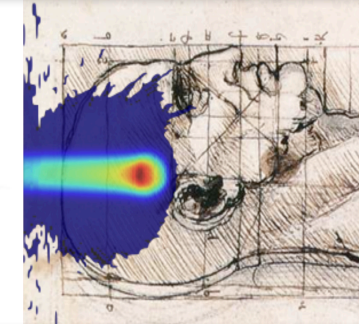
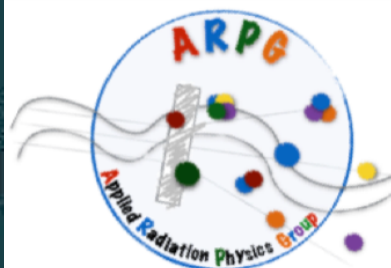




SAPIENZA
UNIVERSITÀ DI ROMA



CENTRO RICERCHE
ENRICO FERMI



Development of a Treatment Control System for IORT FLASH beam

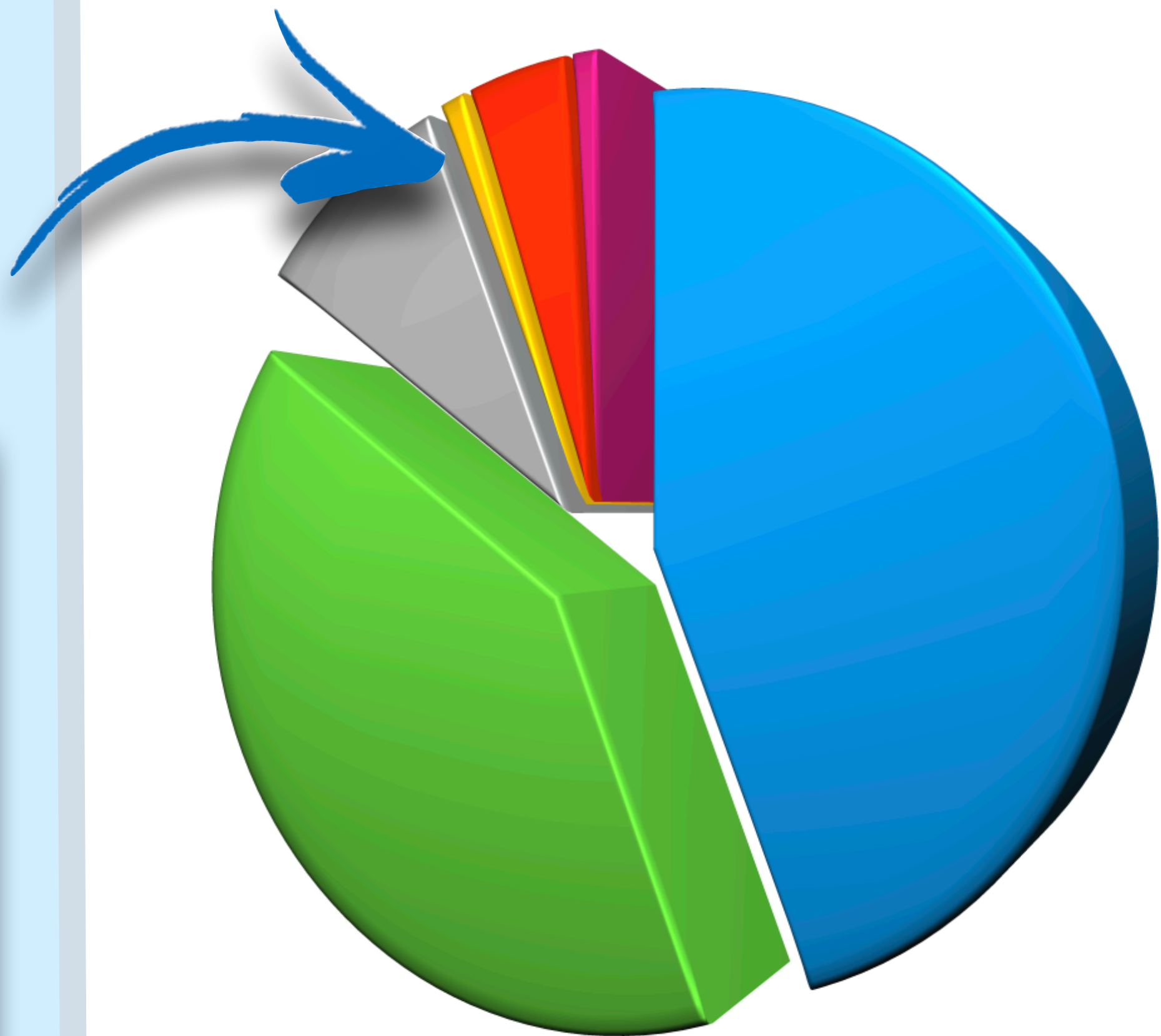
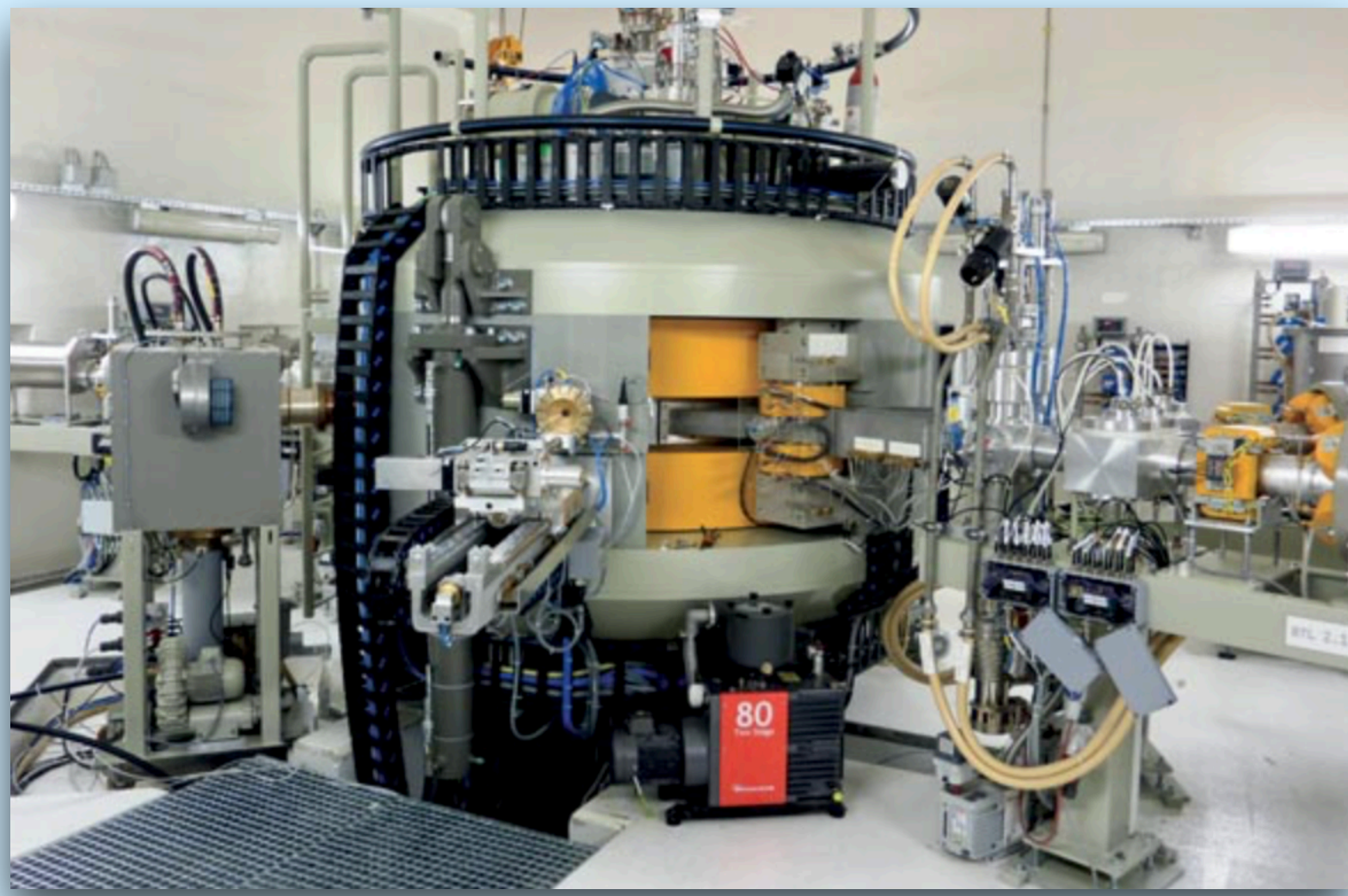
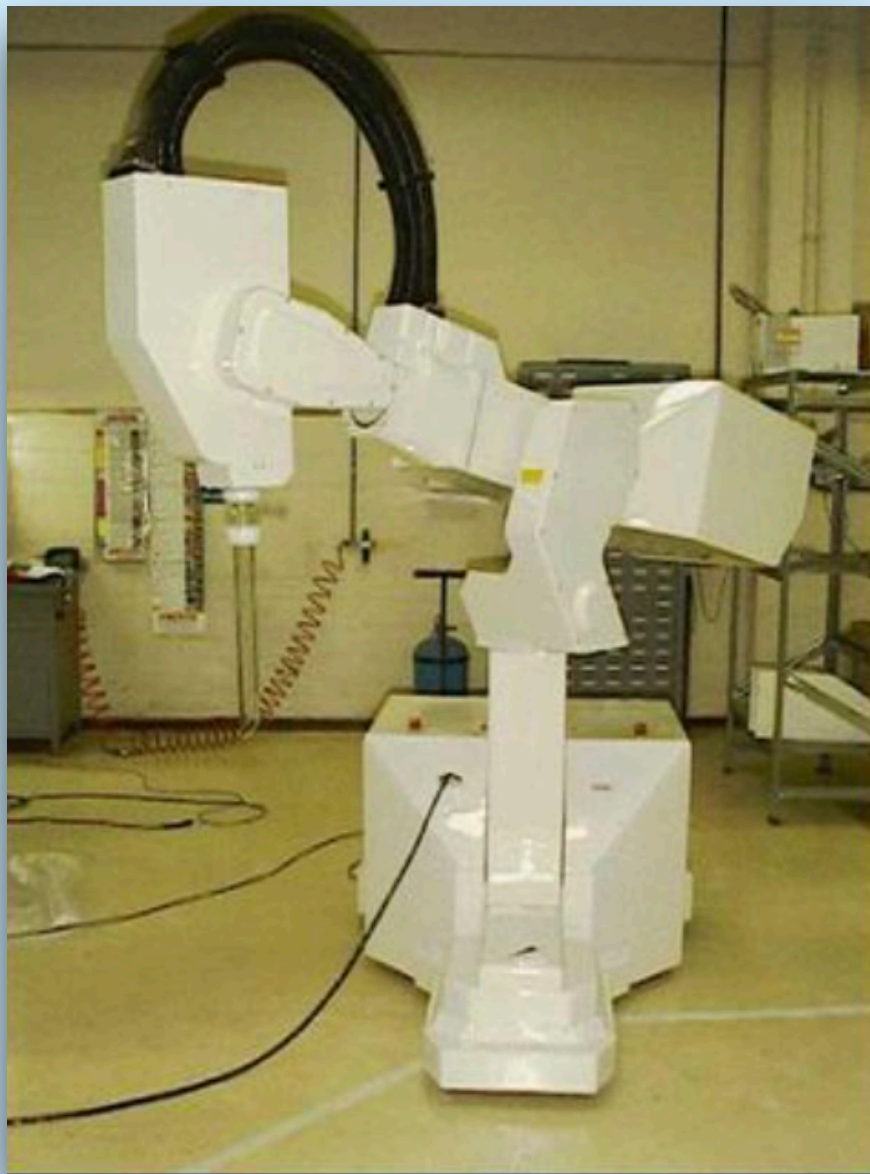
PhD in *Accelerator Physics*, XXXV cycle
Sapienza University of Rome

Gaia Franciosini
Supervisor: **Vincenzo Patera**

Rome 02/11/2021

Accelerators usage worldwide

44% Radiotherapy
41% Ion Implementers & Surface Modification
9% Industrial Processing and Research
1% > 1GeV for research
4% Research (incl. biomedical)
1% Medical Radioisotopes



Treatment Planning System

The Treatment Planning System (**TPS**) combines the characteristics of the particles at the energies of interest with the accelerator machine parameters to be applied in order to optimise the dose distribution to the patient. In radio-particle therapy it can be analytic or Monte Carlo driven.

The **TPS** provides information to the beam control system:

- Position
- Intensity
- Direction

Physician Prescription

			Relative Importance
Prostate PTV	100	74.0	1.0
Prostate PTV	5.0	72.0	1.0
Prostate PTV	10.0	76.0	1.0
Rectum	90.0	10.0	0.5
Rectum	50.0	20.0	0.5
Rectum	10.0	30.0	0.5
Bladder	90.0	10.0	0.2
Bladder	50.0	20.0	0.2
Bladder	10.0	30.0	0.2
Femoral heads	90.0	10.0	0.2
Femoral heads	50.0	20.0	0.2
Femoral heads	10.0	40.0	0.2

Patient anatomic data (CT, MRI, PET)

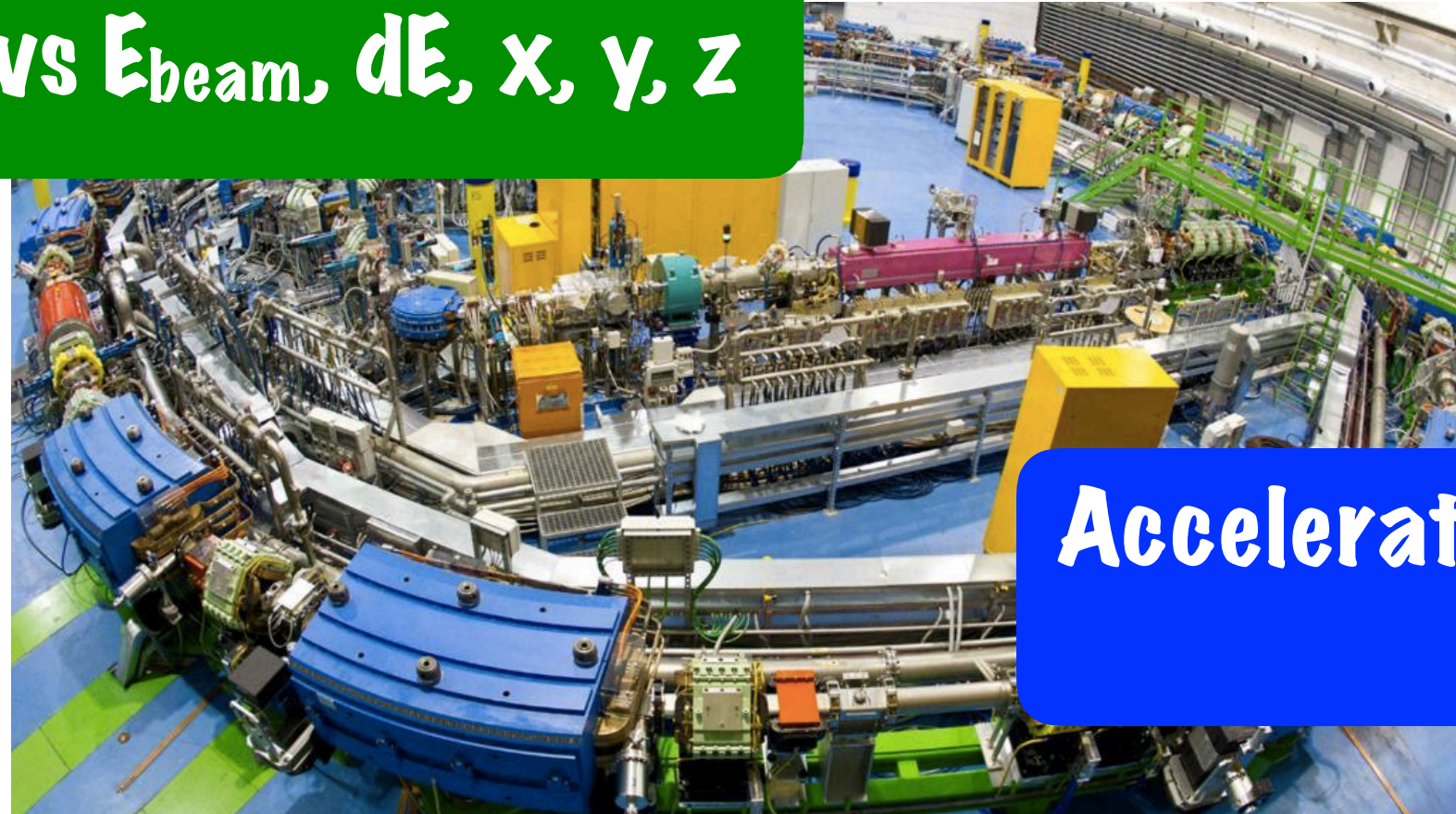
TPS

Accelerators Parameters: Fluences for each beam spot

Table of:

- dE vs E_{beam} , x , y , z
- RBE vs E_{beam} , dE , x , y , z

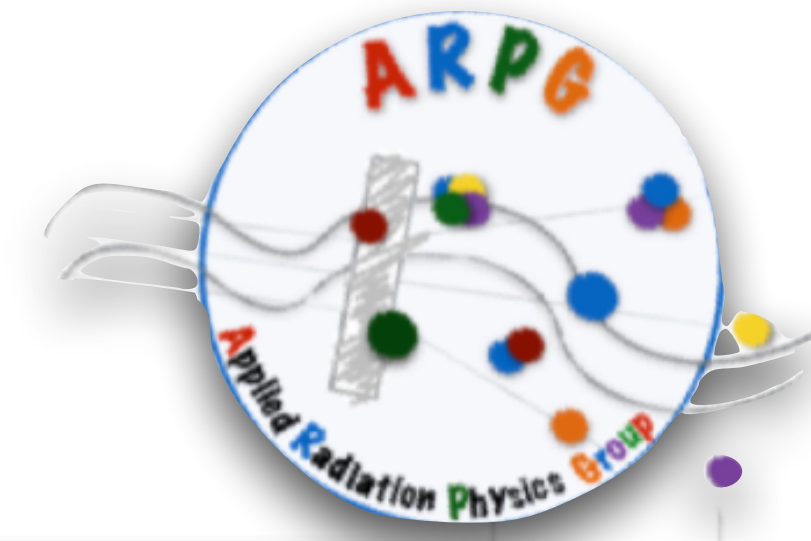
(required) Kinetic Energy (MeV)	Stopping Power (MeV cm ² /g)			Range		
	Electronic	Nuclear	Total	CSDA (g/cm ²)	Projected (g/cm ²)	Detour Factor Projected / CSDA
1.000E-03	1.337E+02	4.315E+01	1.769E+02	6.319E-06	2.878E-06	0.4555
1.500E-03	1.638E+02	3.460E+01	1.984E+02	8.969E-06	4.400E-06	0.4906
2.000E-03	1.891E+02	2.927E+01	2.184E+02	1.137E-05	5.909E-06	0.5197
2.500E-03	2.114E+02	2.557E+01	2.370E+02	1.357E-05	7.380E-06	0.5440
3.000E-03	2.316E+02	2.281E+01	2.544E+02	1.560E-05	8.811E-06	0.5647
4.000E-03	2.675E+02	1.894E+01	2.864E+02	1.930E-05	1.155E-05	0.5986
5.000E-03	2.990E+02	1.631E+01	3.153E+02	2.262E-05	1.415E-05	0.6254
6.000E-03	3.276E+02	1.439E+01	3.420E+02	2.567E-05	1.661E-05	0.6473
7.000E-03	3.538E+02	1.292E+01	3.667E+02	2.849E-05	1.896E-05	0.6656
8.000E-03	3.782E+02	1.175E+01	3.900E+02	3.113E-05	2.121E-05	0.6813
9.000E-03	4.012E+02	1.080E+01	4.120E+02	3.363E-05	2.337E-05	0.6950
1.000E-02	4.229E+02	1.000E+01	4.329E+02	3.599E-05	2.545E-05	0.7070
1.250E-02	4.660E+02	8.485E+00	4.745E+02	4.150E-05	3.037E-05	0.7318
1.500E-02	5.036E+02	7.400E+00	5.110E+02	4.657E-05	3.499E-05	0.7514
1.750E-02	5.372E+02	6.581E+00	5.437E+02	5.131E-05	3.938E-05	0.7674
2.000E-02	5.678E+02	5.900E+00	5.728E+02	5.569E-05	4.356E-05	0.7806
2.250E-02	5.956E+02	5.330E+00	6.000E+02	5.969E-05	4.756E-05	0.7914
2.500E-02	6.208E+02	4.840E+00	6.250E+02	6.336E-05	5.139E-05	0.8000
2.750E-02	6.436E+02	4.420E+00	6.480E+02	6.674E-05	5.507E-05	0.8067
3.000E-02	6.640E+02	4.060E+00	6.680E+02	7.000E-05	5.861E-05	0.8117
3.500E-02	7.100E+02	3.300E+00	7.130E+02	7.800E-05	6.500E-05	0.8170
4.000E-02	7.450E+02	2.700E+00	7.470E+02	8.450E-05	7.050E-05	0.8210
4.500E-02	7.720E+02	2.200E+00	7.720E+02	9.000E-05	7.500E-05	0.8240



FRED: Fast paRticle thErapy Dose evaluator

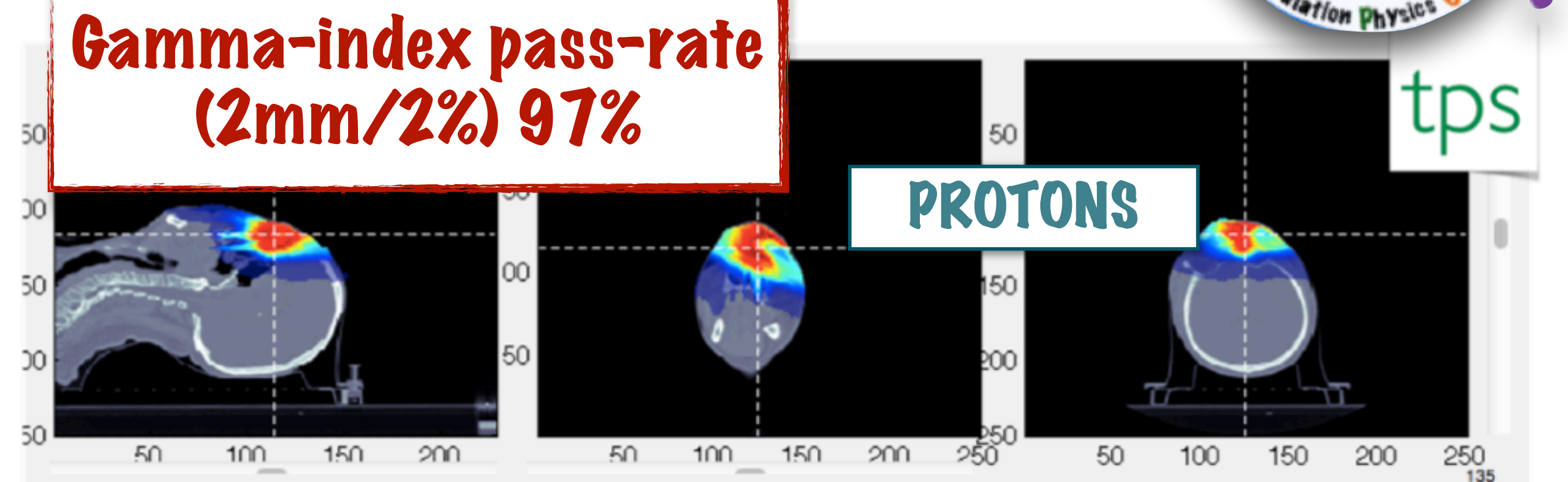
FRED [4] is a fast Monte Carlo code for the transport of particles in heterogeneous media that allows for a quick recalculation of the deposition of the dose. It has been developed in the context of Particle Therapy.

FRED has been developed to work on **GPU (Graphics Processing Unit)** and it reduces the simulation time by a factor of 1000 for proton treatments compared to a standard MC.

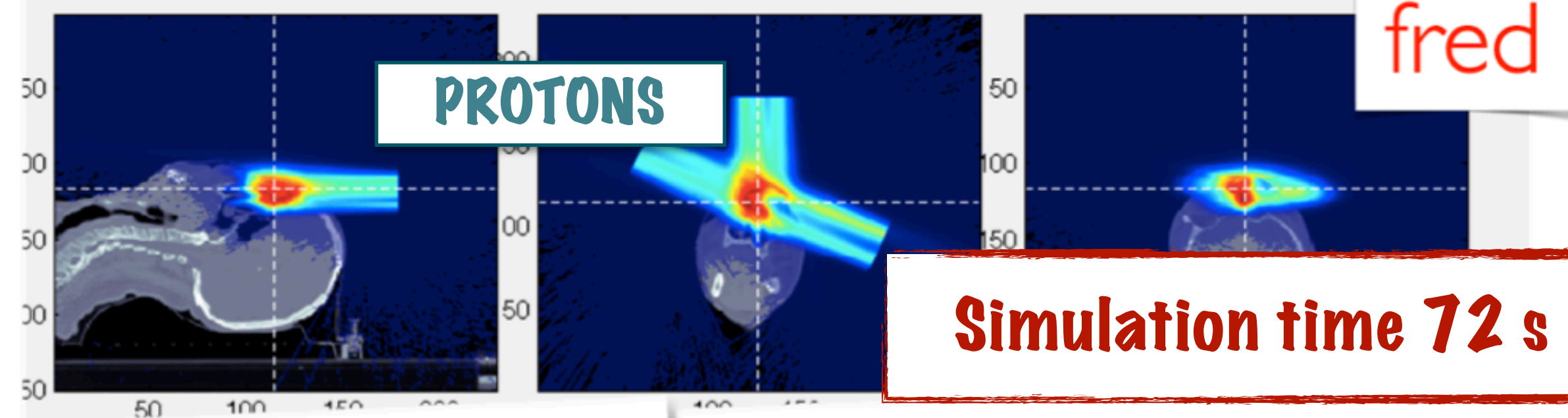


Today FRED protons is used as a tool for the **quality control of TPS** in various medical and research centres throughout Europe.

- MedAustron (Vienna),
- APSS (Trento),
- MAASTRO (Maastricht)
- CNAO (Pavia).



Schiavi A. et al, Physics in Medicine and Biology **62** (2017)



[4] A. Schiavi et al. "FRED: a GPU-accelerated fast-Monte Carlo code for rapid treatment plan recalculation in ion beam therapy" PMB 62 (2017) 18 doi: 10.1088/1361-6560/aa8134

My PhD thesis

For the exceptional speed of the proton and recently also of the carbon tracking algorithms implemented in FRED and for the excellent results achieved, the ARPGroup has decided to implement the tracking of e^- , e^+ and γ in FRED in order to extend the use of this MC- on-GPU based software to the Intra Operative Radio Therapy (IORT) and to the IORT-Flash Therapy.

My PhD thesis

For the exceptional speed of the proton and recently also of the carbon tracking algorithms implemented in FRED and for the excellent results achieved, the ARPGroup has decided to implement the tracking of e^- , e^+ and γ in FRED in order to extend the use of this MC- on-GPU based software to the Intra Operative Radio Therapy (IORT) and to the IORT-Flash Therapy.



FRED-em project

My PhD thesis

For the exceptional speed of the proton and recently also of the carbon tracking algorithms implemented in FRED and for the excellent results achieved, the ARPGroup has decided to implement the tracking of e^- , e^+ and γ in FRED in order to extend the use of this MC- on-GPU based software to the Intra Operative Radio Therapy (IORT) and to the IORT-Flash Therapy.



FRED-em project

First phase

- ➔ Implementation of the electromagnetic models in FRED in CPU (Central Processing Unit)
- ➔ Benchmark of the EM-model
- ➔ Test of the FRED-em code for IORT application

Second phase

- ➔ Porting on GPU and code optimization
- ➔ TPS for IORT

My PhD thesis

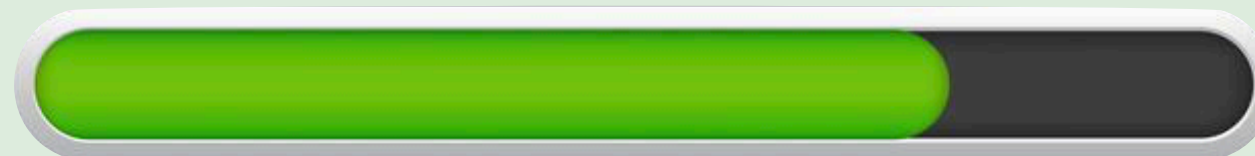
For the exceptional speed of the proton and recently also of the carbon tracking algorithms implemented in FRED and for the excellent results achieved, the ARPGroup has decided to implement the tracking of e^- , e^+ and γ in FRED in order to extend the use of this MC- on-GPU based software to the Intra Operative Radio Therapy (IORT) and to the IORT-Flash Therapy.



FRED-em project

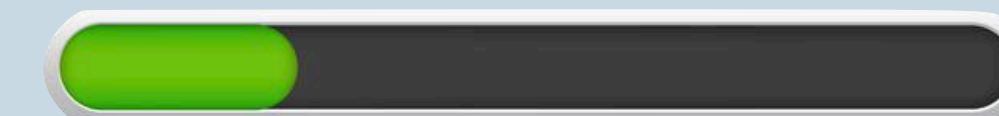
First phase

- ➔ Implementation of the electromagnetic models in FRED in CPU (Central Processing Unit)
- ➔ Benchmark of the EM-model
- ➔ Test of the FRED-em code for IORT application **80%**



Second phase

- ➔ Porting on GPU and code optimization **55%**
- ➔ TPS for IORT **15%**



IOeRT Technique

The Intra Operative Radio Therapy with electron (**IOeRT**) is a technique that, after the surgical tumour removal, delivers a dose of ionising radiation directly to the surgery bed [1]. The goal is to eradicate the microscopic residual tumour cells that surgery was not able to remove completely.



[1] *Intraoperative Irradiation. Techniques and Results*, Calvo FA, Gunderson LL et al., *Current Clinical Oncology*, Second Edition, 2011

IOeRT Technique

The Intra Operative Radio Therapy with electron (**IOeRT**) is a technique that, after the surgical tumour removal, delivers a dose of ionising radiation directly to the surgery bed [1]. The goal is to eradicate the microscopic residual tumour cells that surgery was not able to remove completely.



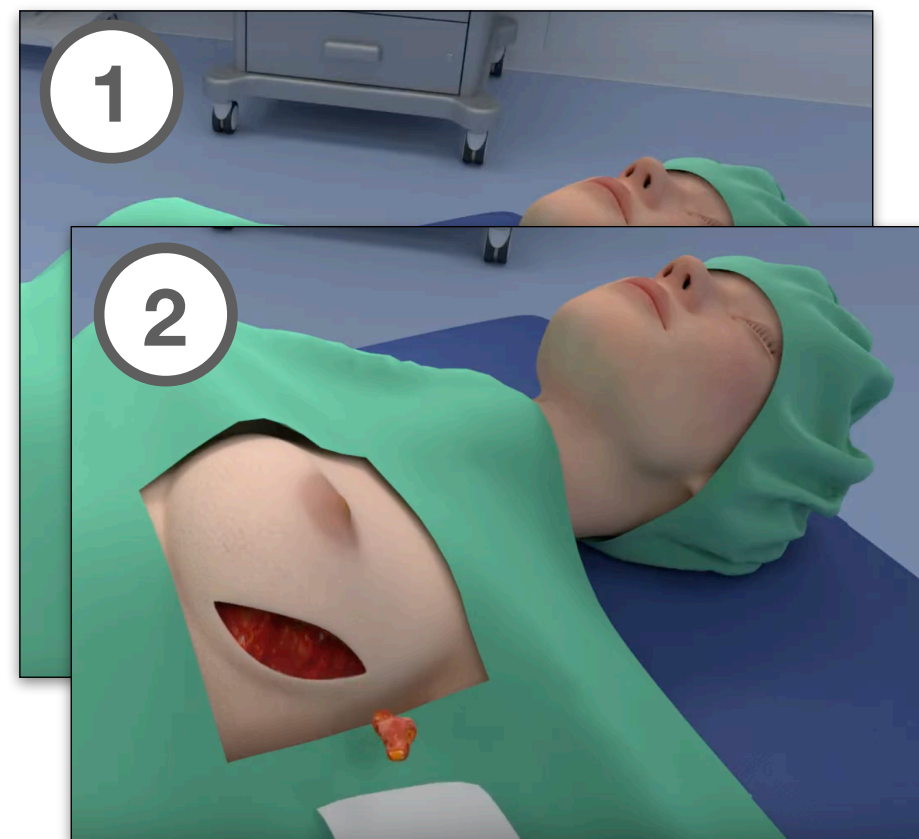
The patient is surgically treated and the tumour is removed by the medical personal.



[1] Intraoperative Irradiation. Techniques and Results, Calvo FA, Gunderson LL et al., Current Clinical Oncology, Second Edition, 2011

IOeRT Technique

The Intra Operative Radio Therapy with electron (**IOeRT**) is a technique that, after the surgical tumour removal, delivers a dose of ionising radiation directly to the surgery bed [1]. The goal is to eradicate the microscopic residual tumour cells that surgery was not able to remove completely.



The patient is surgically treated and the tumour is removed by the medical personal.

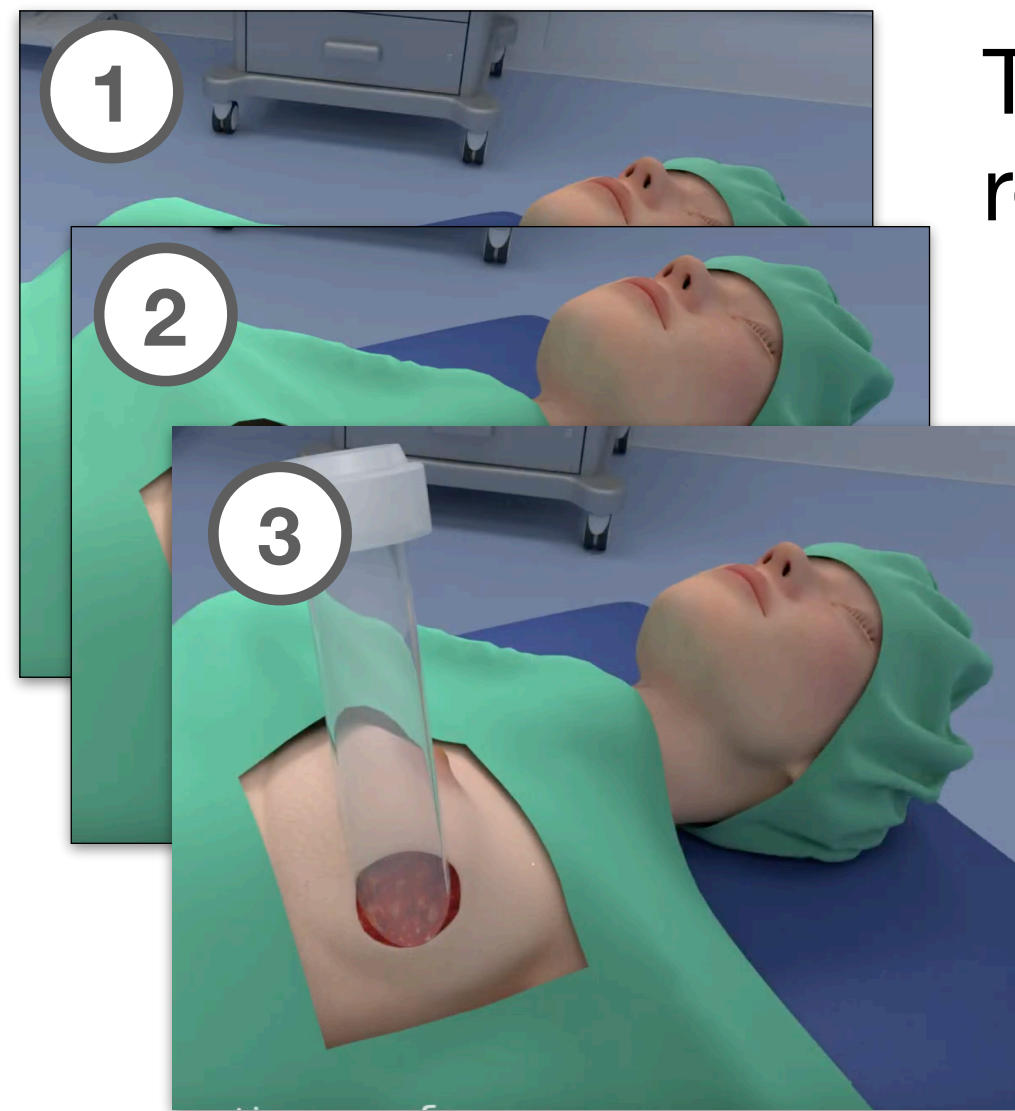
A protective disk is applied in order to preserve the organs from the undesired dose.



[1] *Intraoperative Irradiation. Techniques and Results*, Calvo FA, Gunderson LL et al., *Current Clinical Oncology*, Second Edition, 2011

IOeRT Technique

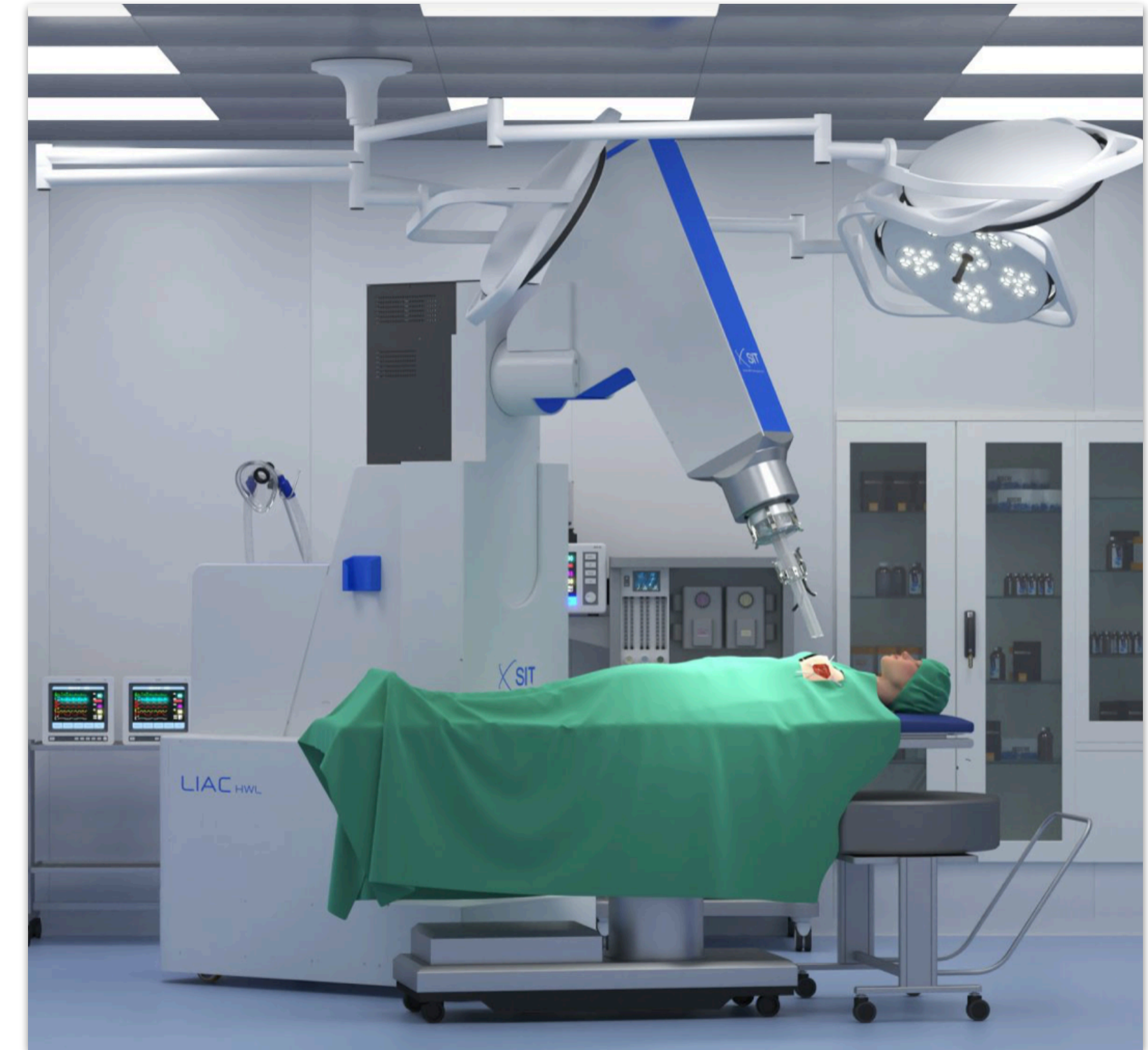
The Intra Operative Radio Therapy with electron (IOeRT) is a technique that, after the surgical tumour removal, delivers a dose of ionising radiation directly to the surgery bed [1]. The goal is to eradicate the microscopic residual tumour cells that surgery was not able to remove completely.



1 The patient is surgically treated and the tumour is removed by the medical personal.

2 A protective disk is applied in order to preserve the organs from the undesired dose.

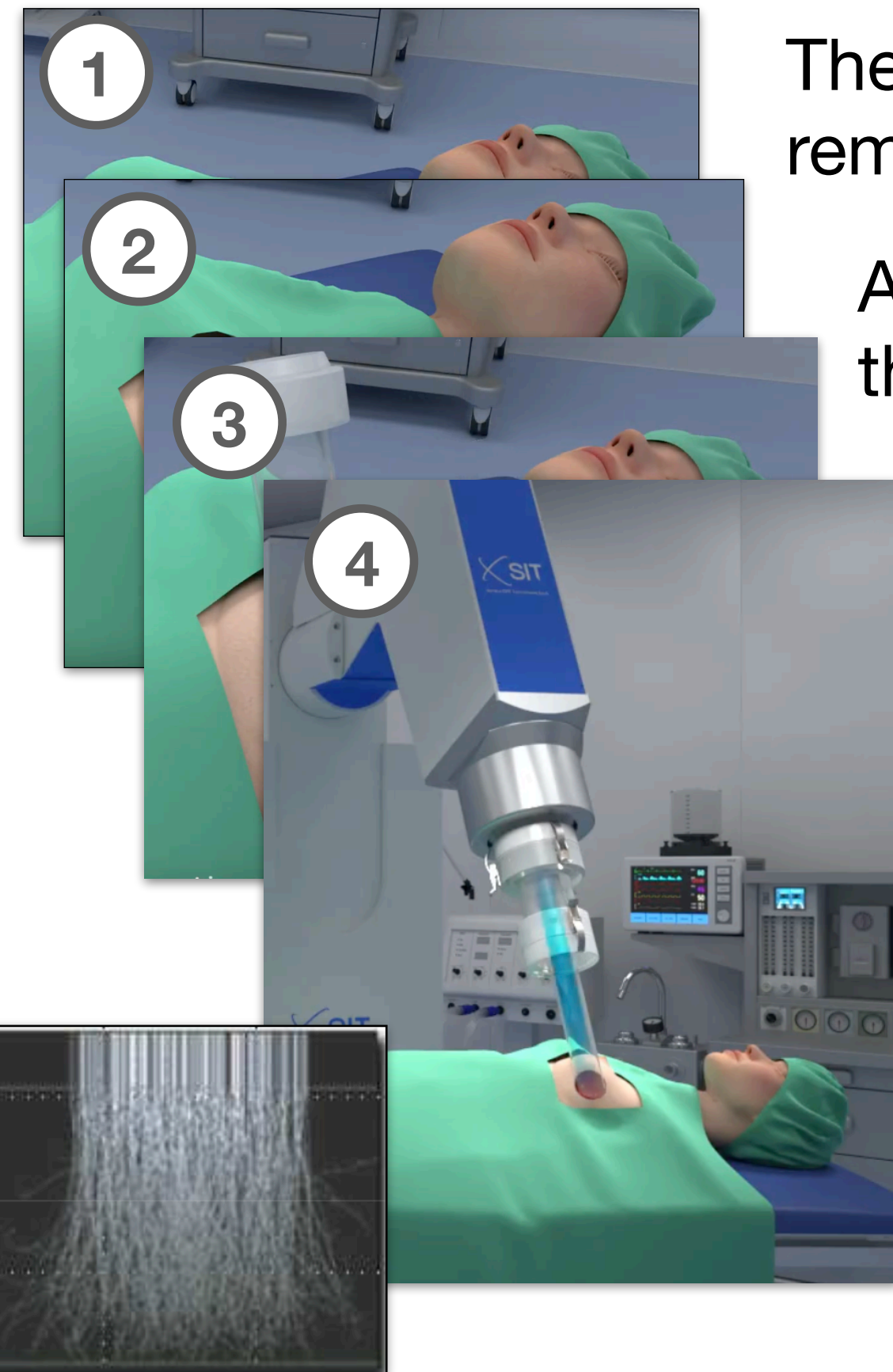
3 The beam is passively collimated by means of PMMA hollow tubes (applicator), targeting only the tumour cells while preserving the surrounding healthy tissues.



[1] Intraoperative Irradiation. Techniques and Results, Calvo FA, Gunderson LL et al., Current Clinical Oncology, Second Edition, 2011

IOeRT Technique

The Intra Operative Radio Therapy with electron (IOeRT) is a technique that, after the surgical tumour removal, delivers a dose of ionising radiation directly to the surgery bed [1]. The goal is to eradicate the microscopic residual tumour cells that surgery was not able to remove completely.



1 The patient is surgically treated and the tumour is removed by the medical personal.

2 A protective disk is applied in order to preserve the organs from the undesired dose.

3 The beam is passively collimated by means of PMMA hollow tubes (applicator), targeting only the tumour cells while preserving the surrounding healthy tissues.

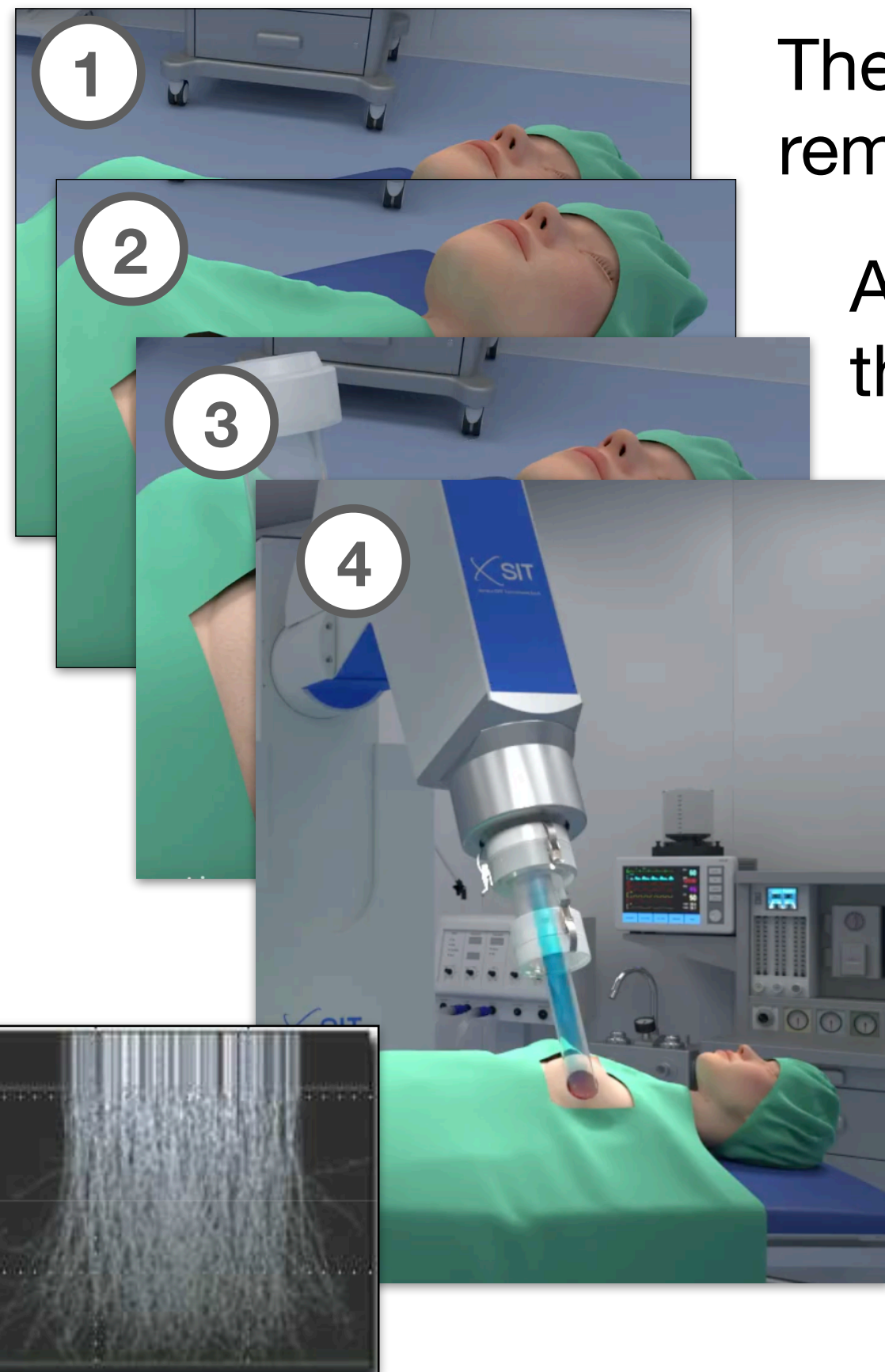
4 The dose is provided by a uniform electron beam produced by a miniaturised LINAC accelerator with energy between 4 and 12 MeV.



[1] Intraoperative Irradiation. Techniques and Results, Calvo FA, Gunderson LL et al., Current Clinical Oncology, Second Edition, 2011

IOeRT Technique

The Intra Operative Radio Therapy with electron (IOeRT) is a technique that, after the surgical tumour removal, delivers a dose of ionising radiation directly to the surgery bed [1]. The goal is to eradicate the microscopic residual tumour cells that surgery was not able to remove completely.



1 The patient is surgically treated and the tumour is removed by the medical personal.

2 A protective disk is applied in order to preserve the organs from the undesired dose.

3 The beam is passively collimated by means of PMMA hollow tubes (applicator), targeting only the tumour cells while preserving the surrounding healthy tissues.

4 The dose is provided by a uniform electron beam produced by a miniaturised LINAC accelerator with energy between 4 and 12 MeV.

No TPS or dose-report



[1] Intraoperative Irradiation. Techniques and Results, Calvo FA, Gunderson LL et al., Current Clinical Oncology, Second Edition, 2011

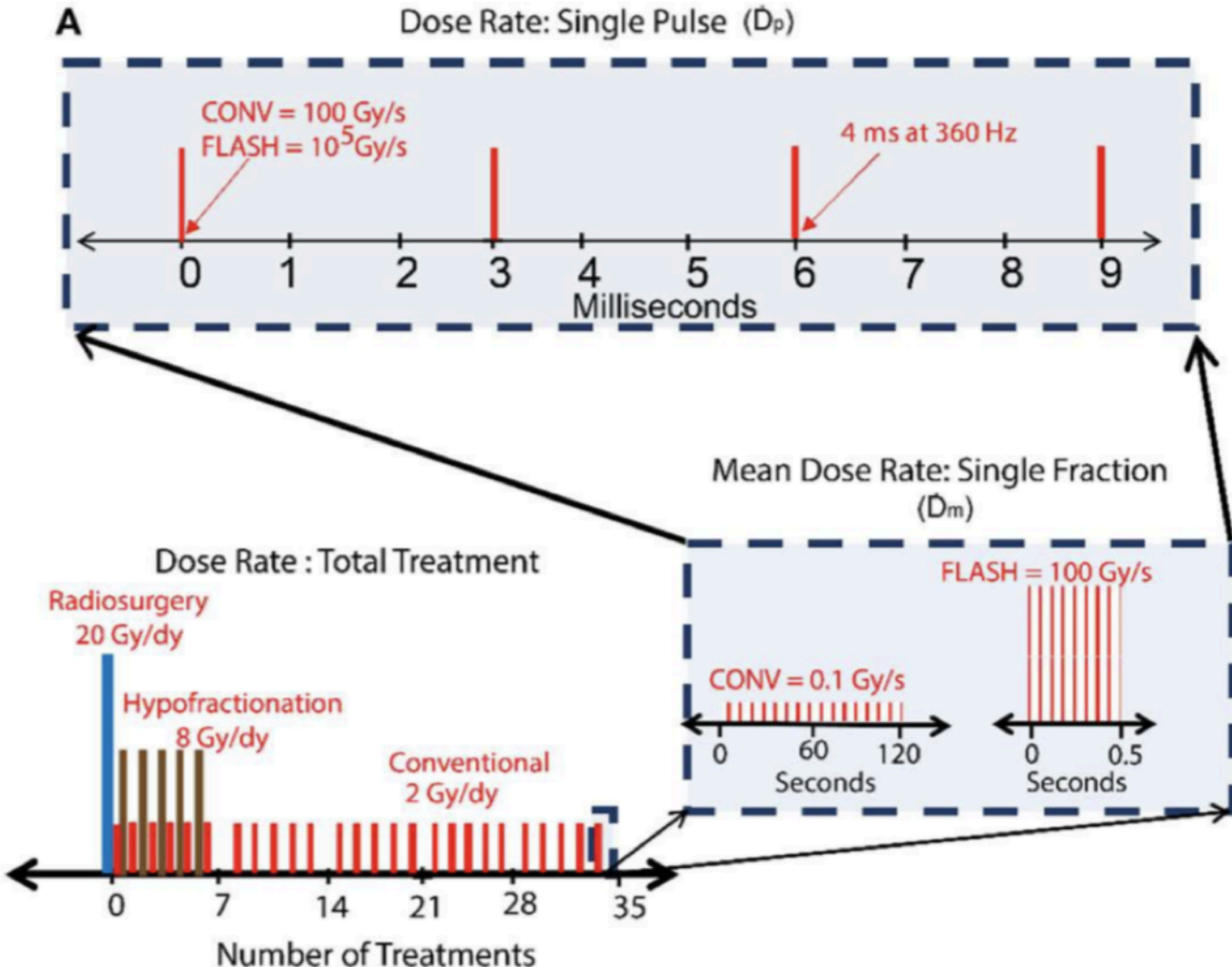
IORT-Flash Technique

From 2014 there is an increasing interest in FLASH radiotherapy. Several pre-clinical studies recently claimed that the toxicity in healthy tissues related to tumour treatments can be significantly reduced (from 80% down to 60%), while keeping the same efficacy in cancer killing, if the dose rate is radically increased (**$\sim 100 \text{ Gy/s}$** , or even more) with respect to conventional treatments (**$\sim 0.01 \text{ Gy/s}$**).



- 1. Tumor response, analogous to the one obtained with conventional RT
- 2. Reduced radiation-induced toxicities in the healthy tissues

Considering this framework, the possibility of readapting existing IORT linac platforms to produce a FLASH beam is particularly attractive.



IOeRT-Flash Technique

From 2014 there is an increasing interest in FLASH radiotherapy. Several pre-clinical studies recently claimed that the toxicity in healthy tissues related to tumour treatments can be significantly reduced (from 80% down to 60%), while keeping the same efficacy in cancer killing, if the dose rate is radically increased (**$\sim 100 \text{ Gy/s}$** , or even more) with respect to conventional treatments (**$\sim 0.01 \text{ Gy/s}$**).



1. Tumor response, analogous to the one obtained with conventional RT
2. Reduced radiation-induced toxicities in the healthy tissues

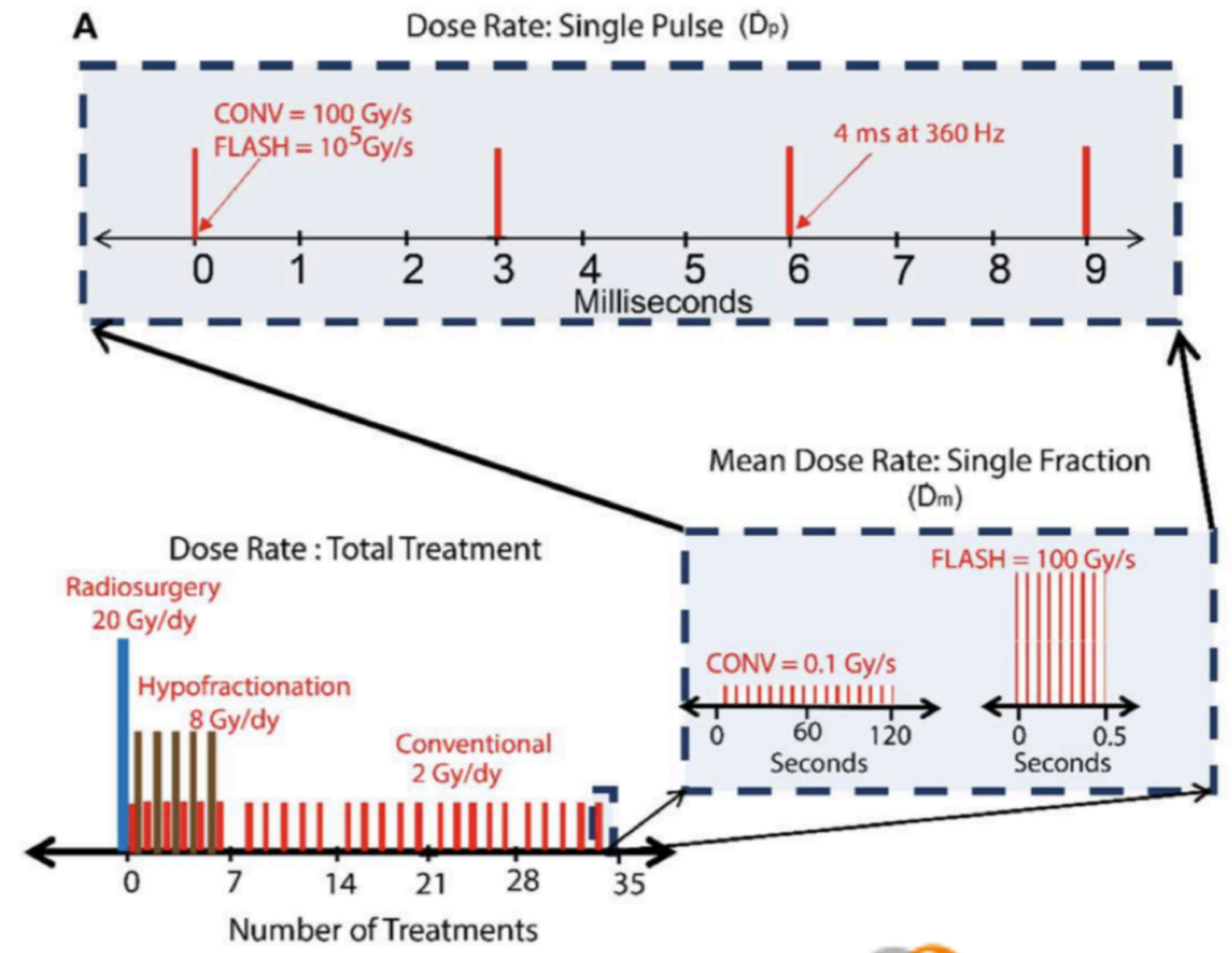
Considering this framework, the possibility of readapting existing IORT linac platforms to produce a FLASH beam is particularly attractive.

In collaboration with the **SIT company** and the **Curie institute** I'm marginally working on this field:

BEAM PARAMETERS AND DOSE RATES MEASUREMENTS OF THE ELECTRON FLASH LINAC AT CURIE INSTITUTE

L. Giuliano, **G. Franciosini**, L. Faillace, M. Migliorati, L. Palumbo
 G. Felici, F. Galante
 A. Patriarca
 M. Dutreix, V. Favaud

to be soon published



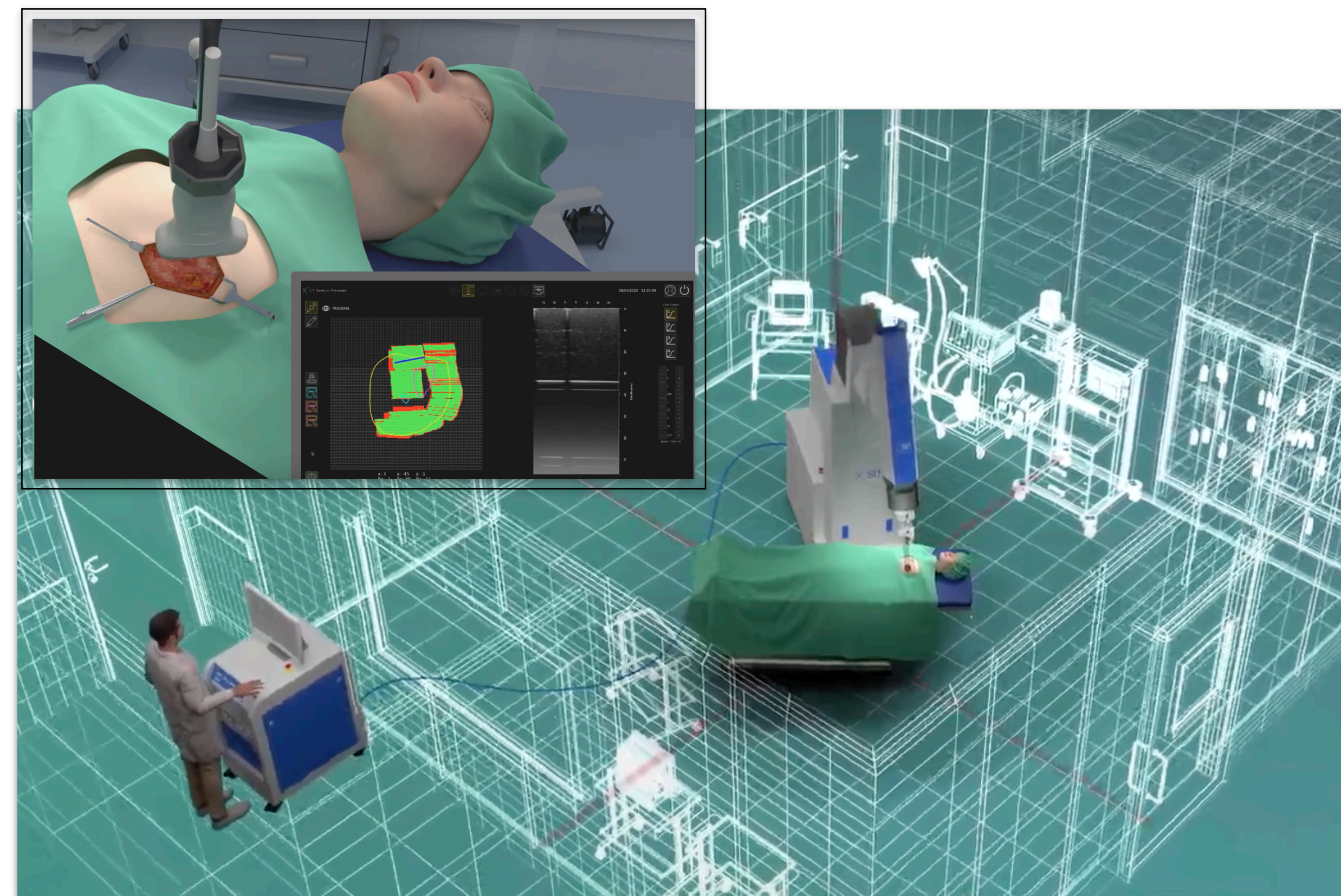
S-band Electron Flash IORT linac commissioning



IOeRT in the future

From 2020, the law (European 2013/59/EURATOM, Italian D.Lgs 101/2020) asks to provide a dosimetric report after each diagnostic exam/treatment that involve radiations surges. **The report has to includes all the organs at risk involved in the exam/treatment.**

- For IOeRT, the dose report is full-filled evaluating analytically the dose to the patient.
- In order to **increase the accuracy a dedicated software is needed**. As the patient undergoes surgical removal of the primary tumour a **real-time imaging** (ecography) and an extremely **TPS** are required.
- **The fast TPS must be able to exploit the aforementioned imaging as input.**



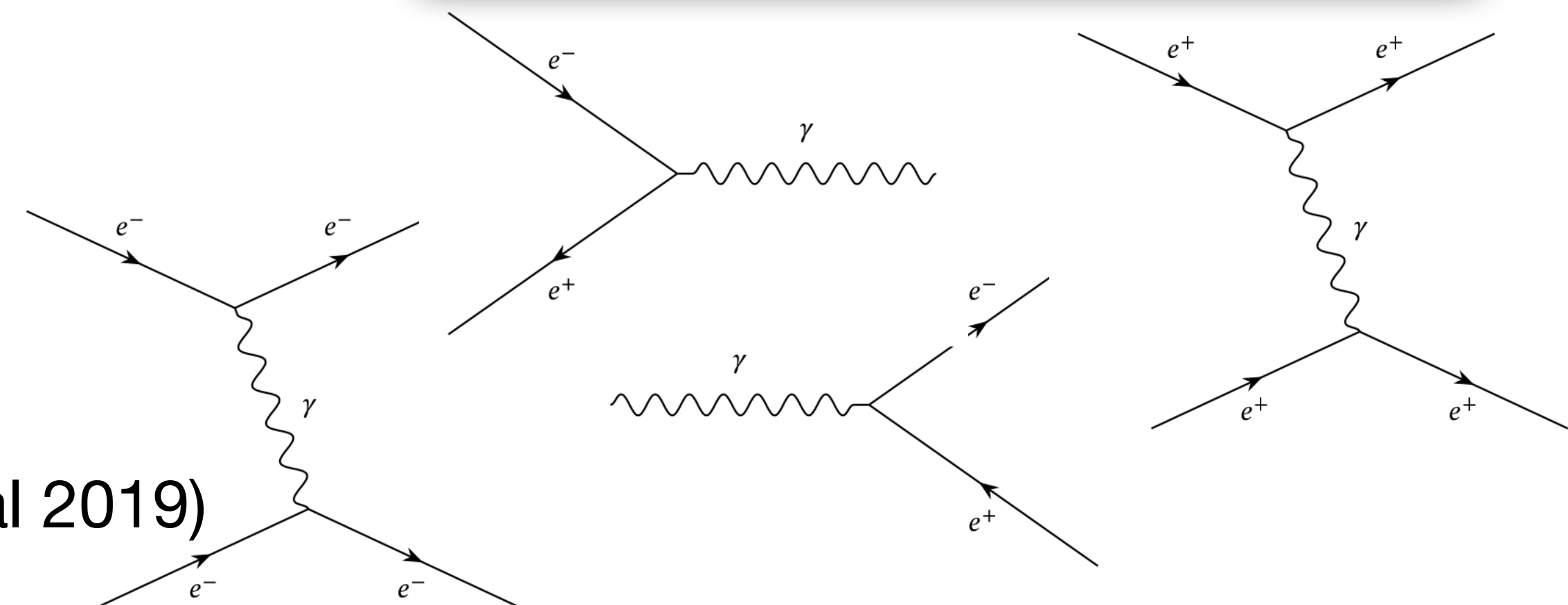
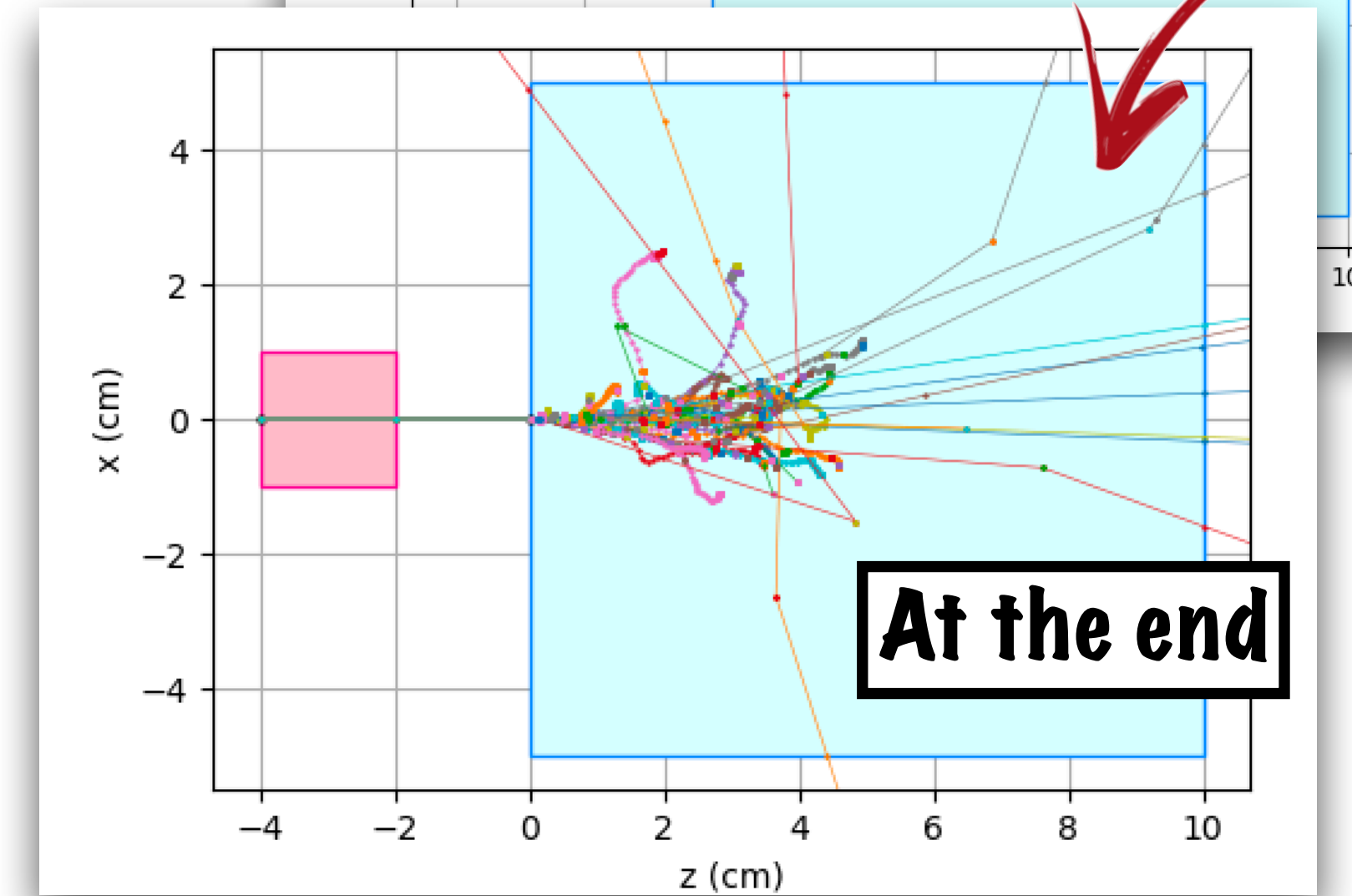
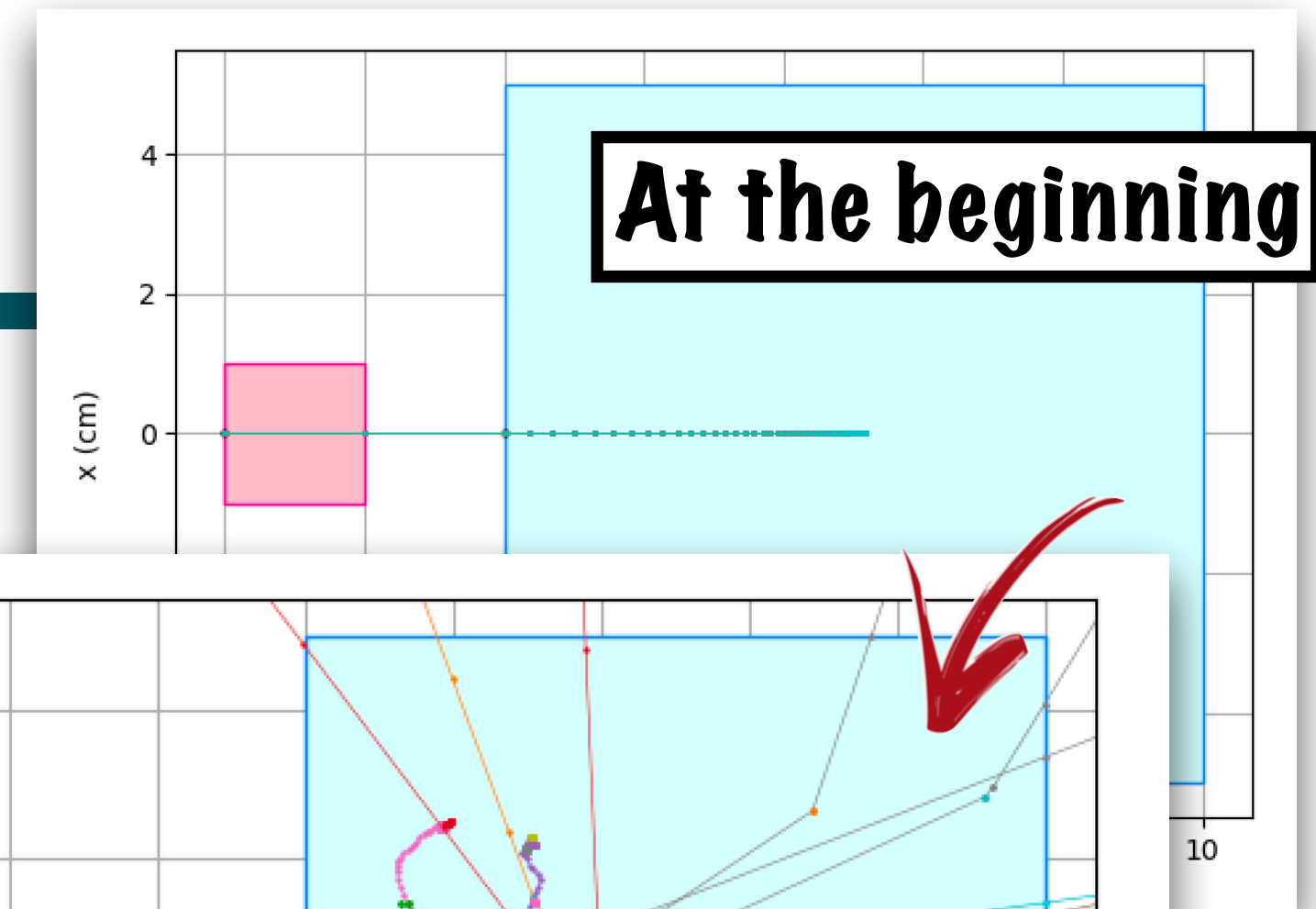
Electromagnetic Model in FRED

Continuous process ($e^- e^+$)

- dE/dx from NIST eSTAR database + **straggling** (GEANT4 physics manual 2019)
- **Multiple scattering** (A. A. Al Beteri, D.E. Raeside, Medical Physics 15, 351 (1988) doi: 10.1118/1596230).

Discrete interactions (e^- , e^+ , γ):

- **Bremsstrahlung** ($d\sigma/dk$ from S.M. Seltzer, M.J. Berger, Data Nucl. Data Tables 35, 345–418 (1986). doi:10.1016/0092-640X(86)90014-8)
- **Moller/Bhabha** scattering (GEANT4 physics manual 2019)
- **Coherent scattering** (XCOM NIST database)
- **Photoelectric** (XCOM NIST database)
- **Compton** (XCOM NIST database)
- **Pair production** (XCOM NIST database)
- **Positron annihilation** at rest/ in flight (GEANT4 physics manual 2019)



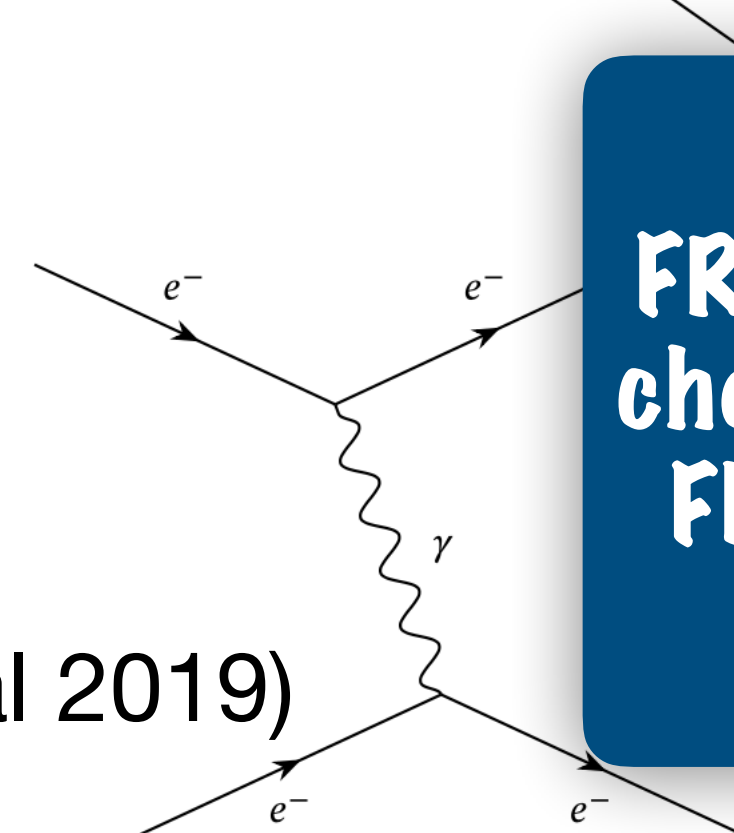
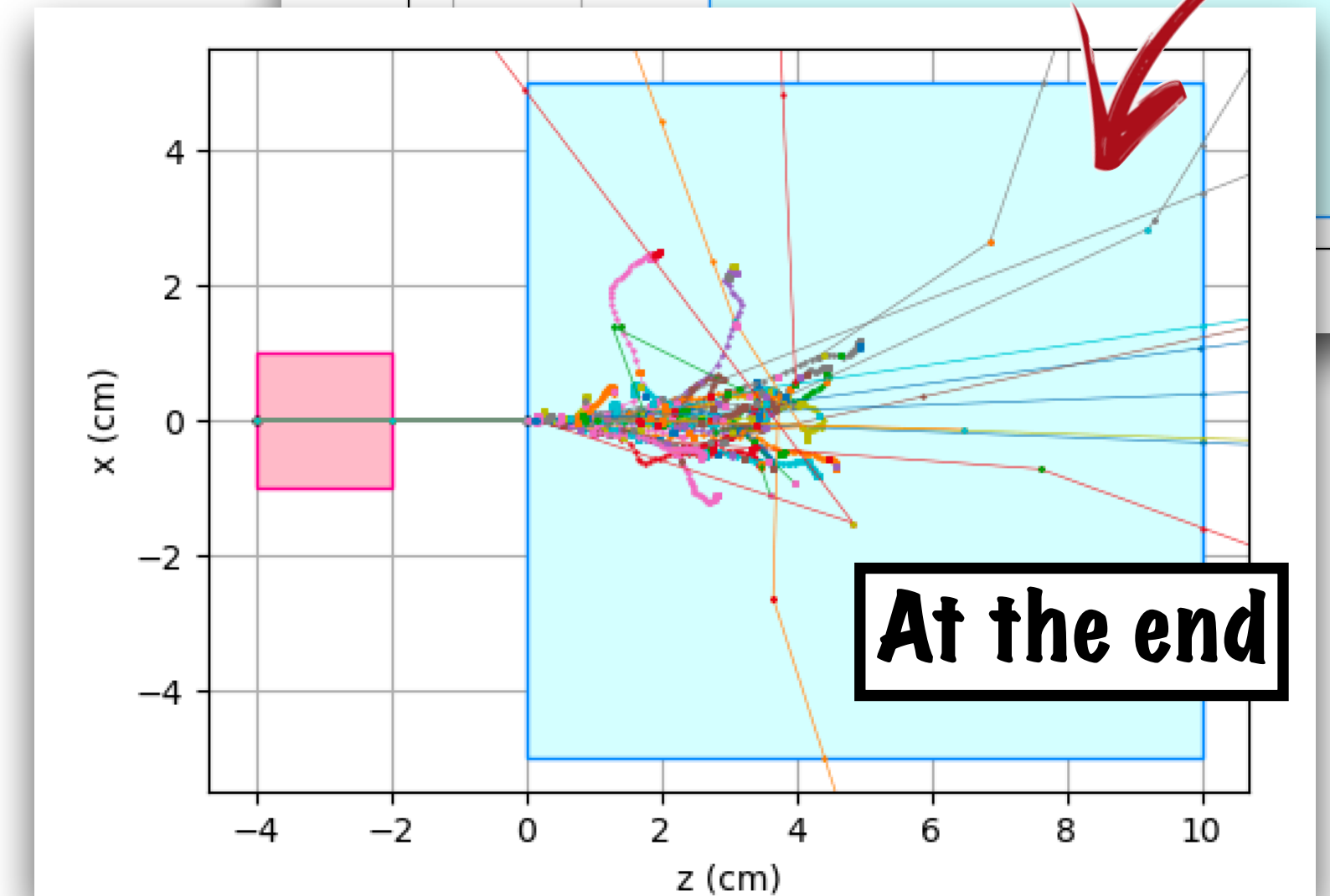
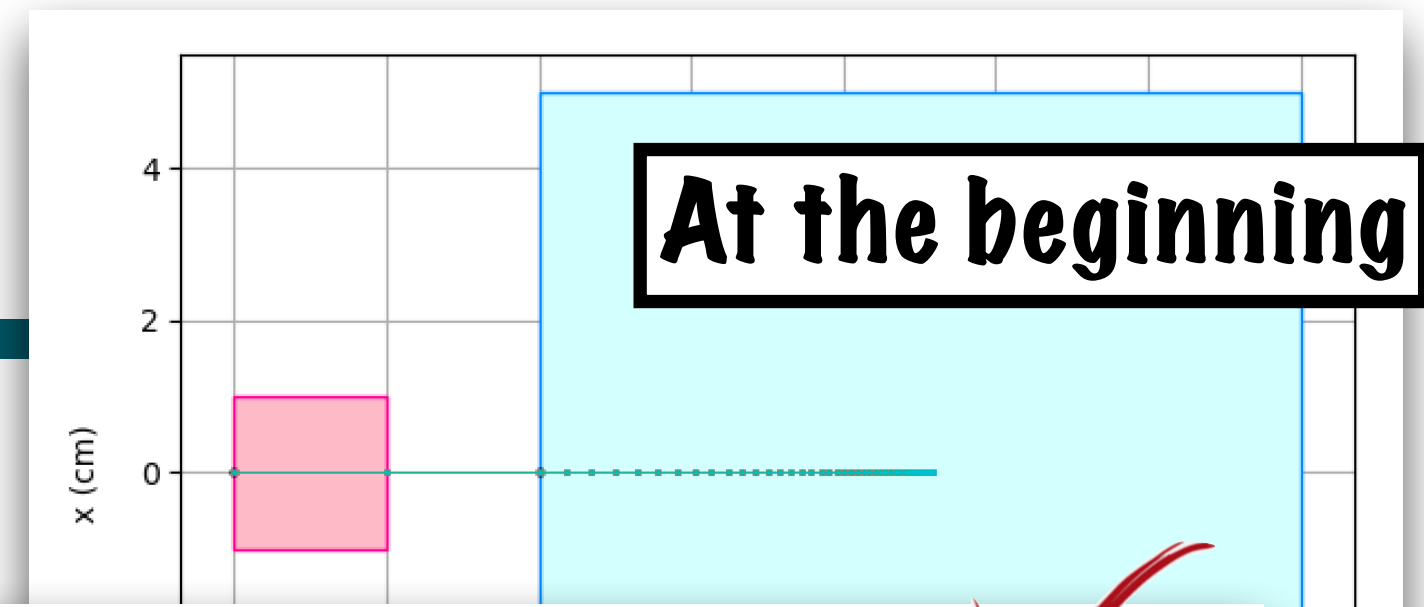
Electromagnetic Model in FRED

Continuous process ($e^- e^+$)

- dE/dx from NIST eSTAR database + **straggling** (GEANT4 physics manual 2019)
- **Multiple scattering** (A. A. Al Beteri, D.E. Raeside, Medical Physics 15, 351 (1988) doi: 10.1118/1596230).

Discrete interactions (e^- , e^+ , γ):

- **Bremsstrahlung** ($d\sigma/dk$ from S.M. Seltzer, M.J. Berger, Data Nucl. Data Tables 35, 345–418 (1986). doi:10.1016/0092-640X(86)90014-8)
- **Moller/Bhabha** scattering (GEANT4 physics manual 2019)
- **Coherent scattering** (XCOM NIST database)
- **Photoelectric** (XCOM NIST database)
- **Compton** (XCOM NIST database)
- **Pair production** (XCOM NIST database)
- **Positron annihilation** at rest/ in flight (GEANT4 physics manual 2019)



FRED-em results have been cross-checked and benchmarked against FLUKA simulations step-by-step

Thin target benchmark

FRED-em models

To check each electromagnetic interaction I have implemented an equal simulation setup in **FRED-em** and **FLUKA**, characterized by a thin target of different materials such as **water**, **PMMA** or element with Z value ranging from 1 (**Hydrogen**) to 79 (**Gold**). I have then cross-checked the **energy and angle distributions** of each interaction in the **energy range of [1-200] MeV**.

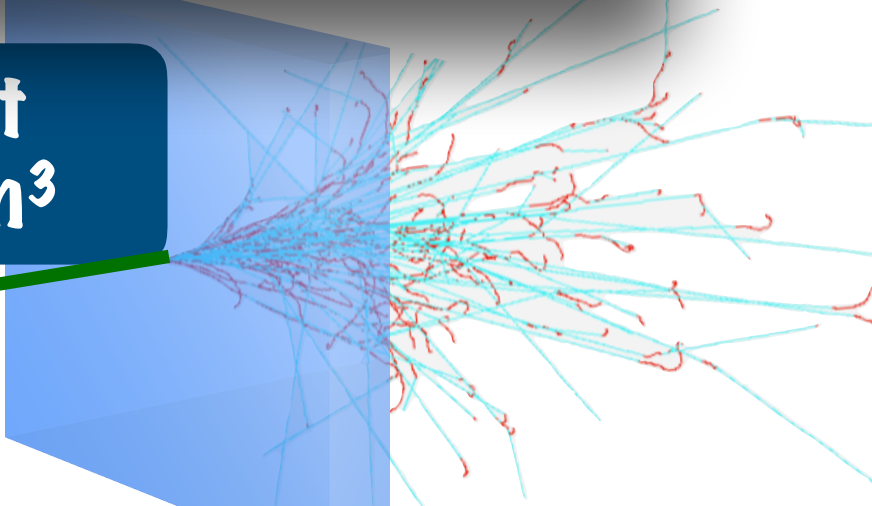
Thin target benchmark

FRED-em models

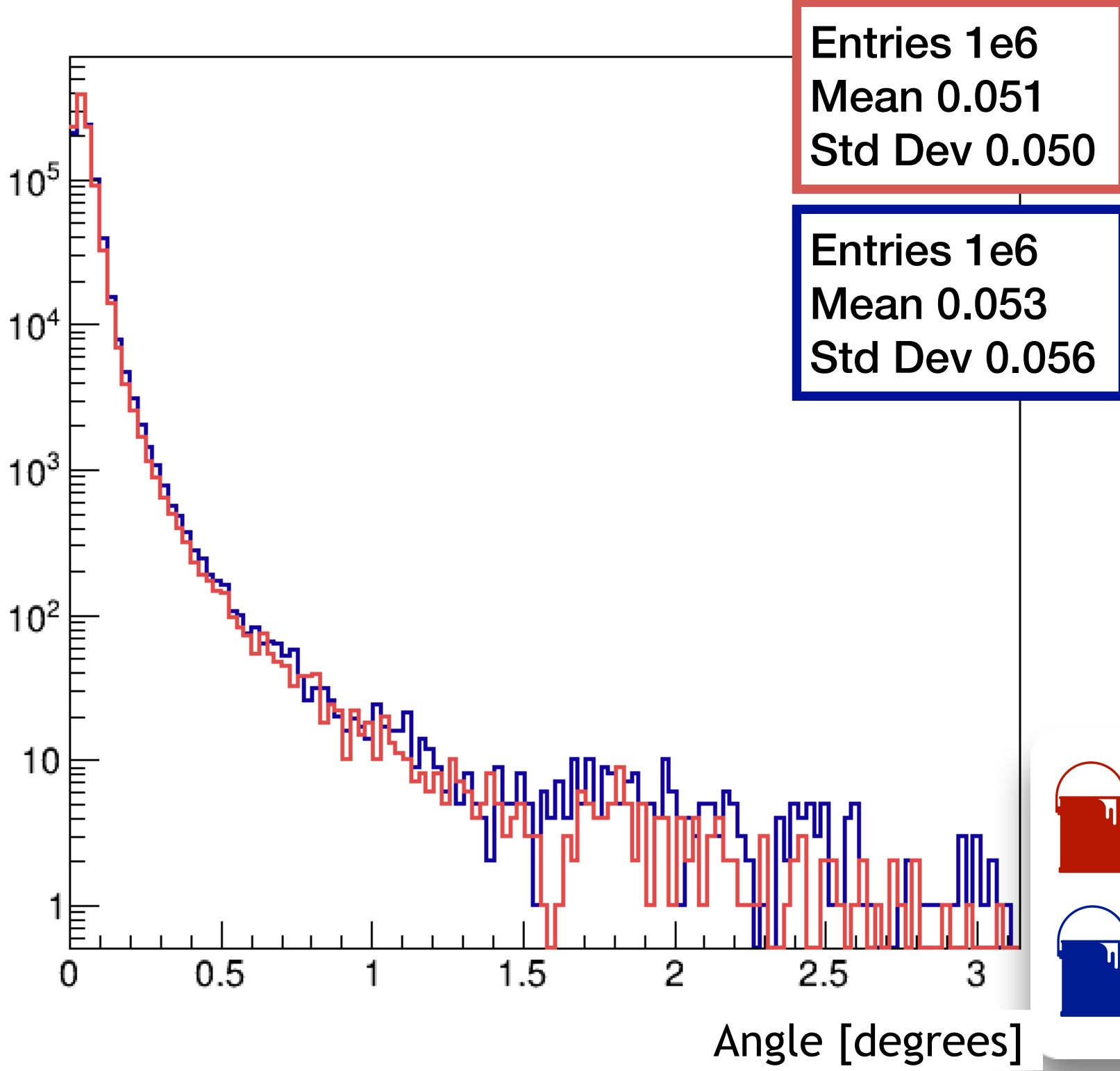
To check each electromagnetic interaction I have implemented an equal simulation setup in **FRED-em** and **FLUKA**, characterized by a thin target of different materials such as **water**, **PMMA** or element with Z value ranging from 1 (**Hydrogen**) to 79 (**Gold**). I have then cross-checked the **energy and angle distributions** of each interaction in the **energy range of [1-200] MeV**.

Water target [5,5,0.05] cm³

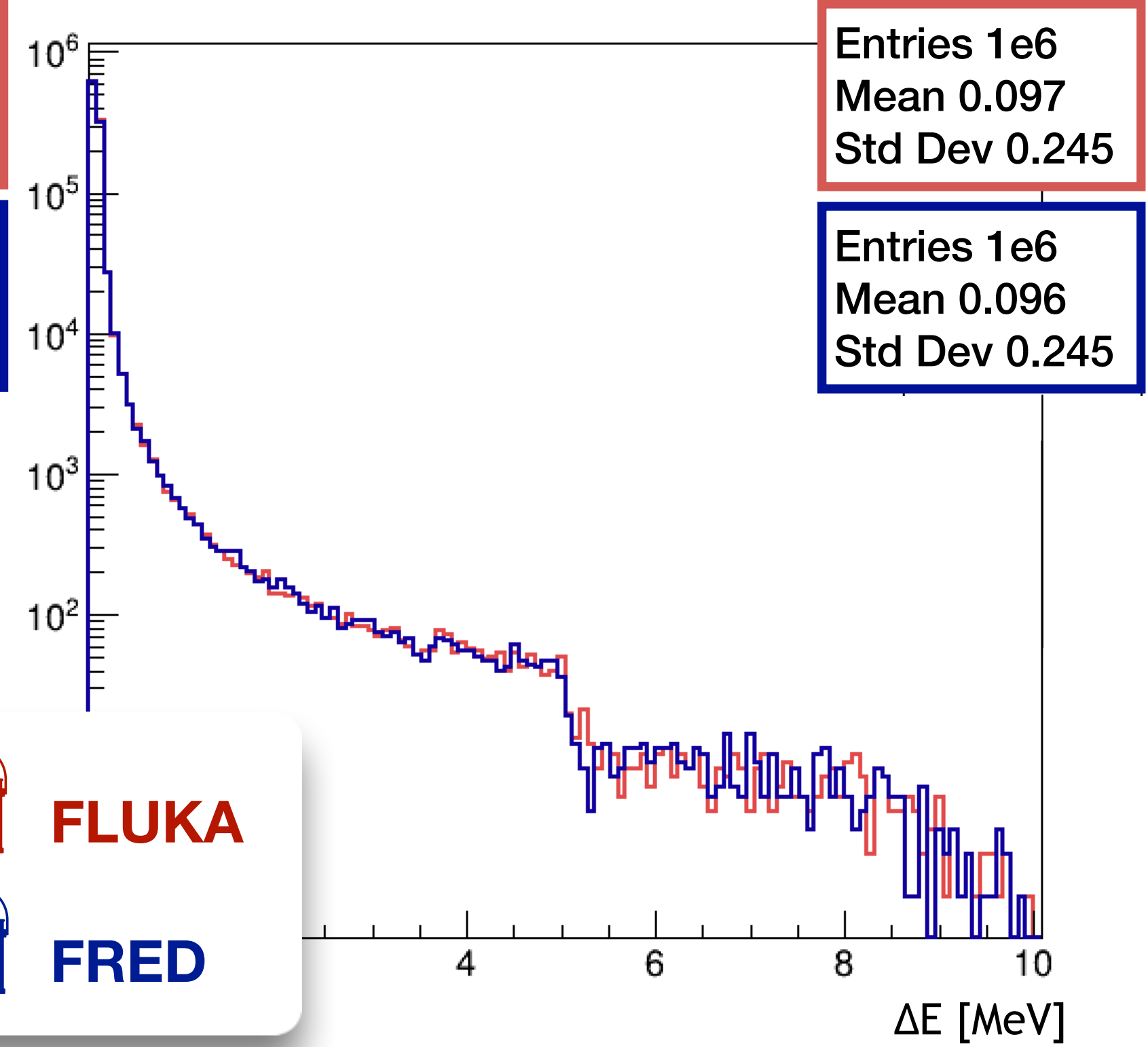
1e7 e⁻ at 10 MeV



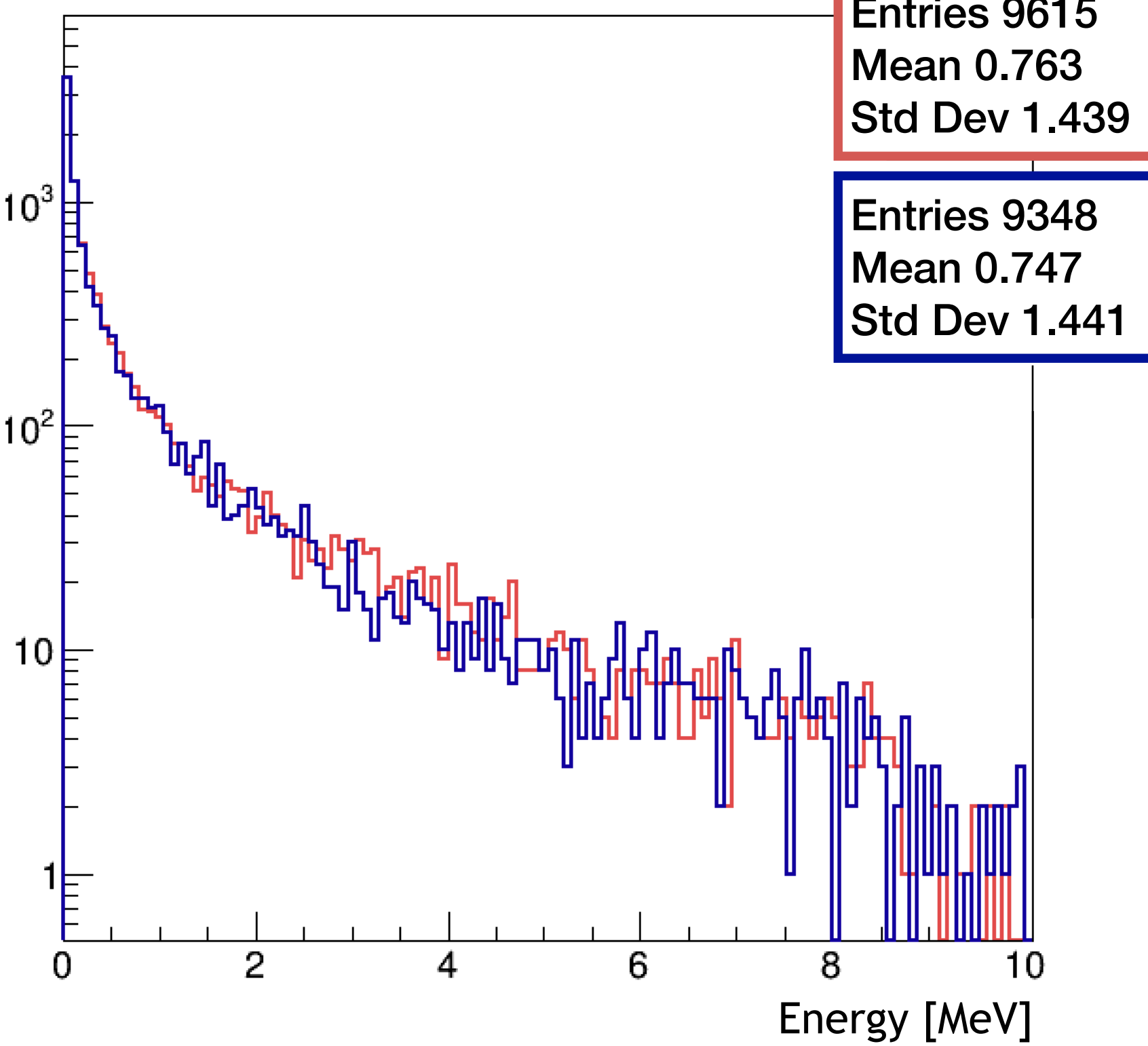
Electrons beam angles @ exit



Energy loss



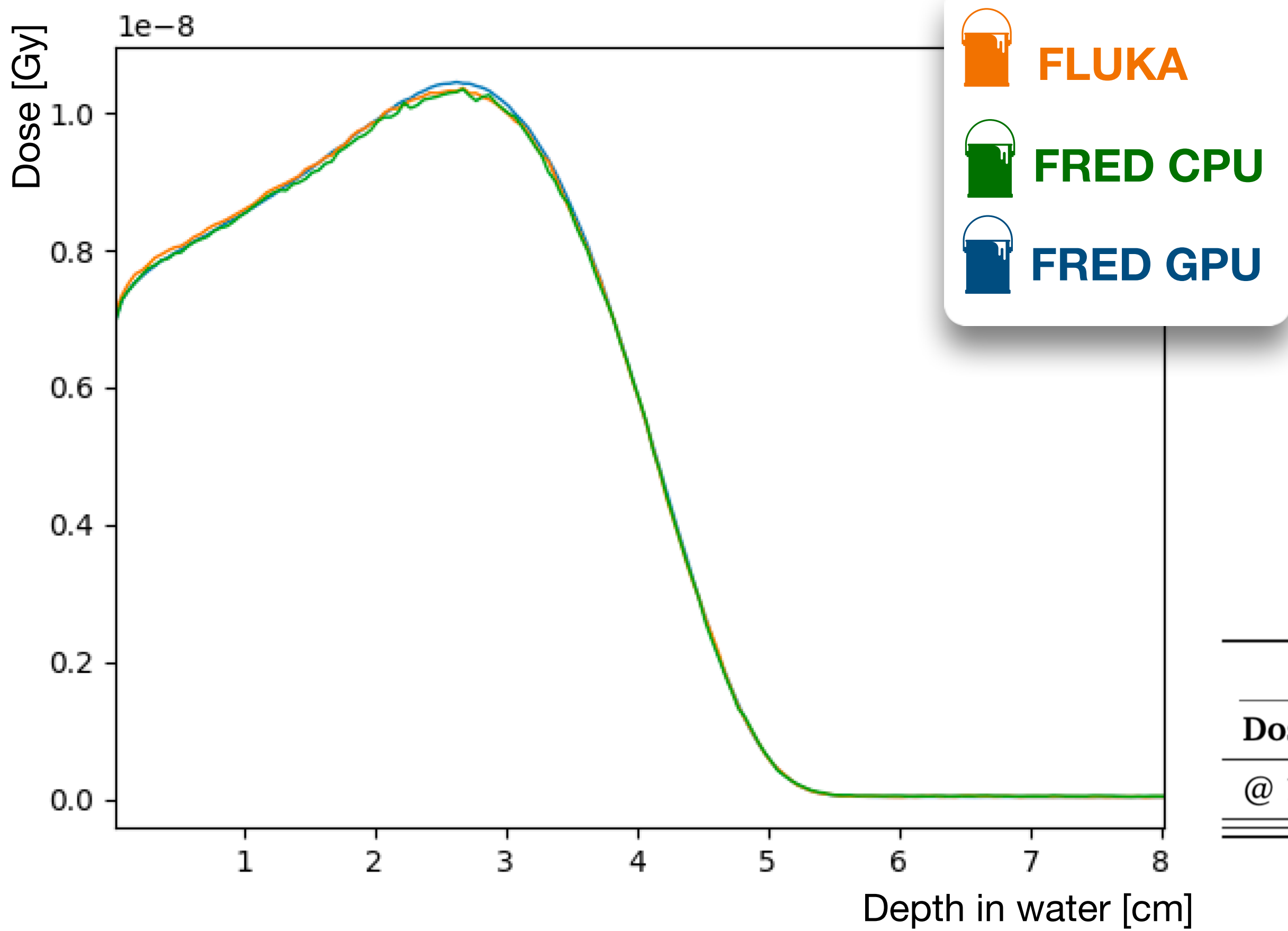
Bremms photon energy @ exit



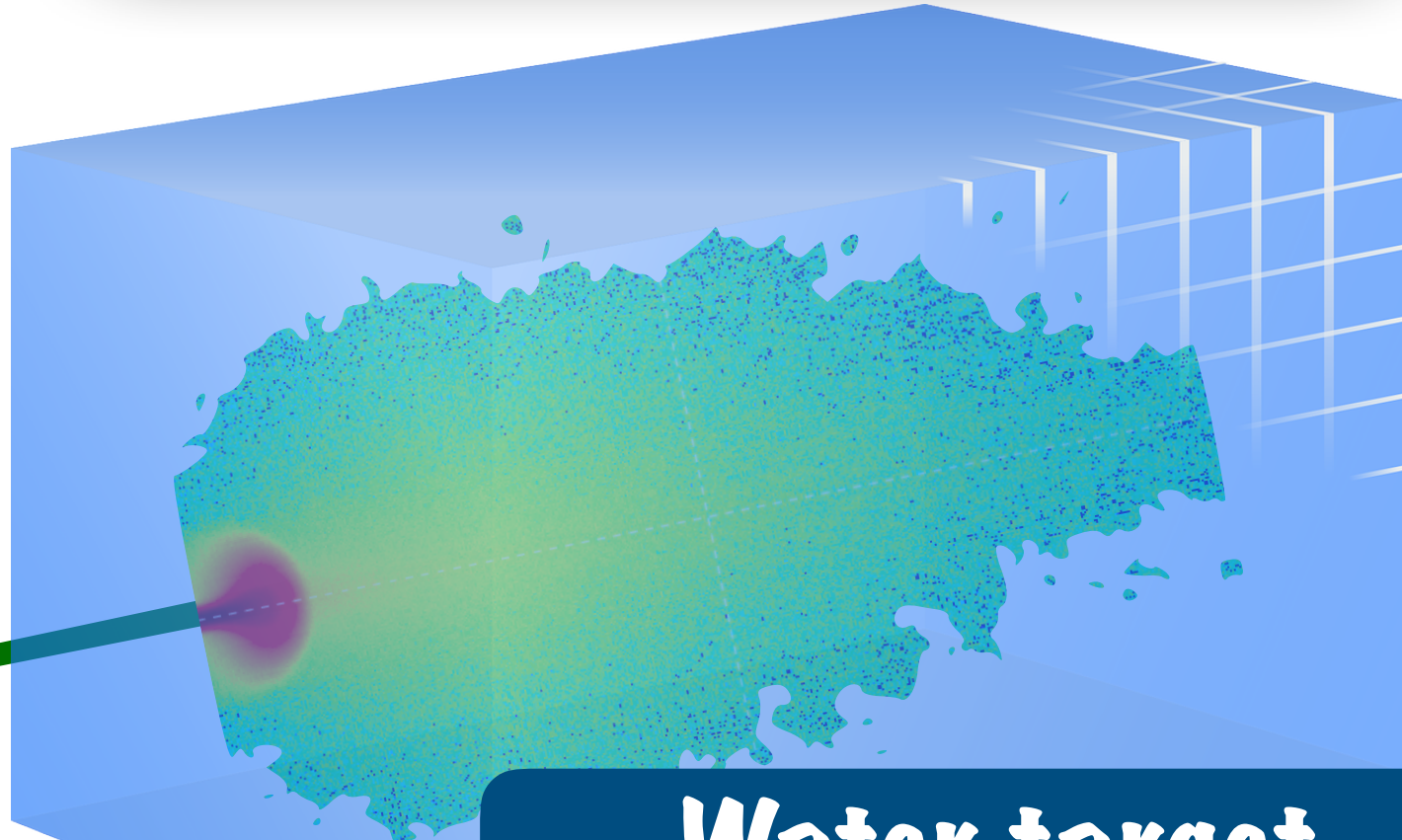
Thick target benchmark

FRED-em dose

Ones I have obtained a successful agreement between the **FLUKA** and **FRED** electromagnetic models, I have checked the **dose distribution** released in different materials in the energy range of **[1-200] MeV**.



1e6 e⁻ at 10 MeV



Water target [40,40,50] cm³

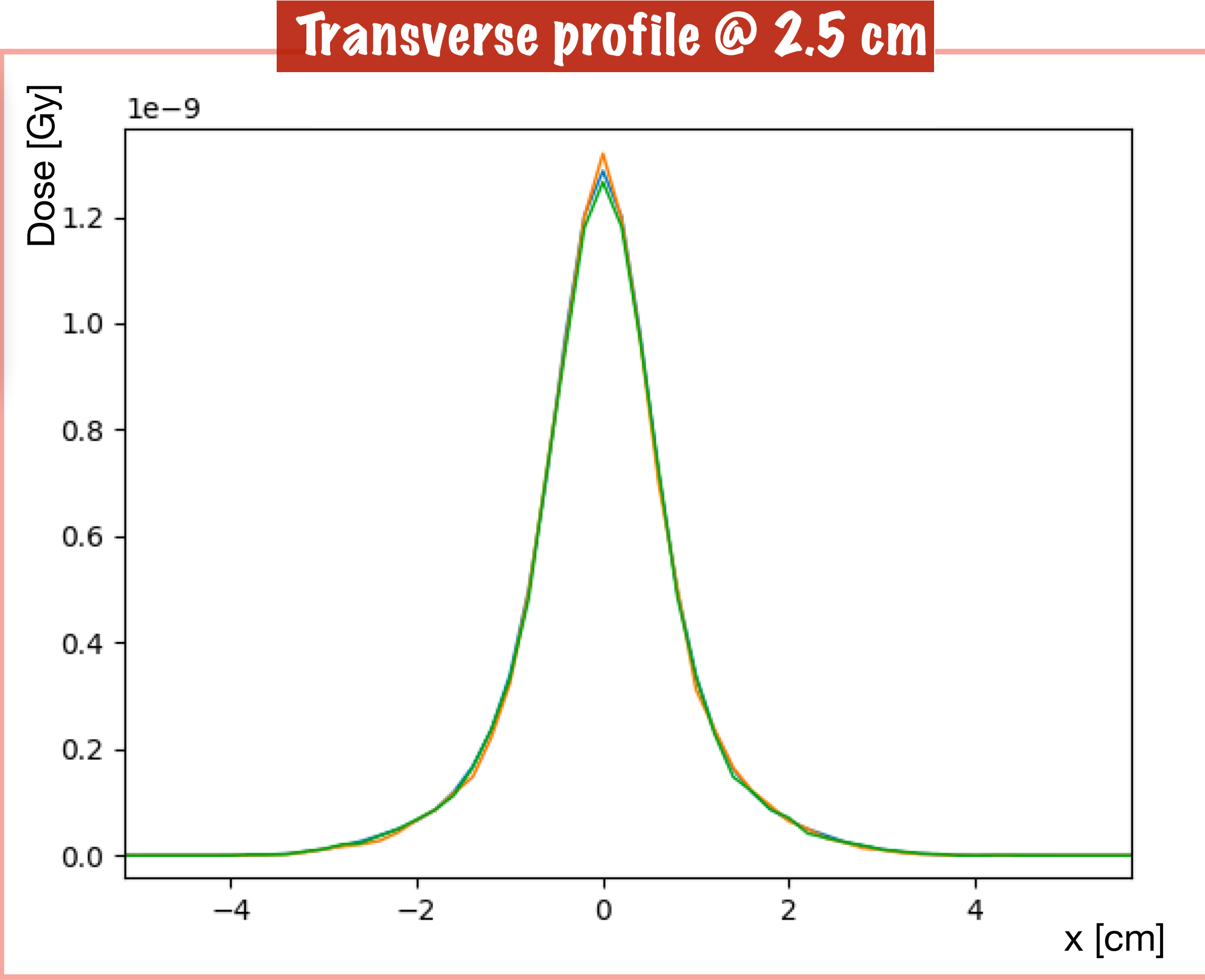
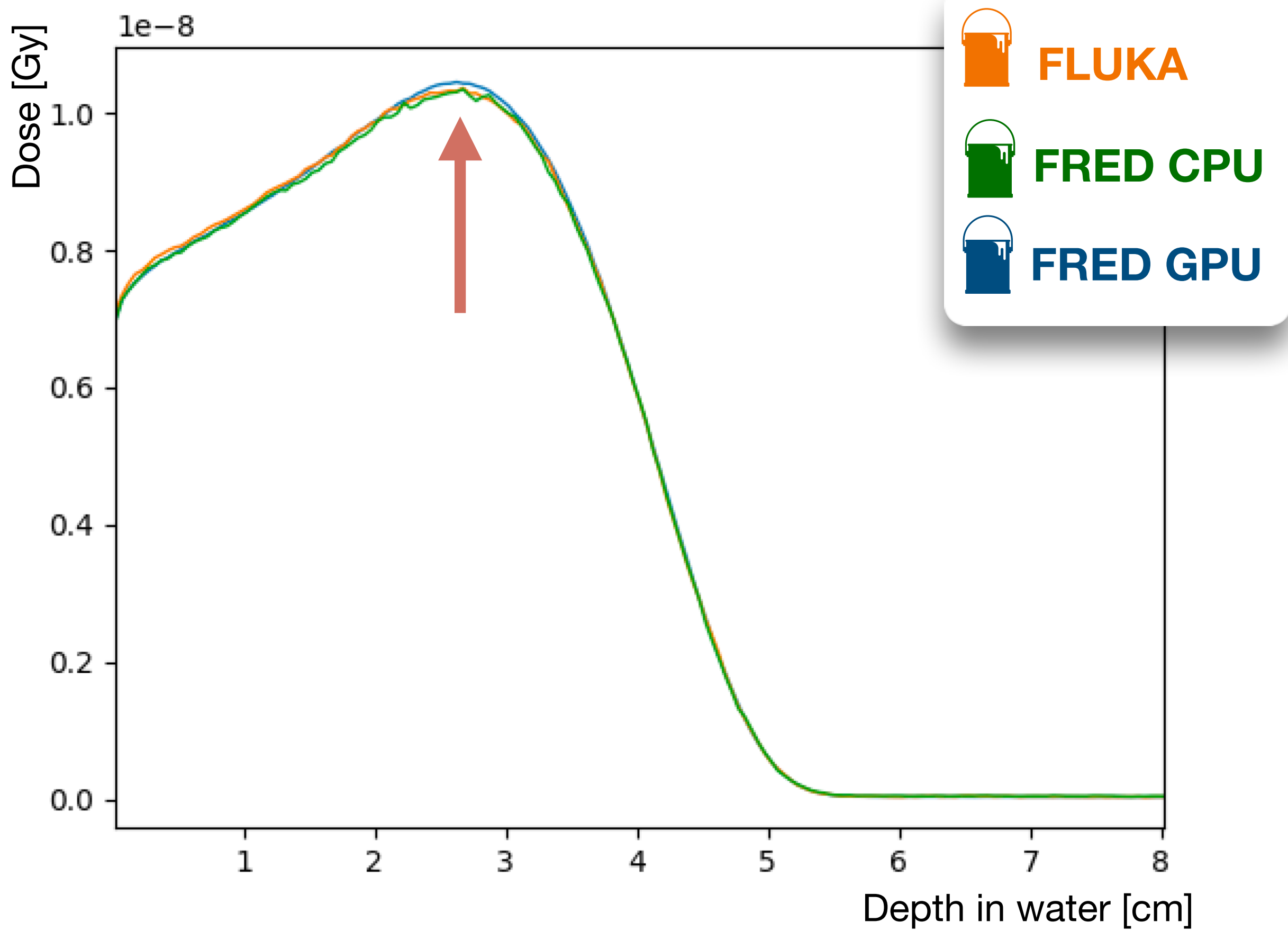
FRED-em performance			
Dose integral	FLUKA	FRED-CPU	FRED-GPU
@ 10 MeV	7.930 · 10 ⁻⁷ Gy/primary	7.889 · 10 ⁻⁷ Gy/primary	7.914 · 10 ⁻⁷ Gy/primary

diff ~ 0.20 %

Thick target benchmark

FRED-em dose

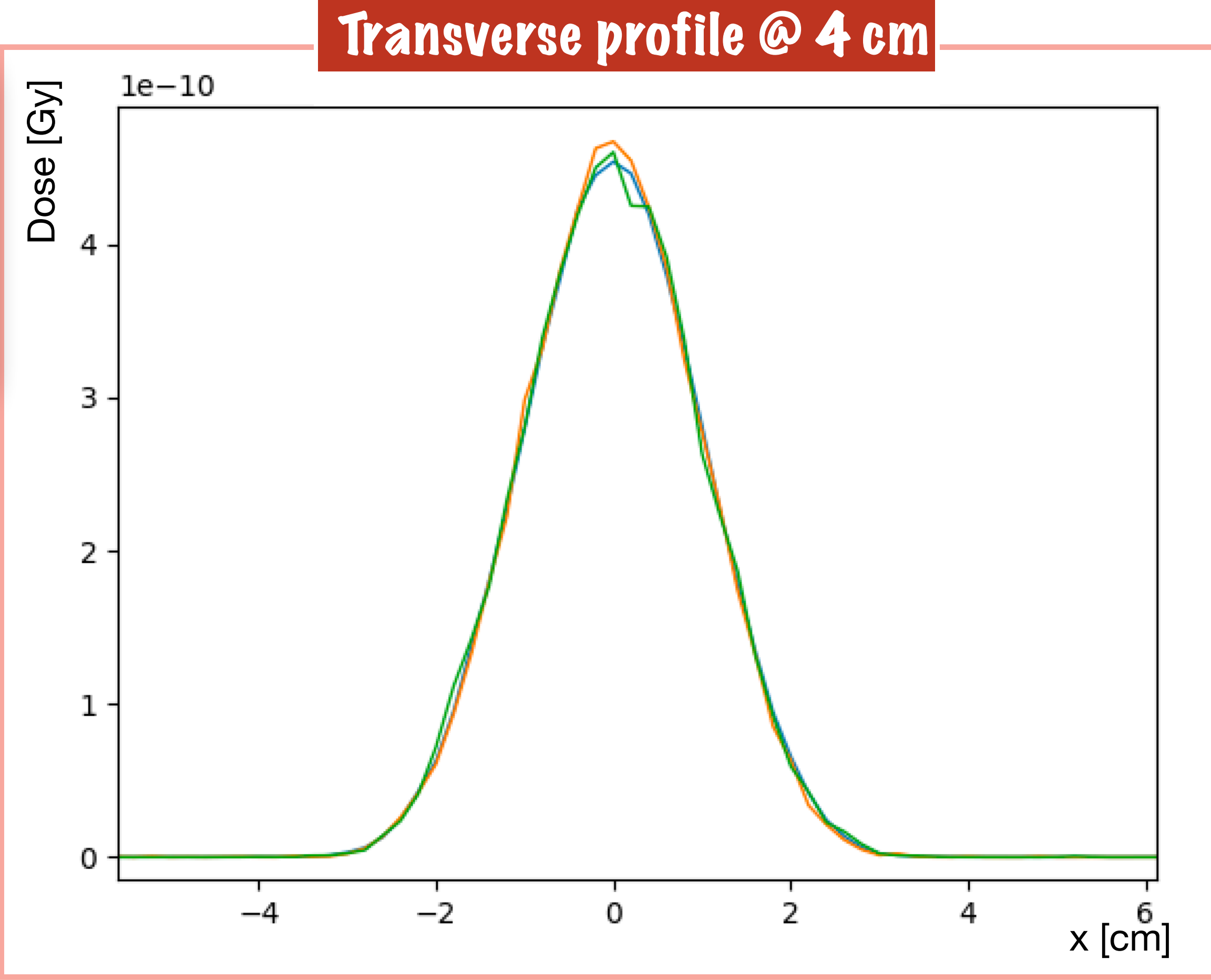
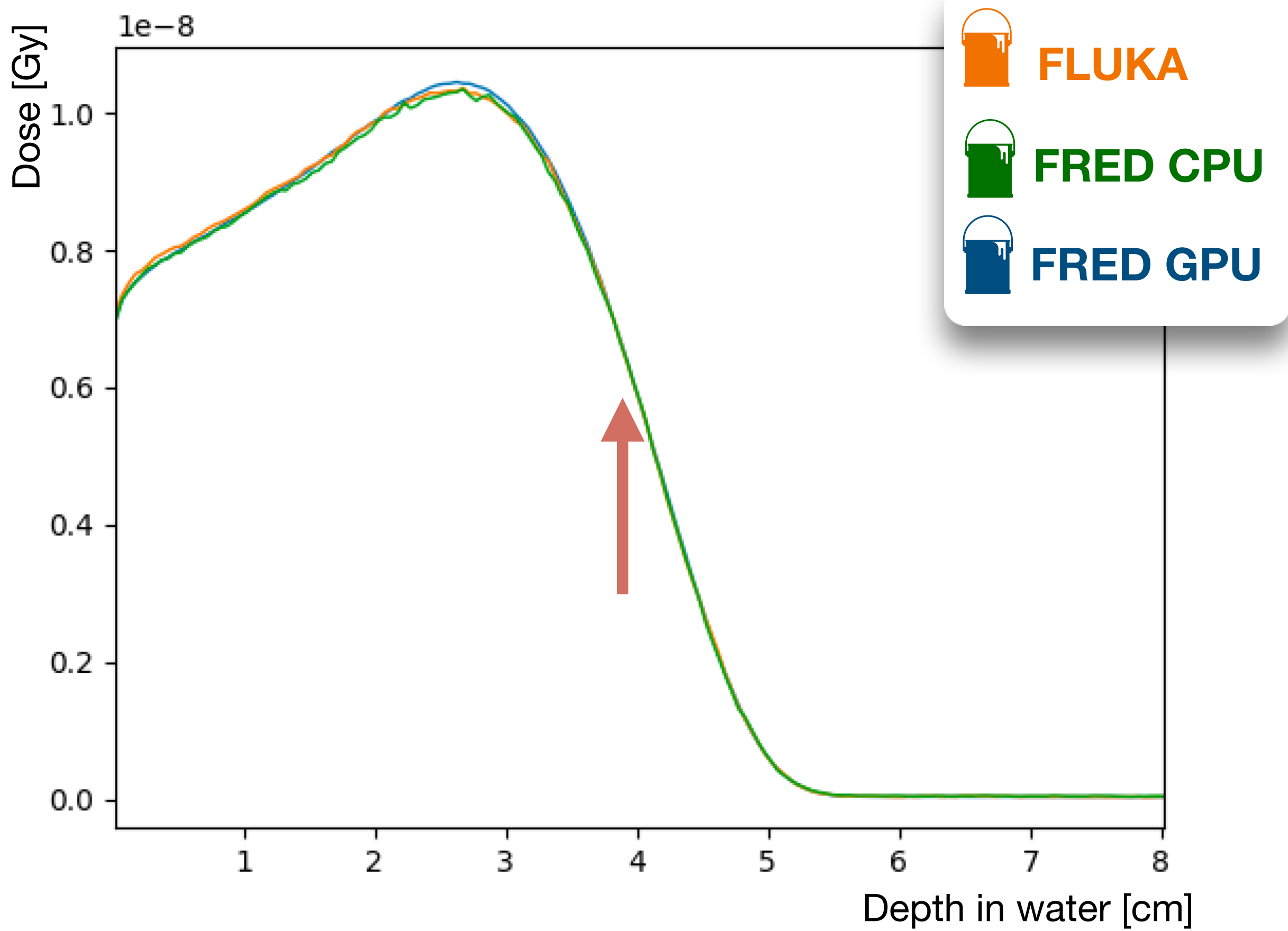
Once I have obtained a successful agreement between the **FLUKA** and **FRED** electromagnetic models, I have checked the **dose distribution** released in different materials in the energy range of **[1-200] MeV**.



Thick target benchmark

FRED-em dose

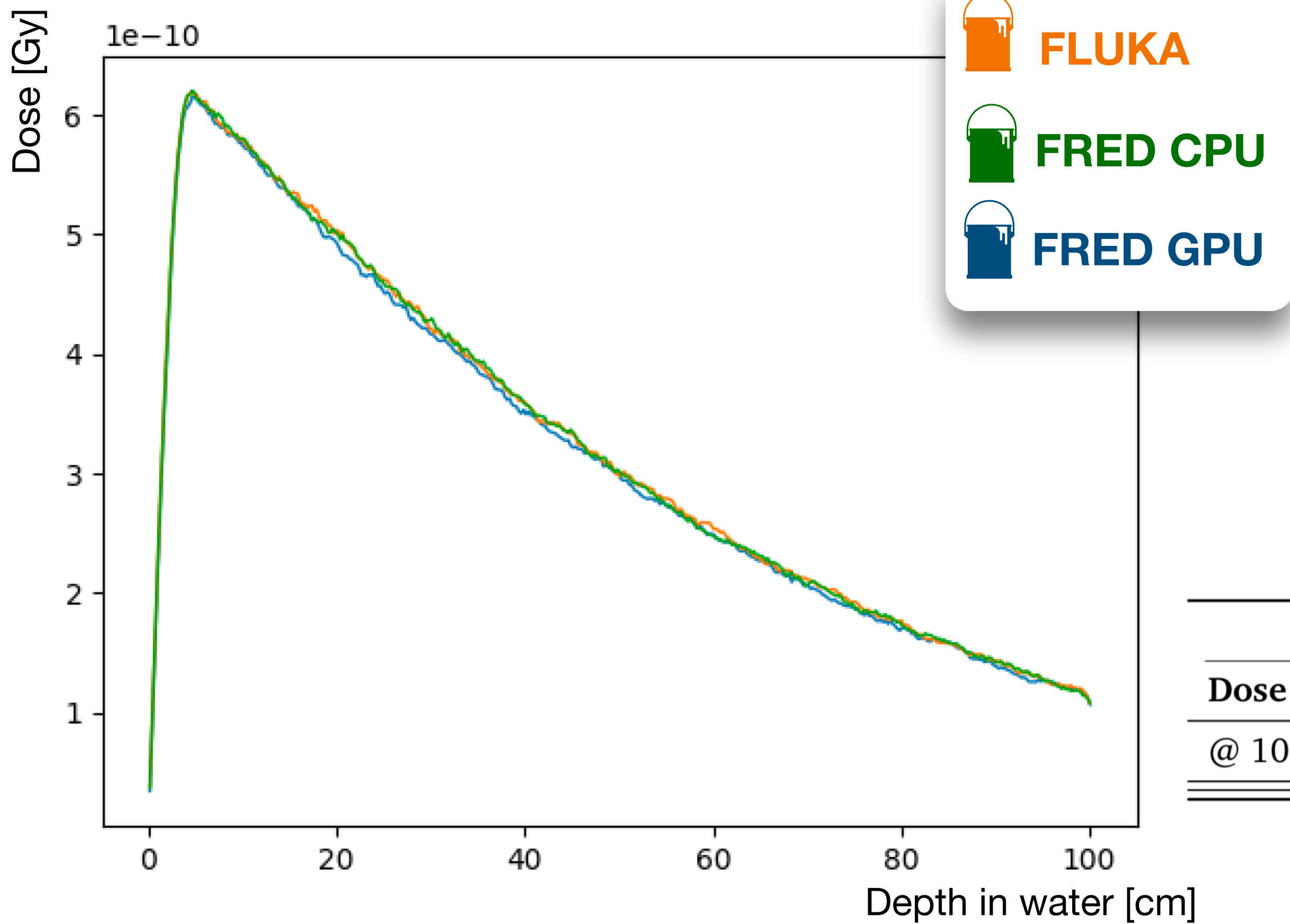
Once I have obtained a successful agreement between the **FLUKA** and **FRED** electromagnetic models, I have checked the **dose distribution** released in different materials in the energy range of **[1-200] MeV**.



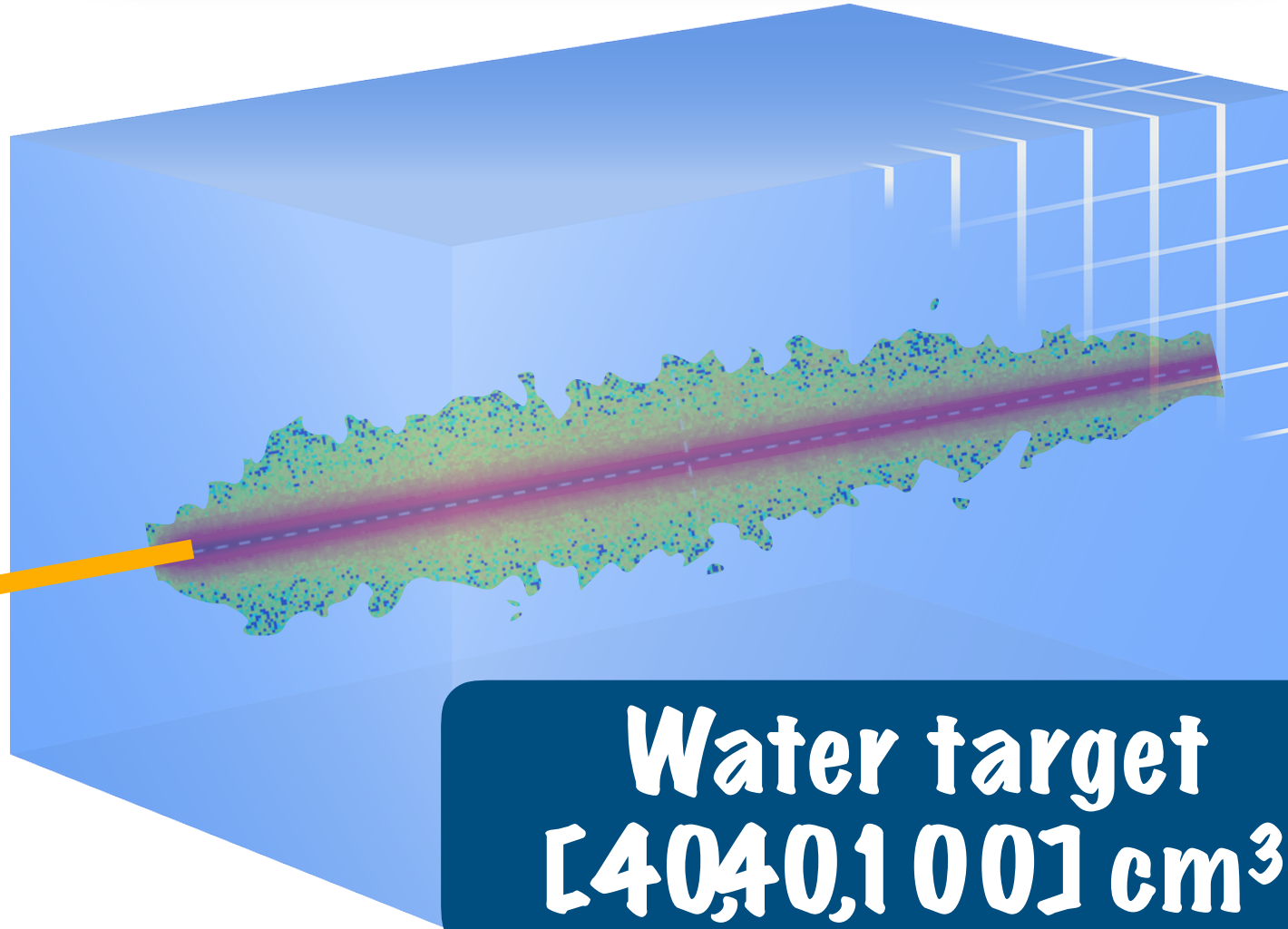
Thick target benchmark

FRED-em dose

Ones I have obtained a successful agreement between the **FLUKA** and **FRED** electromagnetic models, I have checked the **dose distribution** released in different materials in the energy range of **[1-200] MeV**.



1e6 γ at 10 MeV



Water target [40,40,100] cm³

FRED-em performance			
Dose integral	FLUKA	FRED-CPU	FRED-GPU
@ 100 MeV	1.290 · 10 ⁻⁷ Gy/primary	1.288 · 10 ⁻⁷ Gy/primary	1.293 · 10 ⁻⁷ Gy/primary

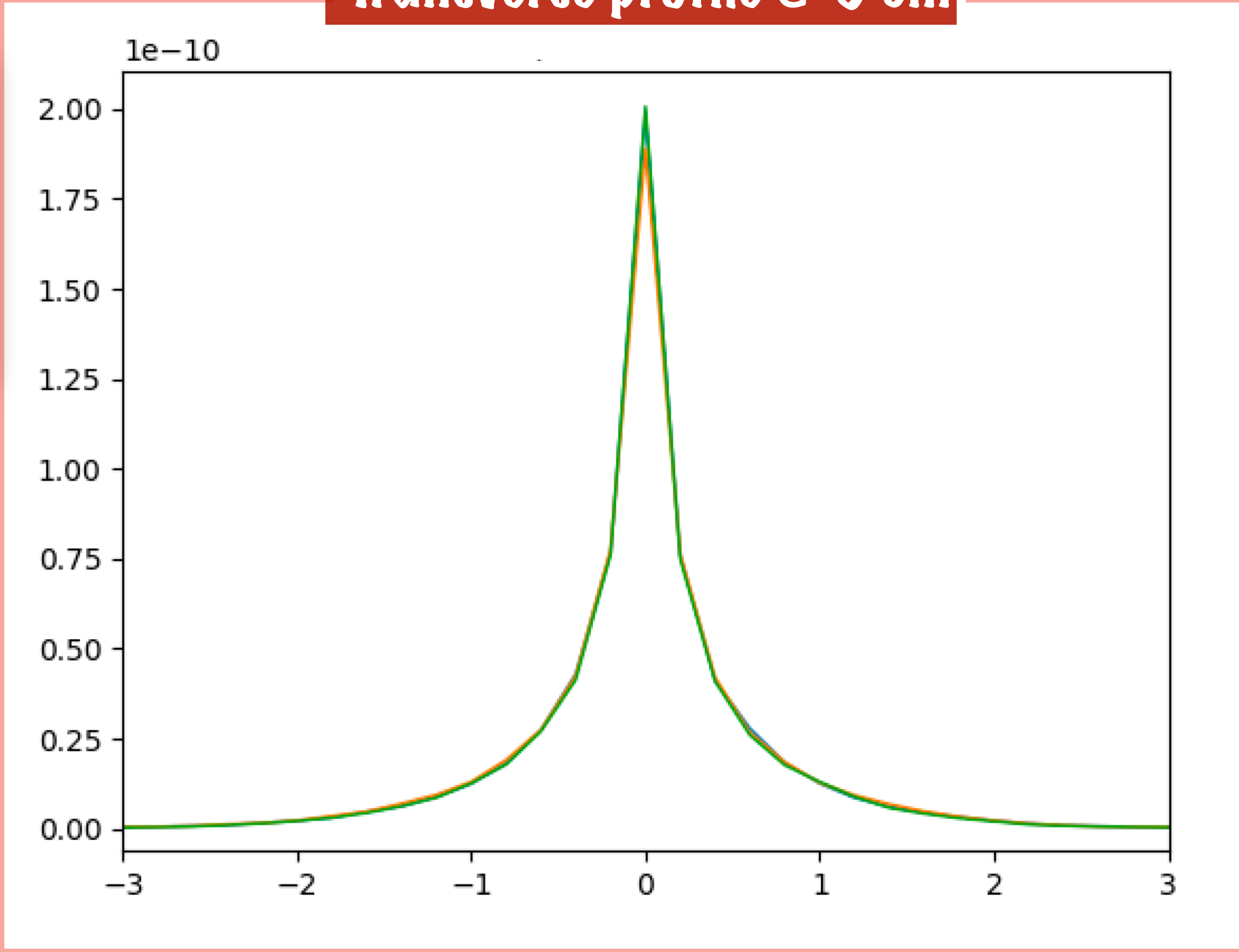
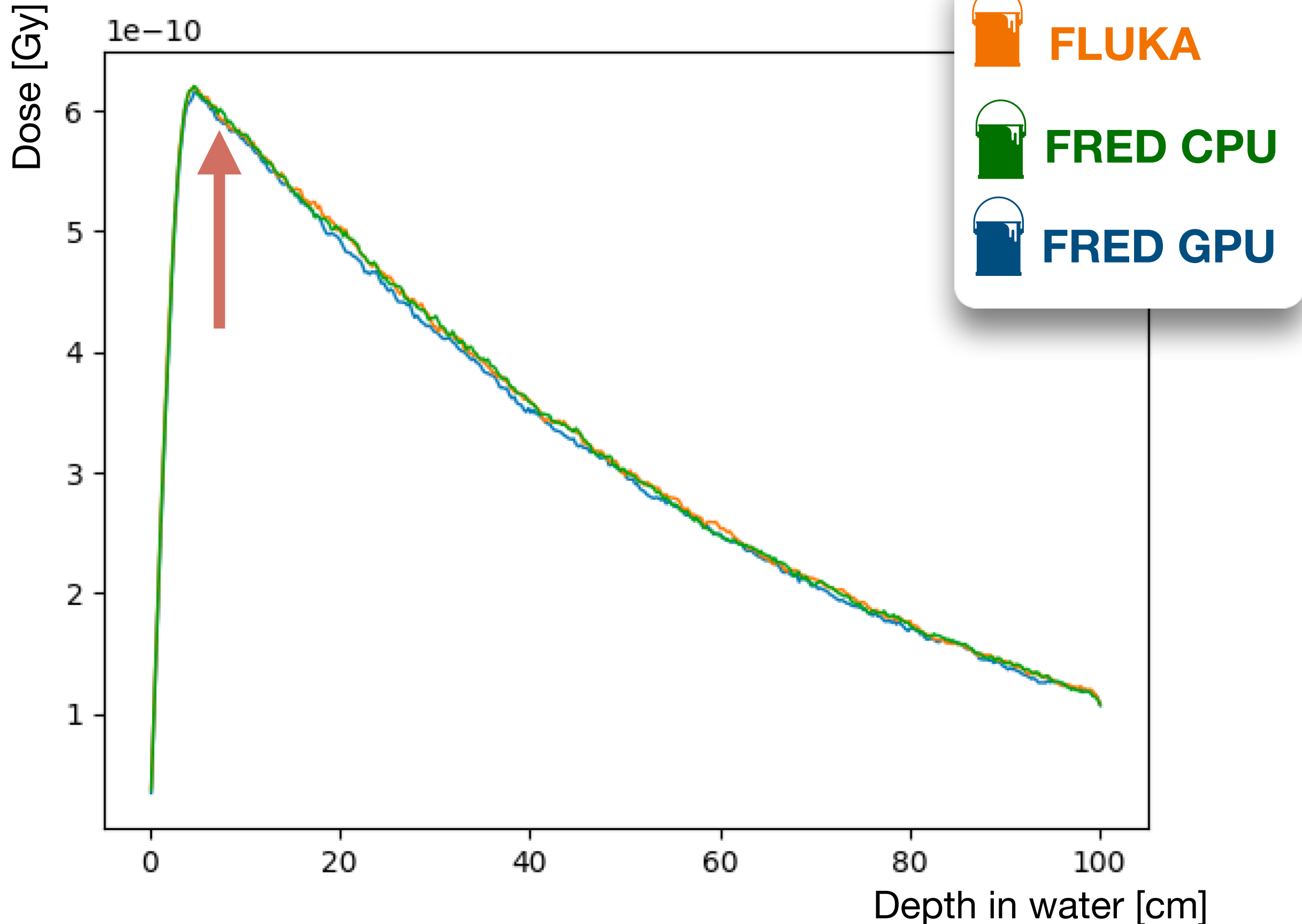
diff ~ 0.23 %

Thick target benchmark

FRED-em dose

Ones I have obtained a successful agreement between the **FLUKA** and **FRED** electromagnetic models, I have checked the **dose distribution** released in different materials in the energy range of **[1-200] MeV**.

Transverse profile @ 5 cm

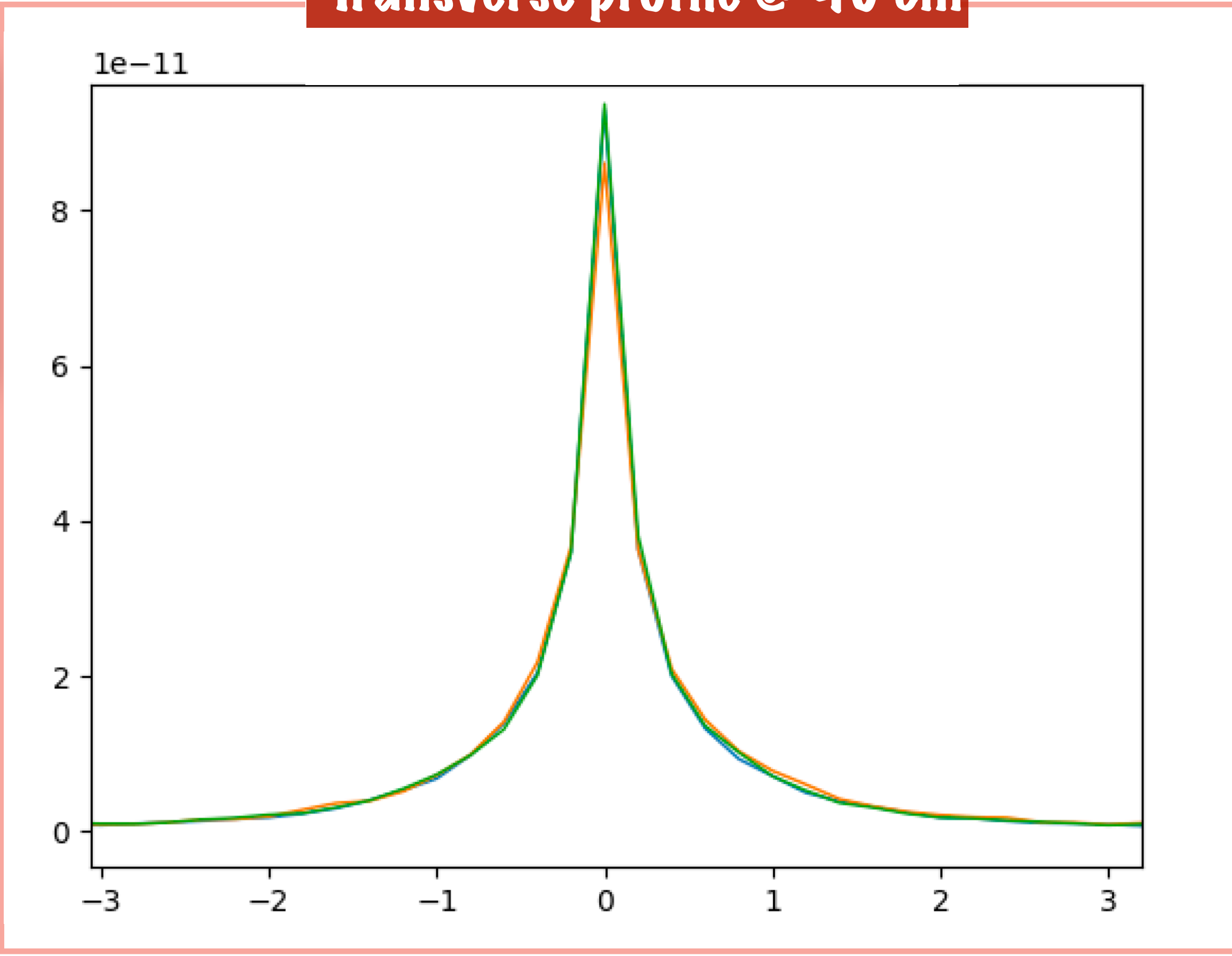
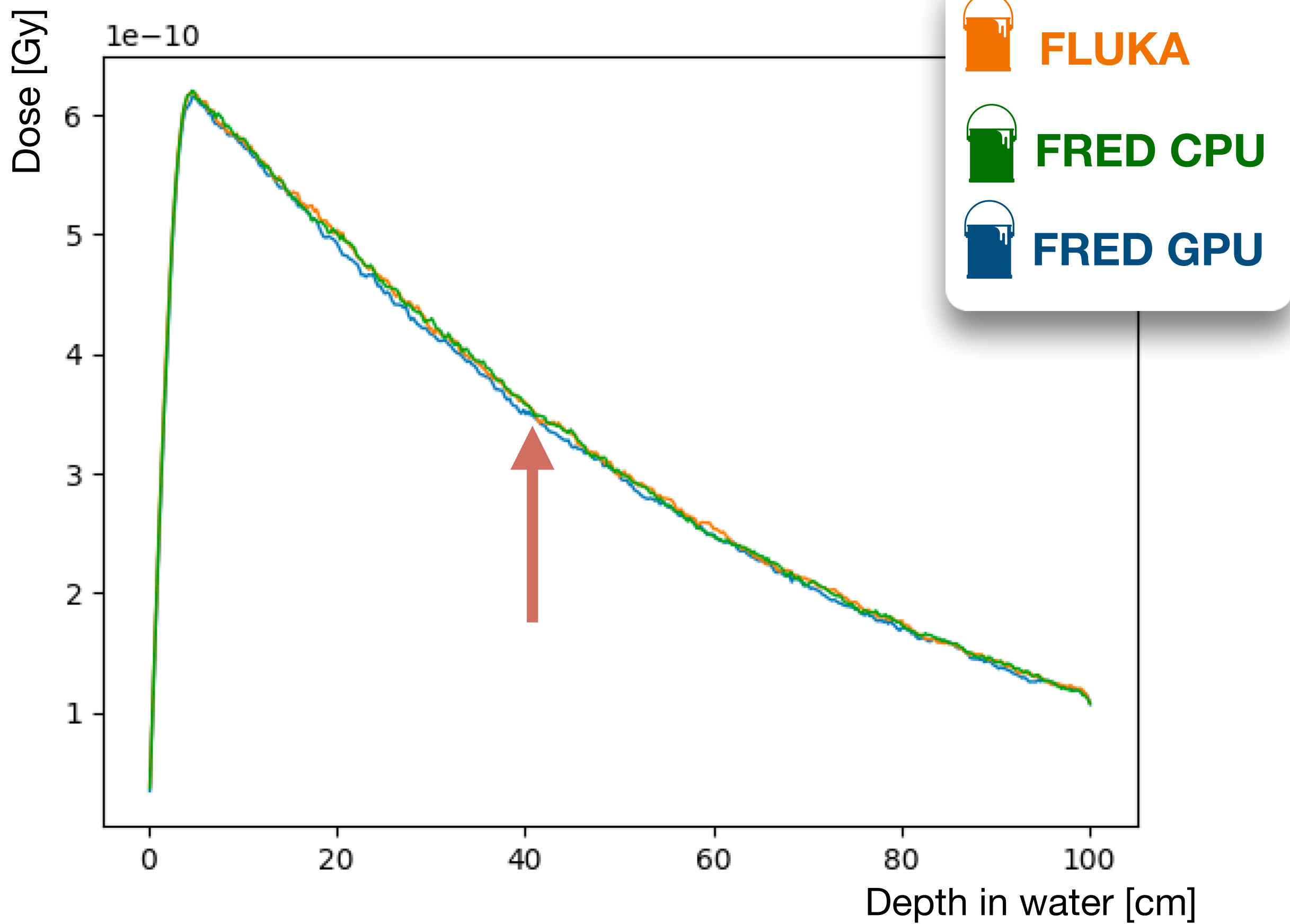


Thick target benchmark

FRED-em dose

Ones I have obtained a successful agreement between the **FLUKA** and **FRED** electromagnetic models, I have checked the **dose distribution** released in different materials in the energy range of **[1-200] MeV**.

Transverse profile @ 40 cm



First FRED-em application



IORT application: NOVAC 11 accelerator

The NOVAC 11 (by Sordina IORT Technologies SpA, Aprilia, Italy) is a linear mobile electron accelerator designed for IORT application:

- Nominal energies: **4, 6, 8** and **10 MeV**;
- Able to treat targets volume with a thickness up to **2.6 cm** inside the 90% isodose;
- The device is able to successfully deliver the full treatment in only 100 seconds (up to **21 Gy at 90% isodose**).

τ_{pulse}

4.5 μs

**Beam
Intensity**

1.5 mA

Dose rate

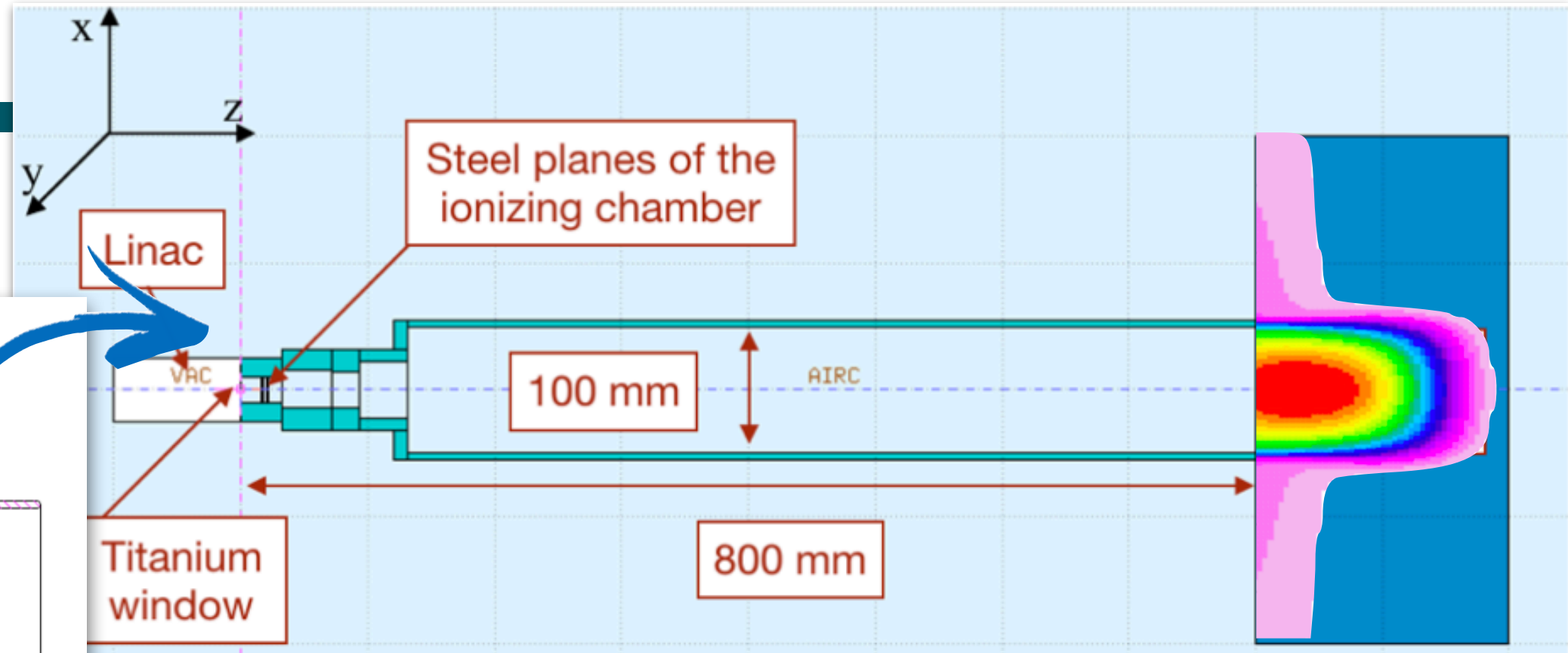
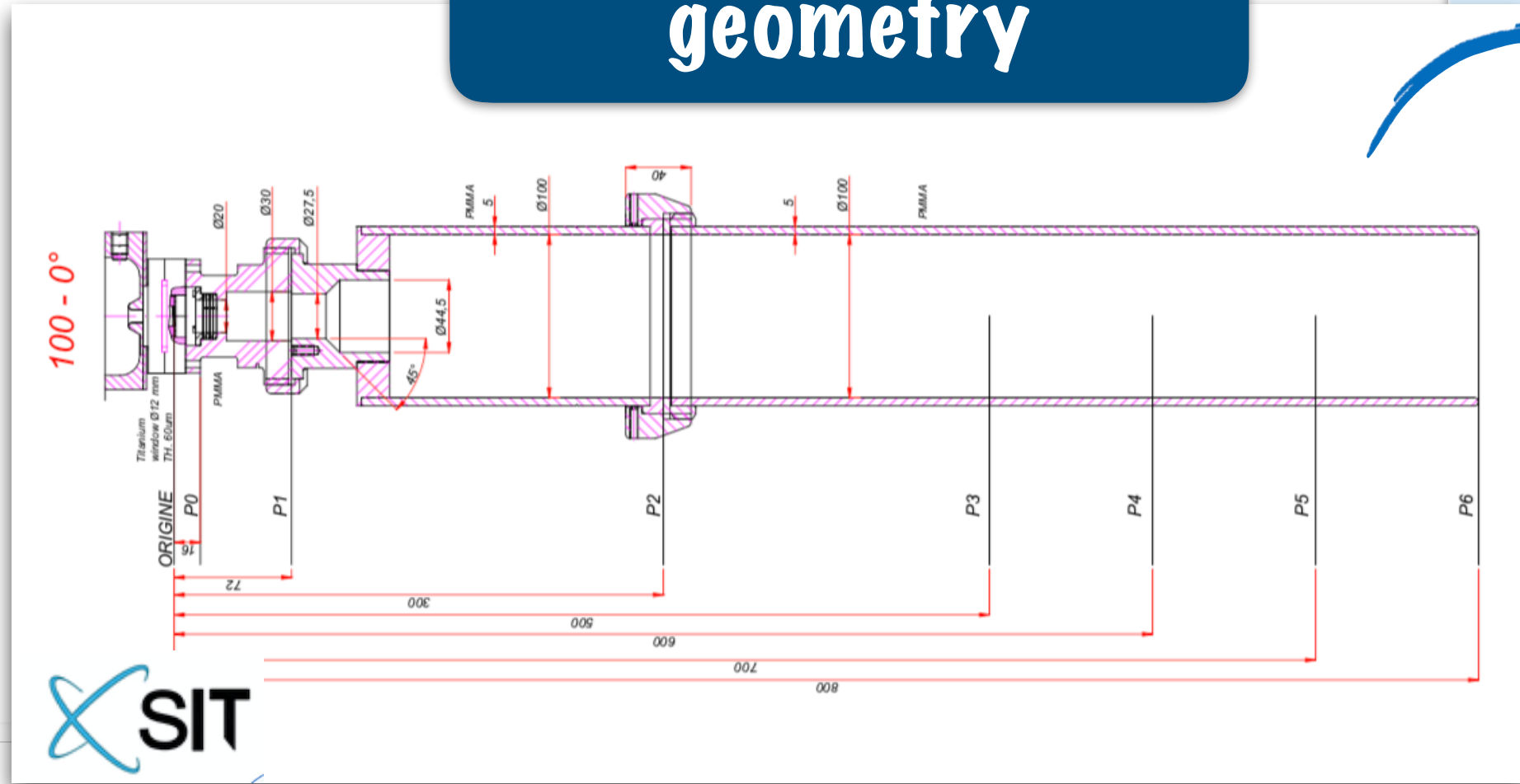
4-30 Gy/min

I used the FRED software to simulated in details the **geometry of the NOVAC 11 and the coupled applicator** in order to **compare the experimental data** of the percentage depth doses (PDDs) and off-axis profiles measured in a water phantom.

First FRED-em application

FRED-em simulation

FRED applicator geometry



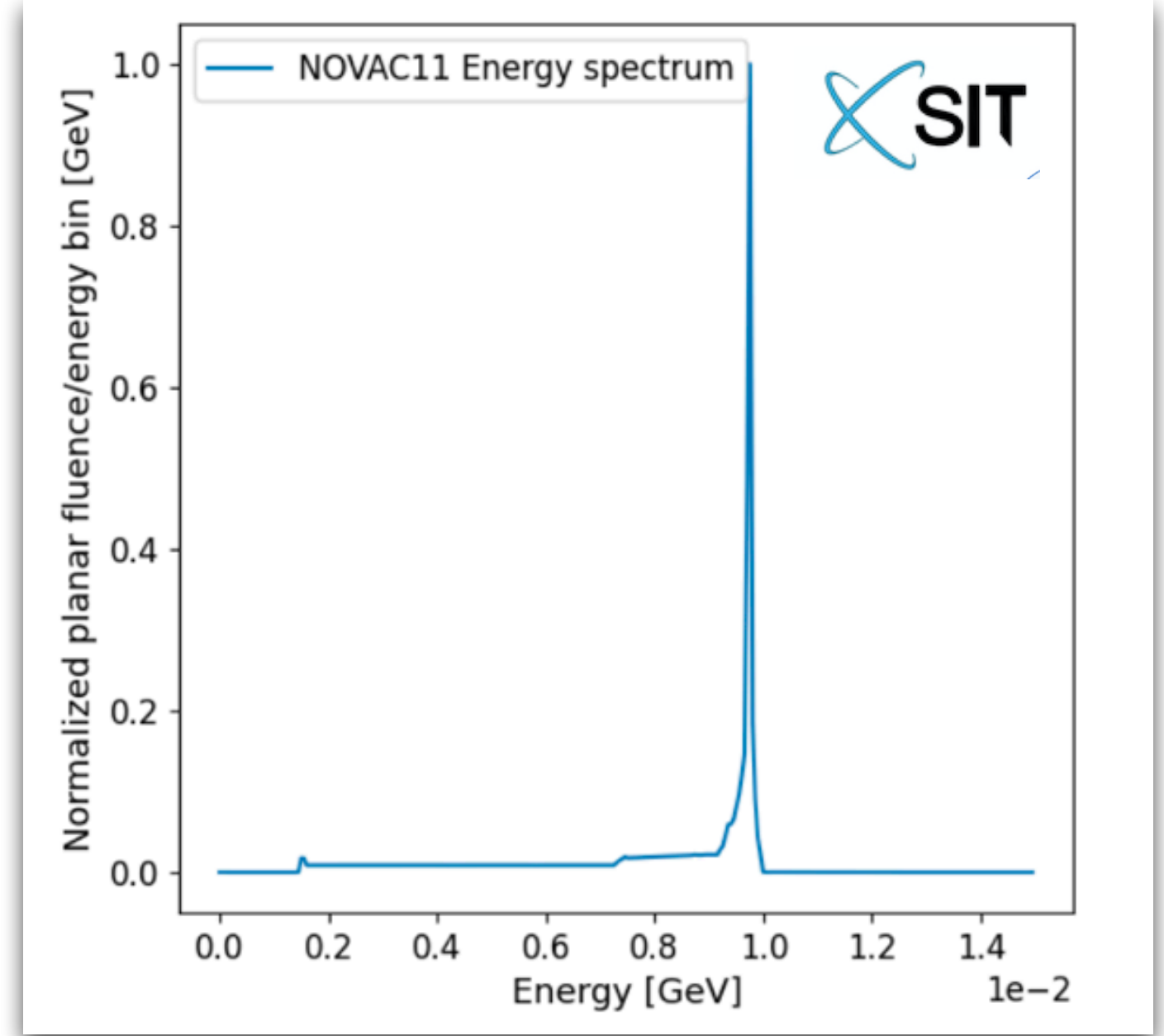
Energy spectrum @ linac exit

GEOMETRY:

- 1. **PMMA cylinders** with different diameters (from 20 to 100 mm)
- 2. Source-to-Skin Distance (**SSD**)=**80 cm**
- 3. **Titanium window (55 μm)**
- 4. **4 steel planes** of the ionizing chamber (**20 μm** each)

SIMULATION PARAMETERS:

- 1. **10 MeV** electrons beam;
- 2. Gauss section with **FWHM=0.13 cm**;
- 3. Transport and production energy cut = **10 keV**



First FRED-em application

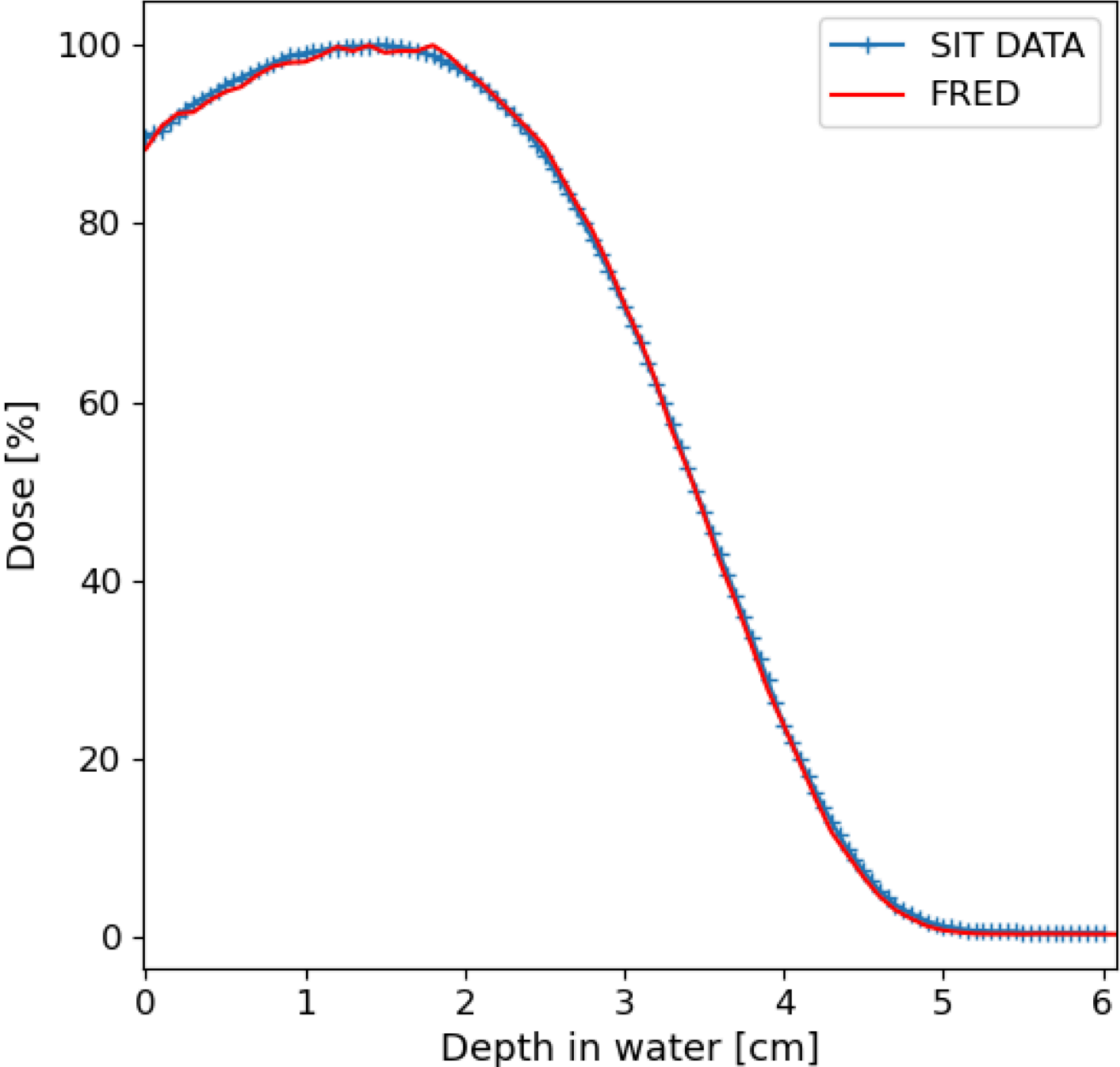
The experimental setup for relative dosimetry, i.e. PDDs and off-axis profiles measurements consisted of a 3D motorized water phantom equipped with an unshielded diode.

For the MC simulation the absorbed dose is evaluated on a water target with a transverse area of $2 \times 2 \text{ mm}^2$, corresponding to the sensitive area of the adopted diode

Gamma index 3mm/3% pass-rate 98.1%



Clinical acceptance >96%



First FRED-em application

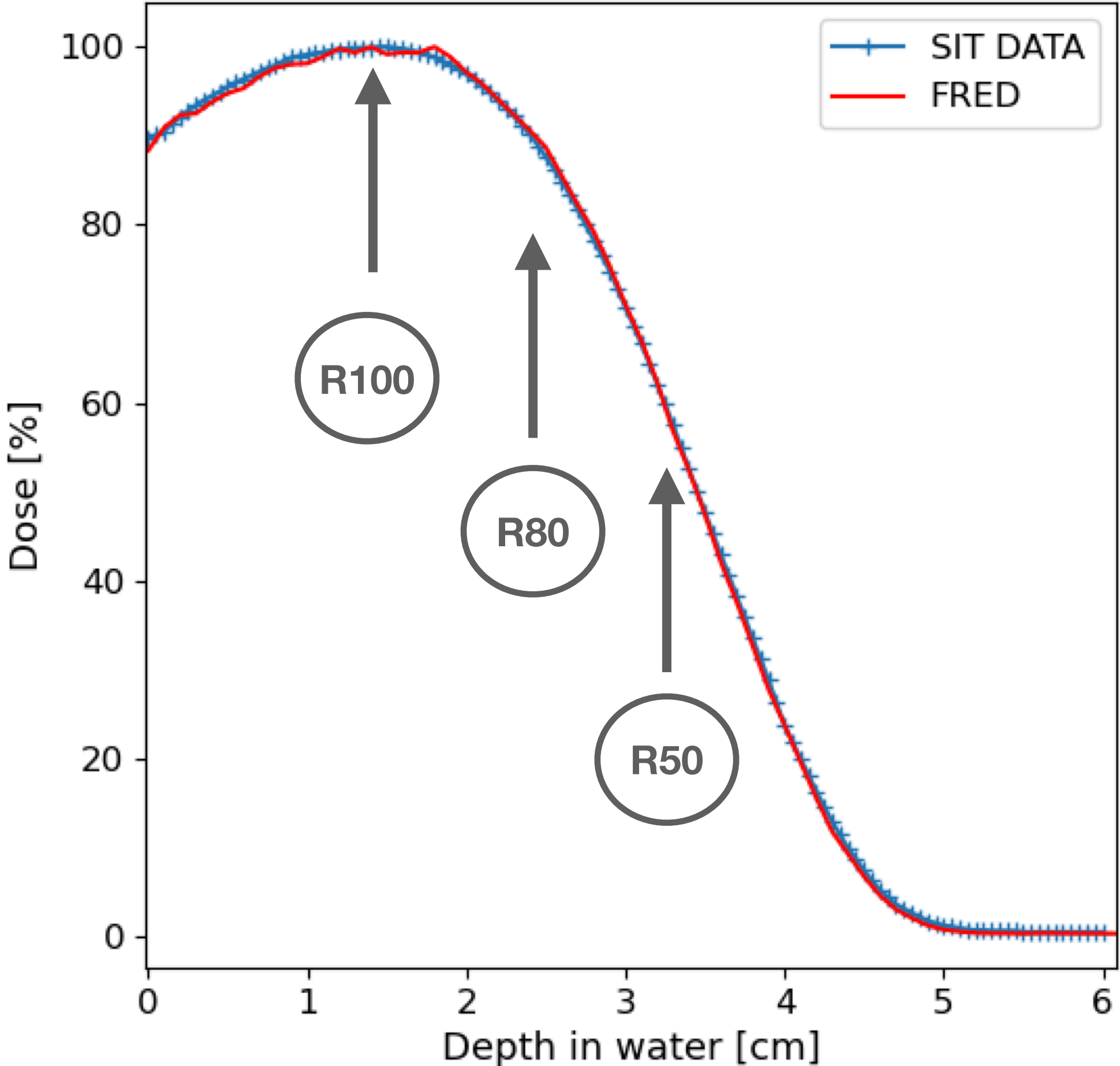
The experimental setup for relative dosimetry, i.e. PDDs and off-axis profiles measurements consisted of a 3D motorized water phantom equipped with an unshielded diode.

For the MC simulation the absorbed dose is evaluated on a water target with a transverse area of $2 \times 2 \text{ mm}^2$, corresponding to the sensitive area of the adopted diode

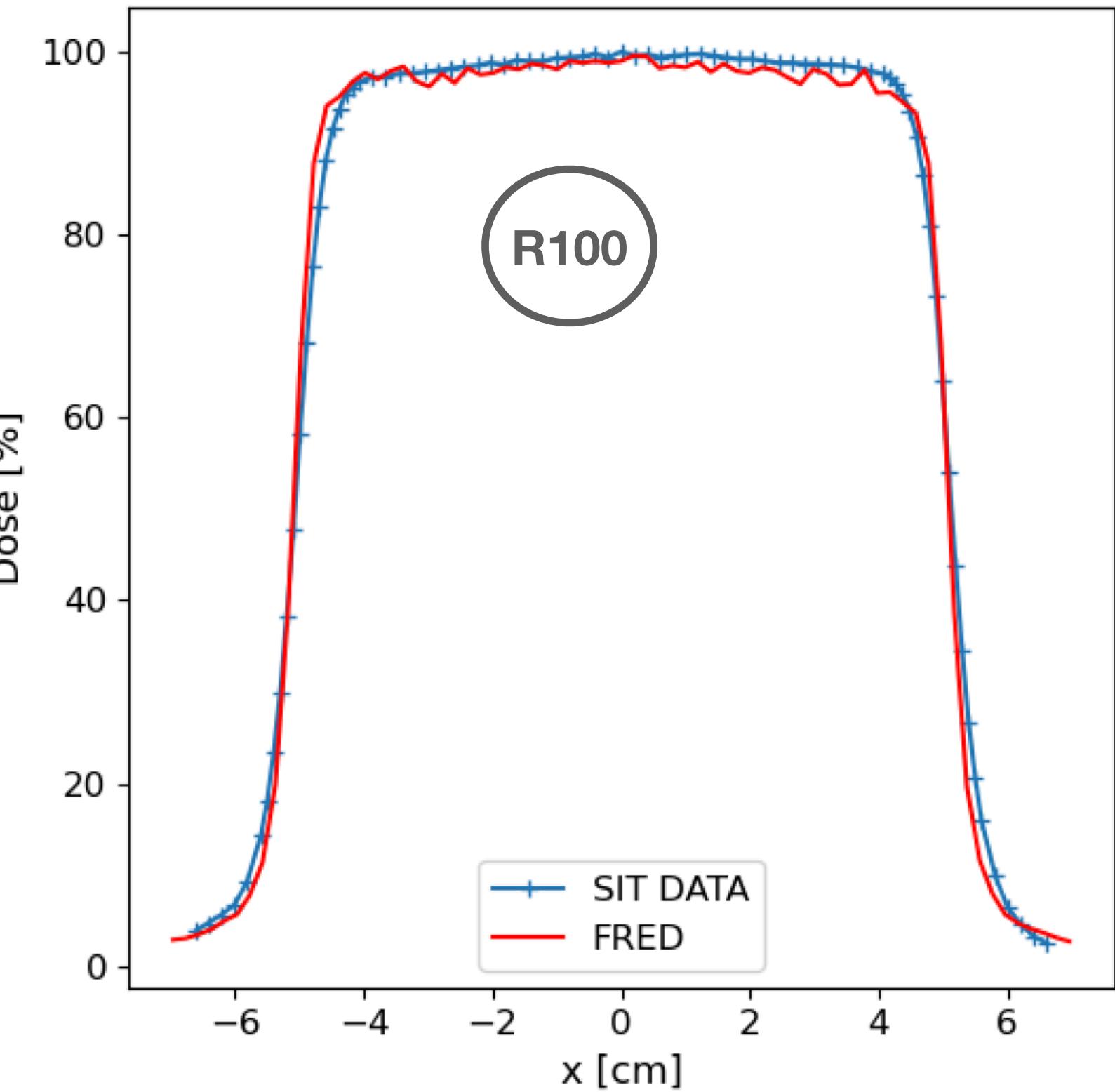
Gamma index 3mm/3% pass-rate 98.1%



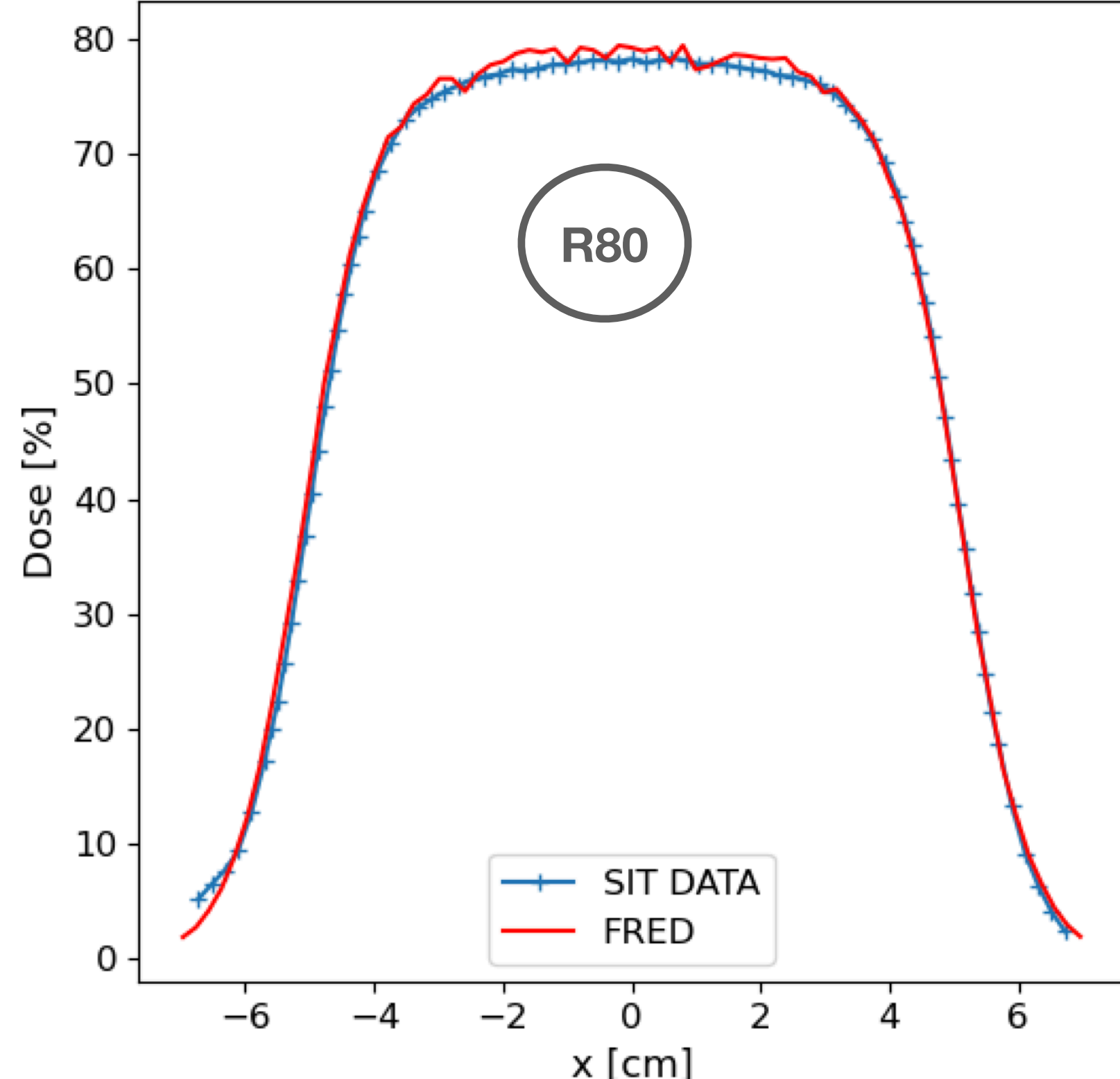
Clinical acceptance >96%



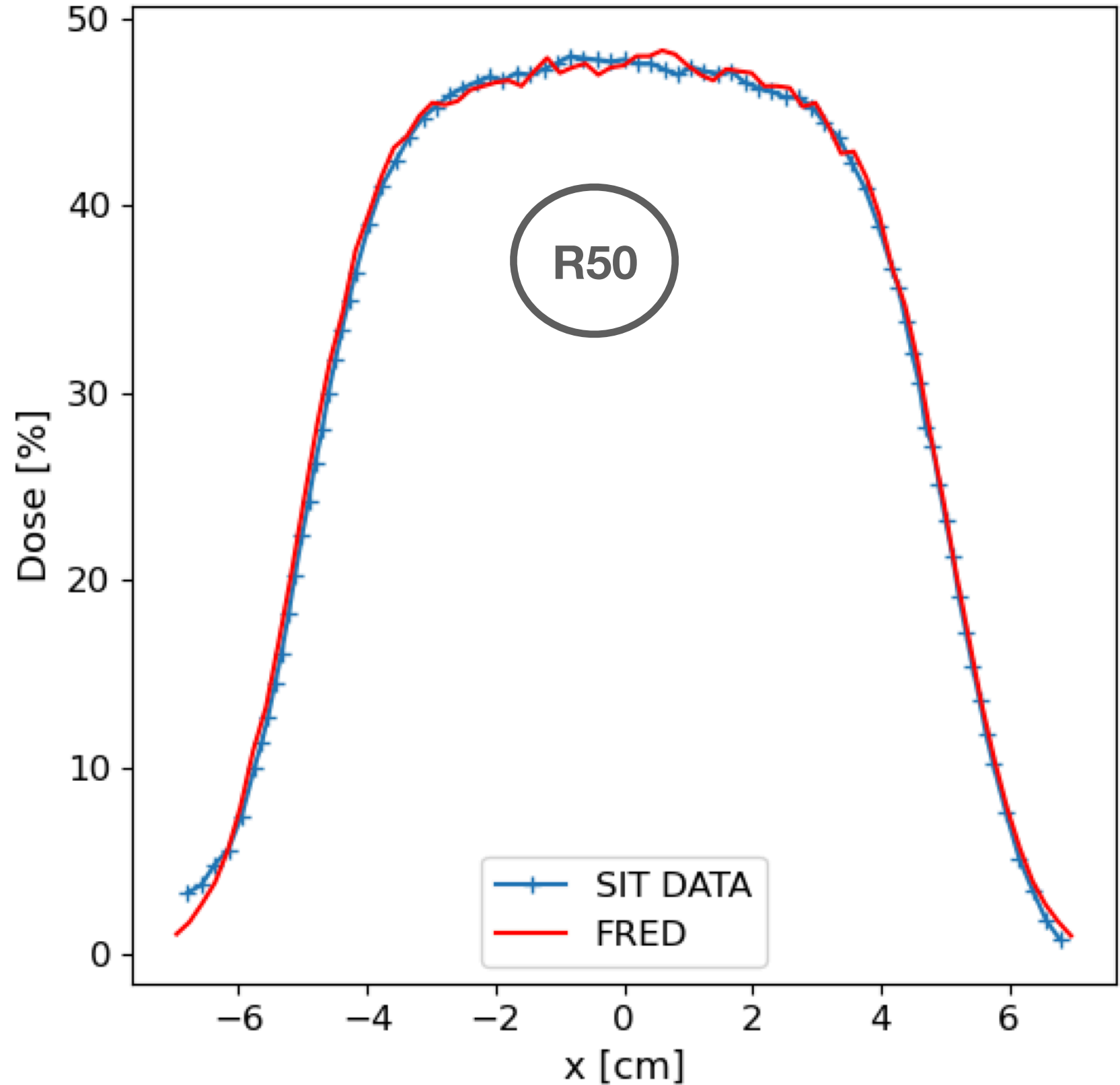
First FRED-em application



Gamma index 3mm/3% pass-rate
84.6%



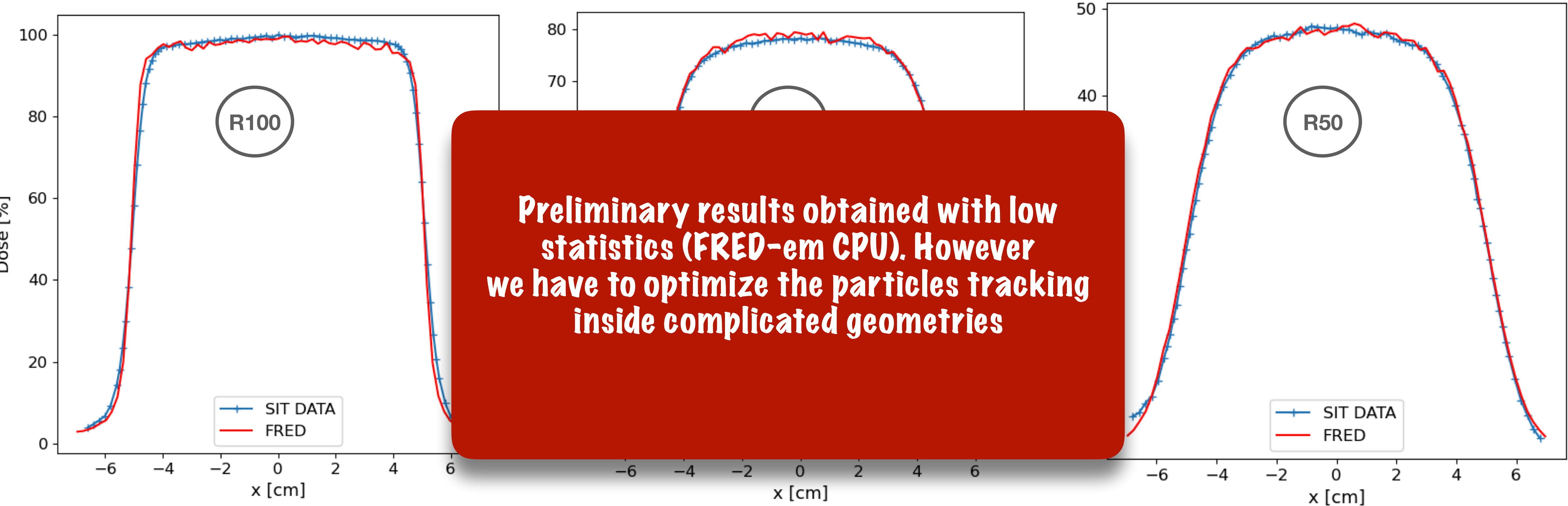
Gamma index 3mm/3% pass-rate
75.3%



Gamma index 3mm/3% pass-rate
82.4%



First FRED-em application



Gamma index 3mm/3% pass-rate
84.6%



Gamma index 3mm/3% pass-rate
75.3%



Gamma index 3mm/3% pass-rate
82.4%



Porting on GPU: preliminary timing performance

Now I'm working on FRED's **porting on GPU**. Exploiting the parallel programming power of GPU architectures, FRED is now capable of tracking millions of primary particles per second on a single GPU card.

The preliminary observed gain in processing time, when comparing to the FLUKA full MC, depending on the energy of the primary beam is here reported .



PRELIMINARY

Tracking rate	Timing performance		
	FLUKA	FRED-CPU	FRED-GPU
@ 1 MeV	$5 \cdot 10^3$ primary/s	$2.5 \cdot 10^3$ primary/s	$6.5 \cdot 10^5$ primary/s
@ 10 MeV	$1 \cdot 10^3$ primary/s	$5 \cdot 10^2$ primary/s	$1.5 \cdot 10^5$ primary/s
@ 100 MeV	$4 \cdot 10^2$ primary/s	$1.3 \cdot 10^2$ primary/s	$2.3 \cdot 10^4$ primary/s

The level of accuracy is driven by the number of primaries AND by the imaging capability.

Preliminary TPS exercise: $1e8$ primary electrons at 10 MeV

Computational time	Rude TPS timing performance			
	FLUKA 1 CORE	FLUKA 5 CORE	FRED-GPU 1 CORE	FRED-GPU 5 CORE
$1e8$ primaries	~ 27 hours	~ 6 hours	~ 16 minutes	~ 3 minutes

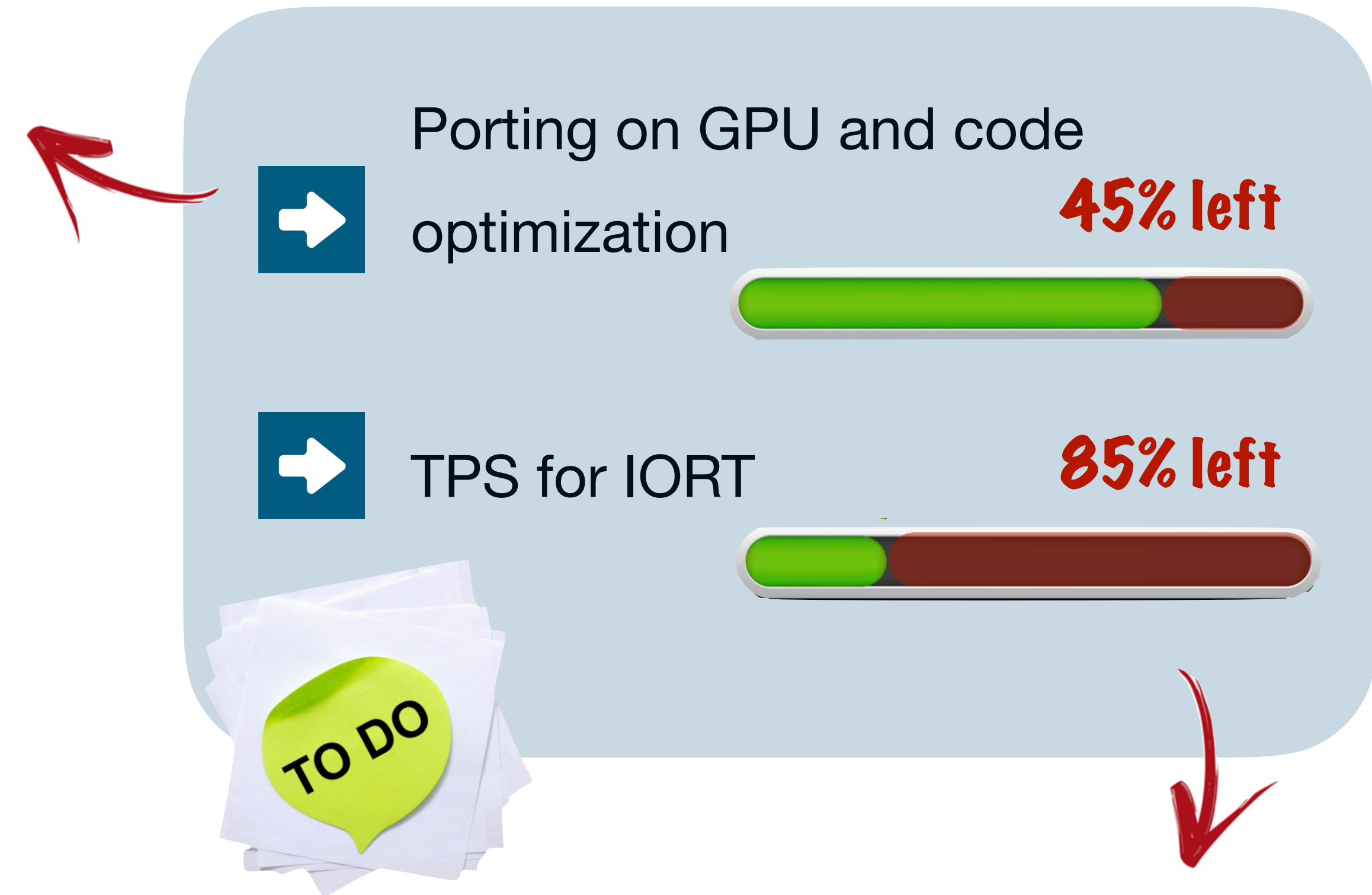
What's next?

With the present electromagnetic models we have obtained promising results but we want to **optimize the em-code** in order to reduce the differences in the dose profiles.

- While porting the FRED-em code on GPU, profiting from the reduced computational time, I will perform different tests to verify the model:

In this phase a **benchmark** against other MC tools such as **GEANT4** or against **experimental data** will be necessary to test and validate our em-model.

- The FRED-em timing performance here reported is preliminary: I have to optimize the **computational timing performance**.



- Starting from the implemented NOVAC 11 simulation, I will investigate the feasibility of developing a TPS for IORT treatments.

Thanks for your attention!



Attended Conferences

- [a] **FOOT experiment (FragmentatiOn Of Target)**, Poster Presentation, 10th Young Researcher Meeting, 18th-21st June 2019, Rome, Italy.
- [b] **Margarita: GSI operation and developments**, Oral Presentation, VI FOOT General Meeting at CNAO (Centro Nazionale di Adroterapia Oncologica), 5th-7th June 2019, Pisa, Italy.
- [c] **Monte Carlo Simulation of an electron beam generated by a mobile iort accelerator**, Poster Presentation, SIRR 2020, XIX Congresso Nazionale (ONLINE) , 10th-12th November 2020, Rome, Italy.
- [d] **Prostate cancer FLASH therapy treatments with electrons of high energy: a feasibility study**, Oral Presentation, PTCOG 59 Annual Conference of the Particle Therapy Co-operative Group (ONLINE) , 4th-7th June 2021, Rome, Italy.
- [e] **Measurements of ¹⁶O fragmentation cross sections on C target with the FOOT apparatus**, Poster Presentation, PTCOG 59 Annual Conference of the Particle Therapy Co-operative Group (ONLINE) , 4th-7th June 2021, Rome, Italy.
- [f] **Inter-fractional monitoring in Particle Therapy treatments with ¹²C ions exploiting the detection of charged secondary particles**, Oral Presentation, ANPC Applied Nuclear Physics Conference 12th-17th September 2021, Prague, Czech Republic.

Publications

- [1] Pellegrini R. et al, *Novel gamma tracker for rapid radiation direction detection for UAV drone use*. Paper presented at the 2019 IEEE Nuclear Science Symposium and Medical Imaging Conference, NSS/MIC 2019, DOI:10.1109/NSS/MIC42101.2019.9059630 (2019)
- [2] M. Fischetti et al, *Inter-fractional monitoring of ¹²C ions treatments: results from a clinical trial at the CNAO facility*, Scientific Reports, 10(1) DOI:10.1038/s41598-020-77843-z (2020).
- [3] M. Toppi et al, *The MONDO Tracker: Characterisation and Study of Secondary Ultrafast Neutrons Production in Carbon Ion Radiotherapy*, Frontiers in Physics, 8 DOI:10.3389/fphy.2020.567990 (2020).
- [4] F. Collamati et al, *Stability and efficiency of a CMOS sensor as detector of low energy β and γ particles*, Journal of Instrumentation, 15(11) DOI:10.1088/1748-0221/15/11/P11003 (2020).
- [5] G. Traini et al, *Performance of the ToF detectors in the foot experiment*, Nuovo Cimento Della Societa Italiana Di Fisica C, 43(1). DOI:10.1393/ncc/i2020-20016-5 (2020).
- [6] E. Fiorina et al, *Detection of interfractional morphological changes in proton therapy: A simulation and in vivo study with the INSIDE in-beam PET* Frontiers in Physics, 8. DOI:10.3389/fphy.2020.578388 (2021)
- [7] G. Battistoni E. et al, *Measuring the Impact of Nuclear Interaction in Particle Therapy and in Radio Protection in Space: the FOOT Experiment*, Frontiers in Physics, 8. DOI:10.3389/fphy.2020.568242 (2021)
- [8] M. Toppi et al, *PAPRICA: The pair production imaging Chamber—Proof of principle*. Frontiers in Physics, 9. DOI:10.3389/fphy.2021.568139 (2021)
- [9] A.C. Kraan et al, *Charge identification of nuclear fragments with the FOOT time-of-flight system*. Nuclear Instruments and Methods in Physics Research, Section A: Accelerators, Spectrometers, Detectors and Associated Equipment, 1001. DOI:10.1016/j.nima.2021.165206 (2021)
- [10] L. Faillace et al., *Compact S-band Linear Accelerator System for FLASH Radiotherapy*. Physical Review Accelerators and Beams (2021). DOI: 10.1103/PhysRevAccelBeams.24.050102
- [11] S. Colombi et al., *Enhancing the understanding of fragmentation processes in hadrontherapy and radioprotection in space with the FOOT experiment*. Physica Scripta, 2021, 96(11), 114013 DOI: <https://doi.org/10.1088/1402-4896/ac186b>
- [12] M. Toppi et al., *Monitoring Carbon Ion Beams Transverse Position Detecting Charged Secondary Fragments: Results From Patient Treatment Performed at CNAO*. Frontiers in Oncology, 2021, 11, 601784 DOI: 10.3389/fonc.2021.601784
- [13] G. Galati et al., *Charge identification of fragments with the emulsion spectrometer of the FOOT experiment*. Open Physics, 19(1), 383-394. DOI:10.1515/phys-2021-0032.

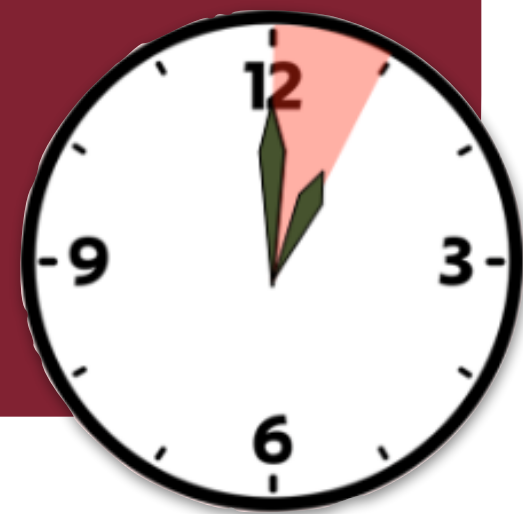
SPARE SLIDES

From full to fast Monte Carlo

ANALYTICAL ALGORITHMS

- Reasonable times for calculating the TPS
- Simplified representation of the tissue: the geometry of the patient is represented in an equivalent volume of water, neglecting the real atomic composition of the tissues.
- Not high accuracy**

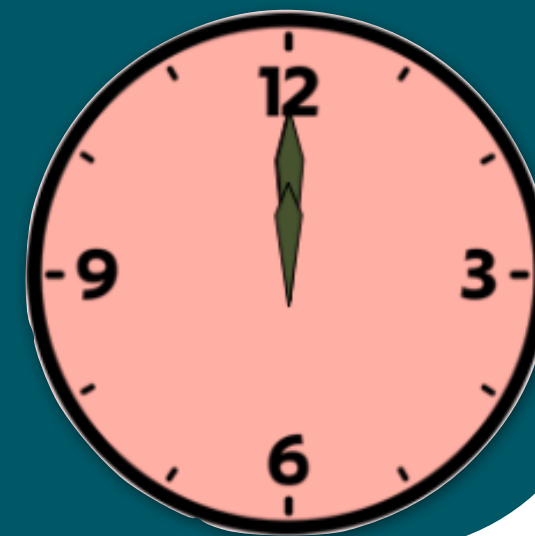
Ex. Proton TPS
~ 1 h/core



MONTE CARLO

- Realistic assessment of body composition
- Extracts accuracy in the description of the transport and the interaction of the particles with matter
- Long times for calculating the TPS**

Ex. Proton TPS
~ days/core



FAST MONTE CARLO

- High accuracy in the description of the transport and of the interaction of particles with matter
- Realistic assessment of body composition
- Very fast calculation of TPS**

Ex. Proton TPS
~ minutes



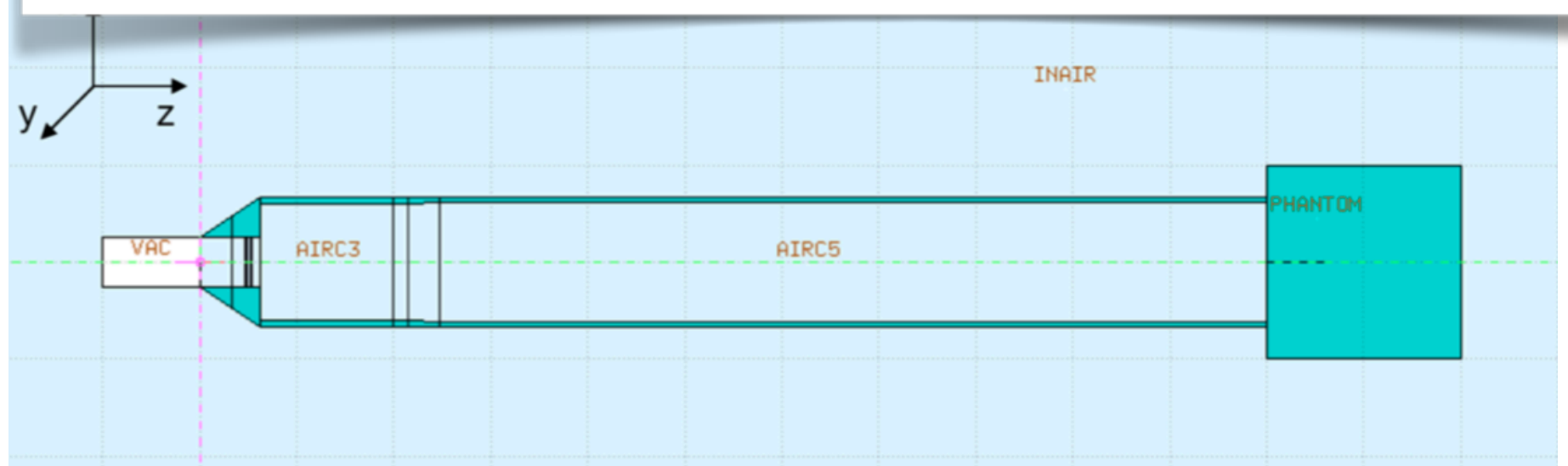
ElectronFlash4000

Characteristics EF4000	Value
Output energy	5 - 7 MeV
Pulse repetition frequency	1 - 250 Hz
Pulse width	0.5 - 4 μ s
Maximum peak beam current	120 mA
Dose rate per pulse	$> 10^6$ Gy/s
Mean Dose rate	1000 Gy/s
Max Dose per pulse	30 Gy in a surface of \varnothing 10 mm

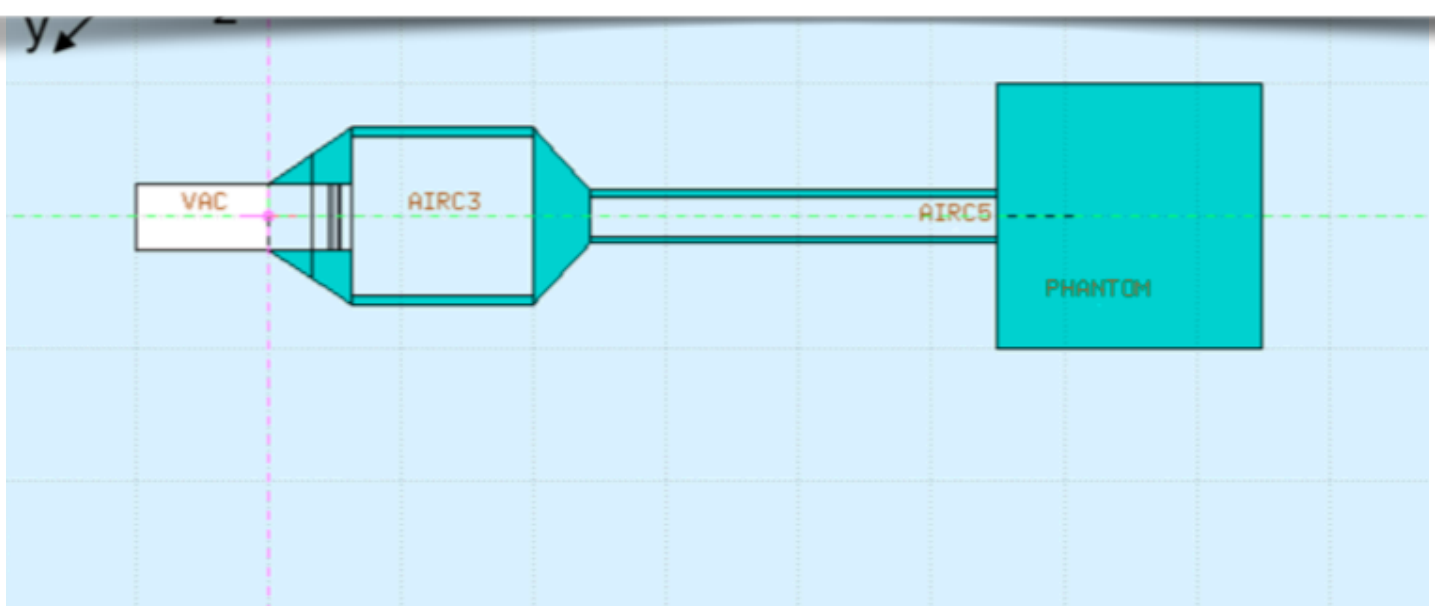
The EF4000 was commissioned by the Curie Institute and it was installed there in August 2020.

I performed the **dosimetric characterization** of the electrons beam produced by the linac by comparing the **experimental data** of the PDD and off-axis profile (Gafchromic EBT-XD films) with the ones obtained with **FLUKA**.

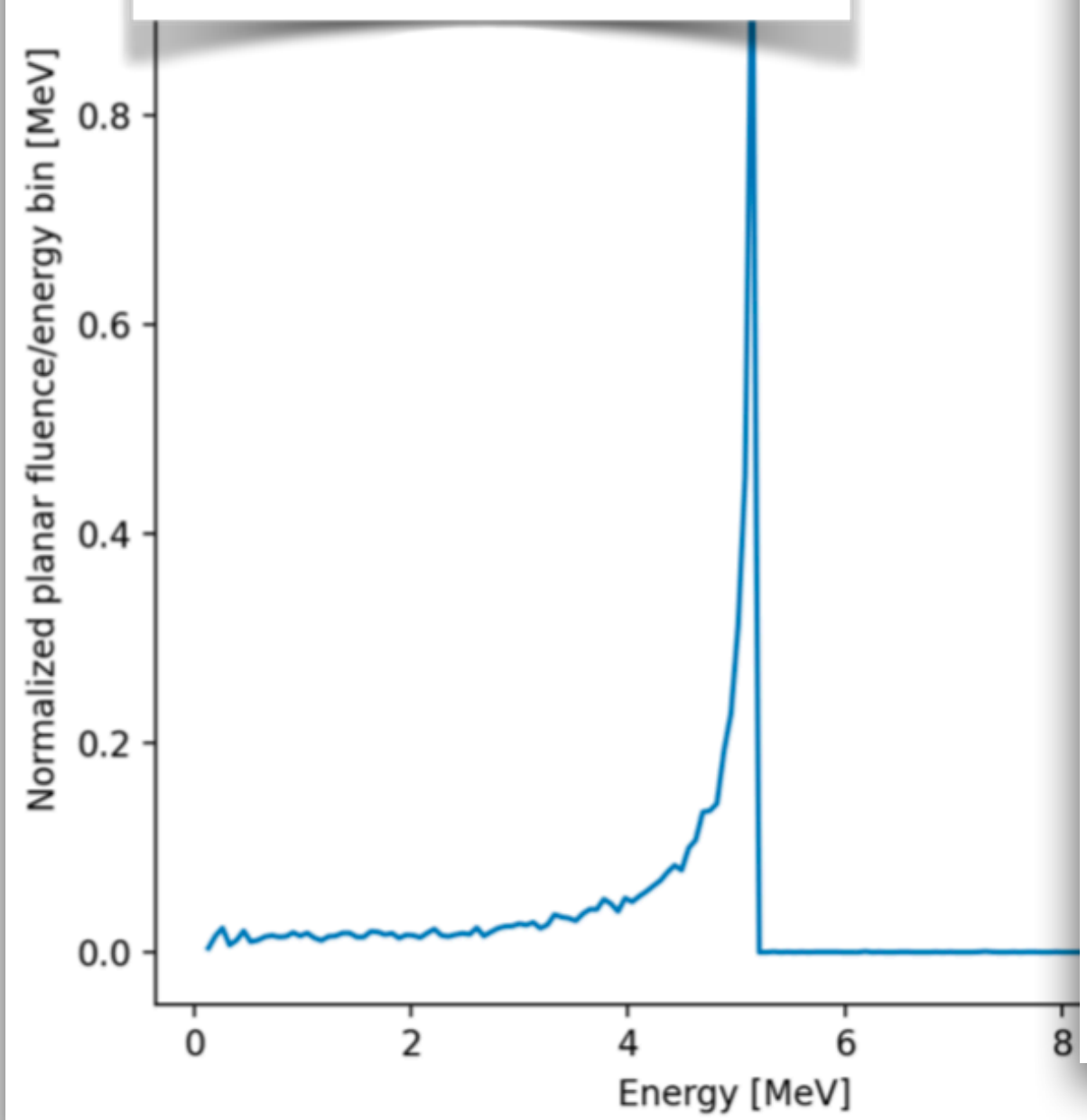
Applicator with d=120 mm and an SSD =1096 mm



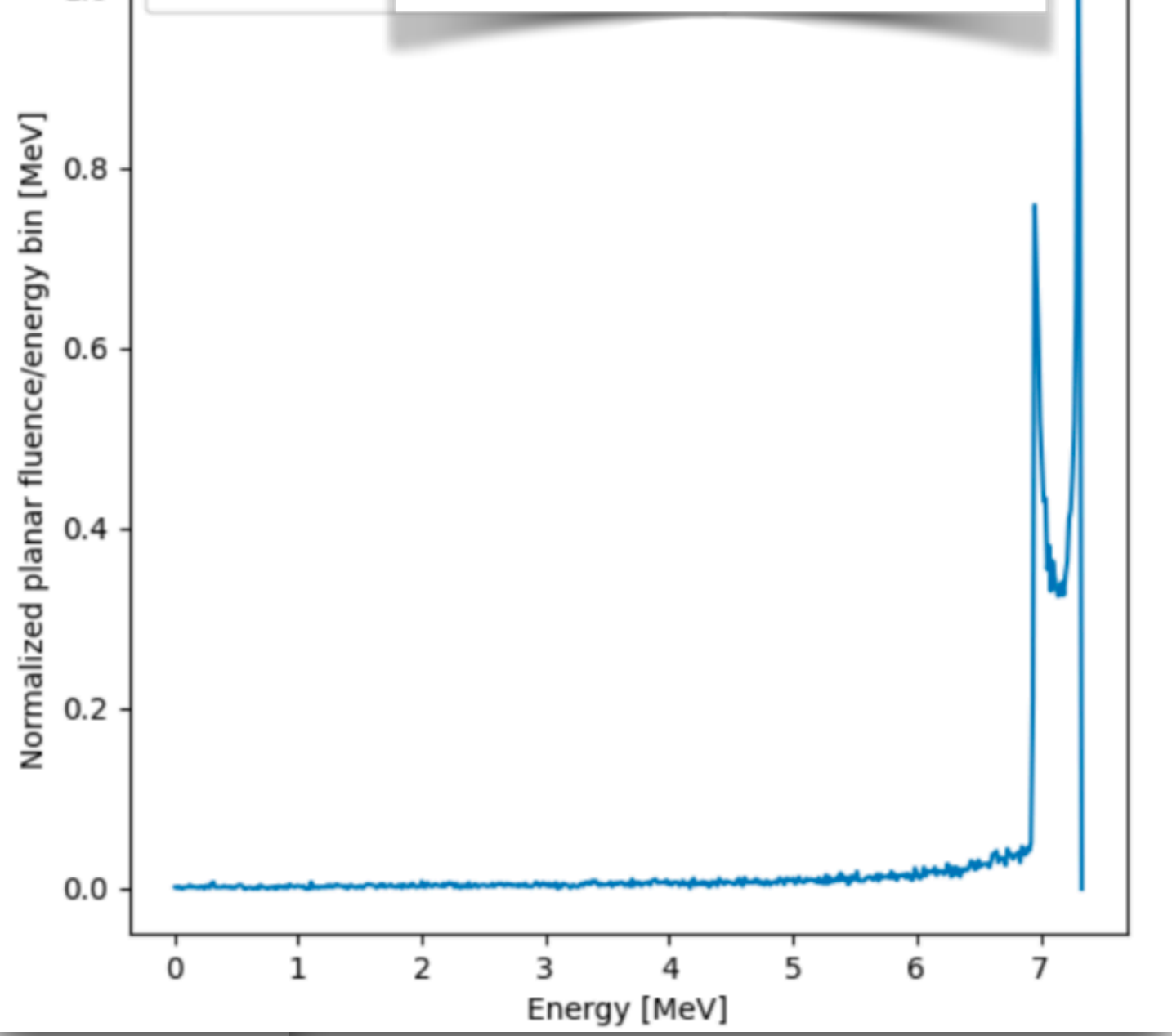
Applicator with d=30 mm and an SSD =549 mm



Energy spectrum @ 5 MeV



Energy spectrum @ 7 MeV

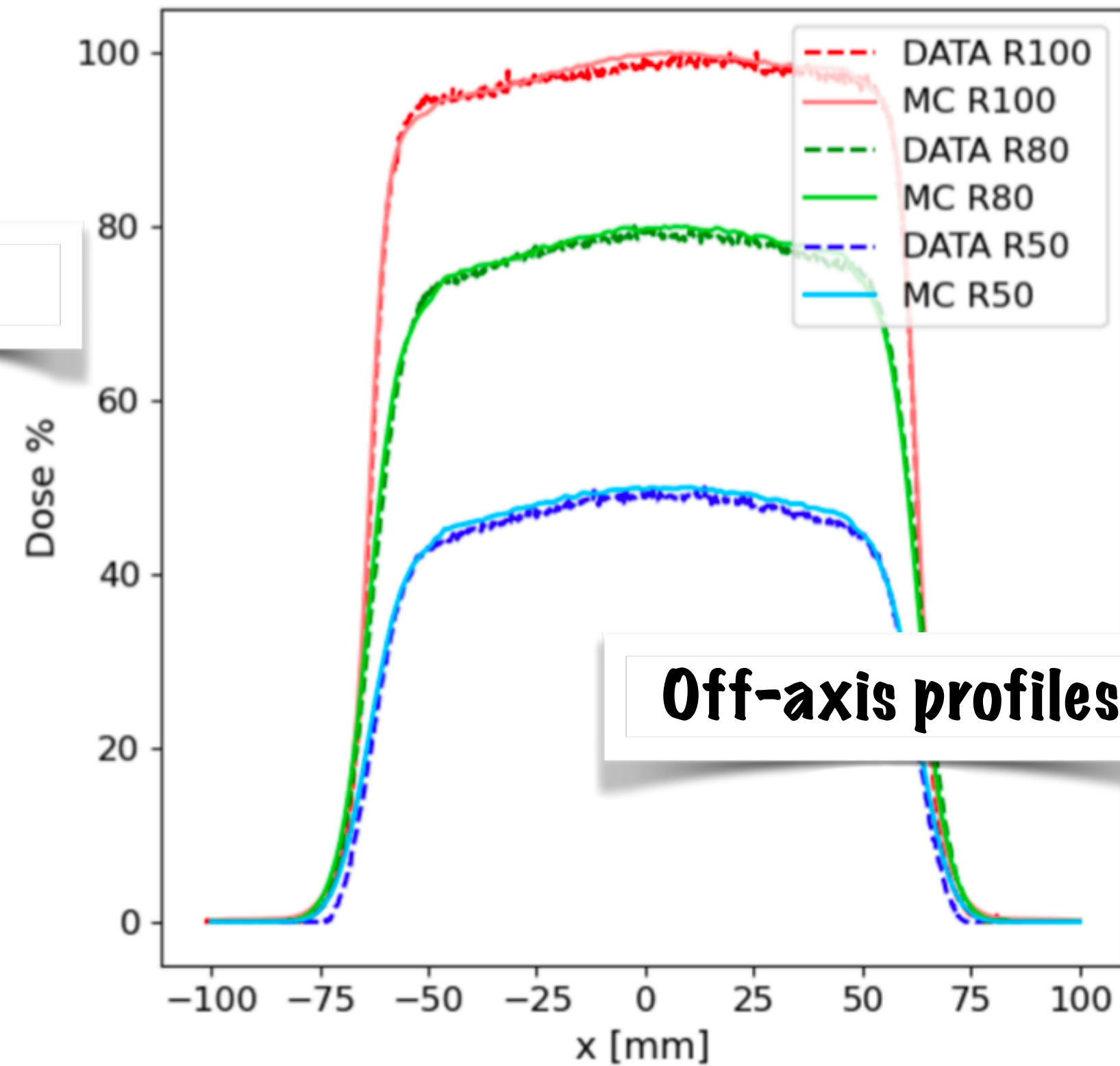
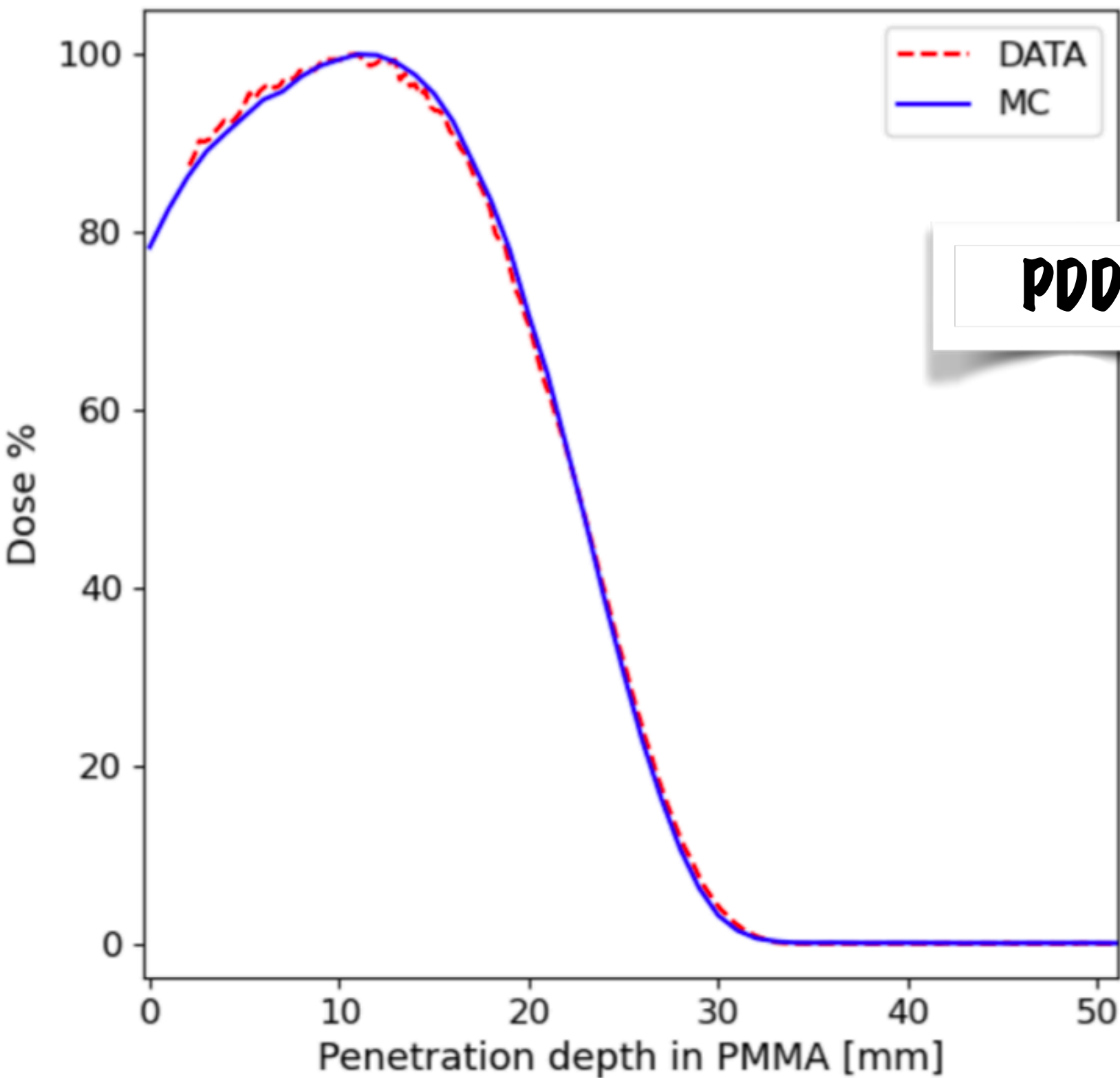


ElectronFlash4000

Characteristics EF4000	Value
Output energy	5 - 7 MeV
Pulse repetition frequency	1 - 250 Hz
Pulse width	0.5 - 4 μ s
Maximum peak beam current	120 mA
Dose rate per pulse	$> 10^6$ Gy/s
Mean Dose rate	1000 Gy/s
Max Dose per pulse	30 Gy in a surface of \varnothing 10 mm

Example of 5 MeV collimated with the applicator with $d=30$ mm

Gamma-index 3mm/3% pass rate:

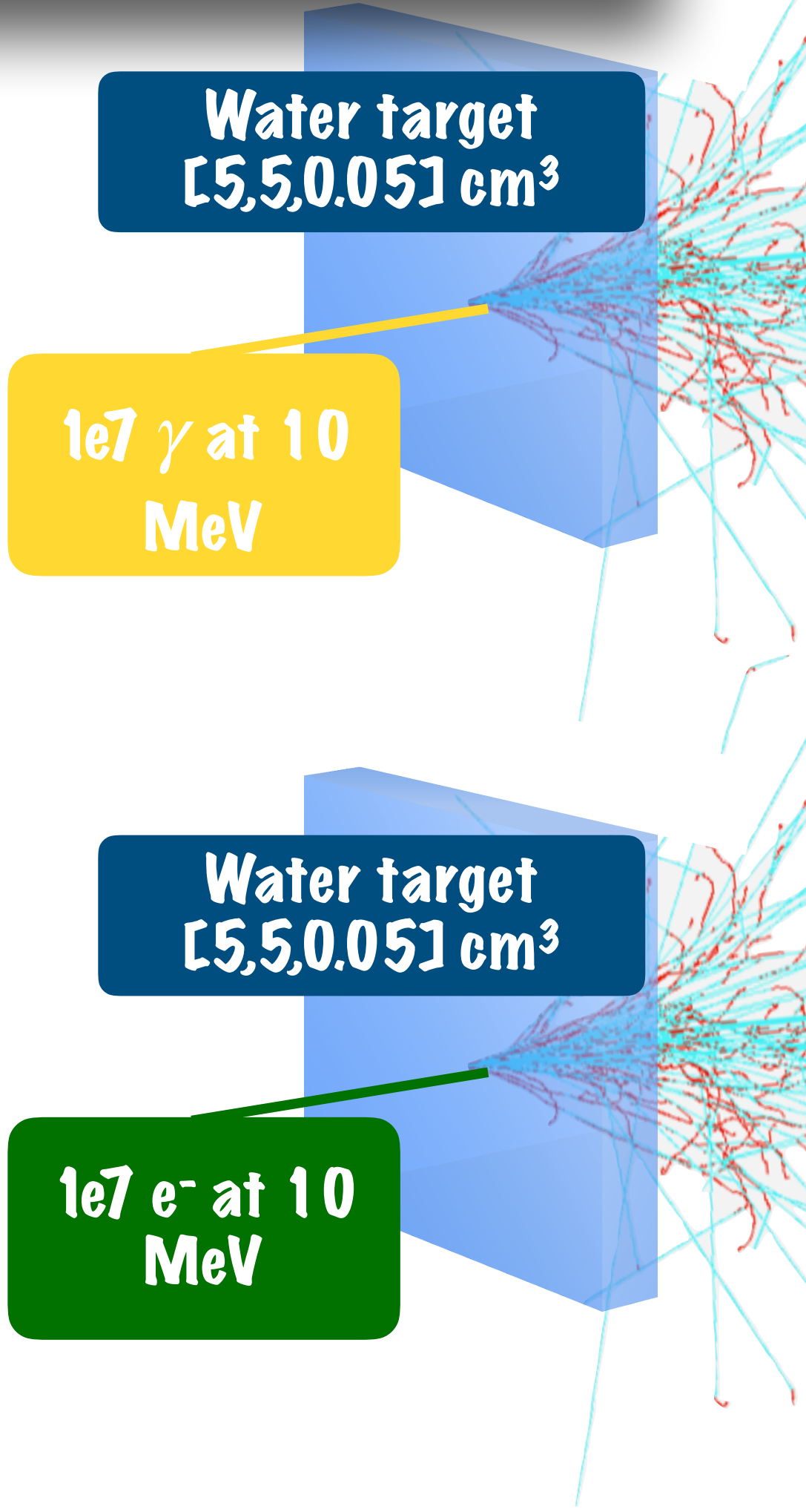
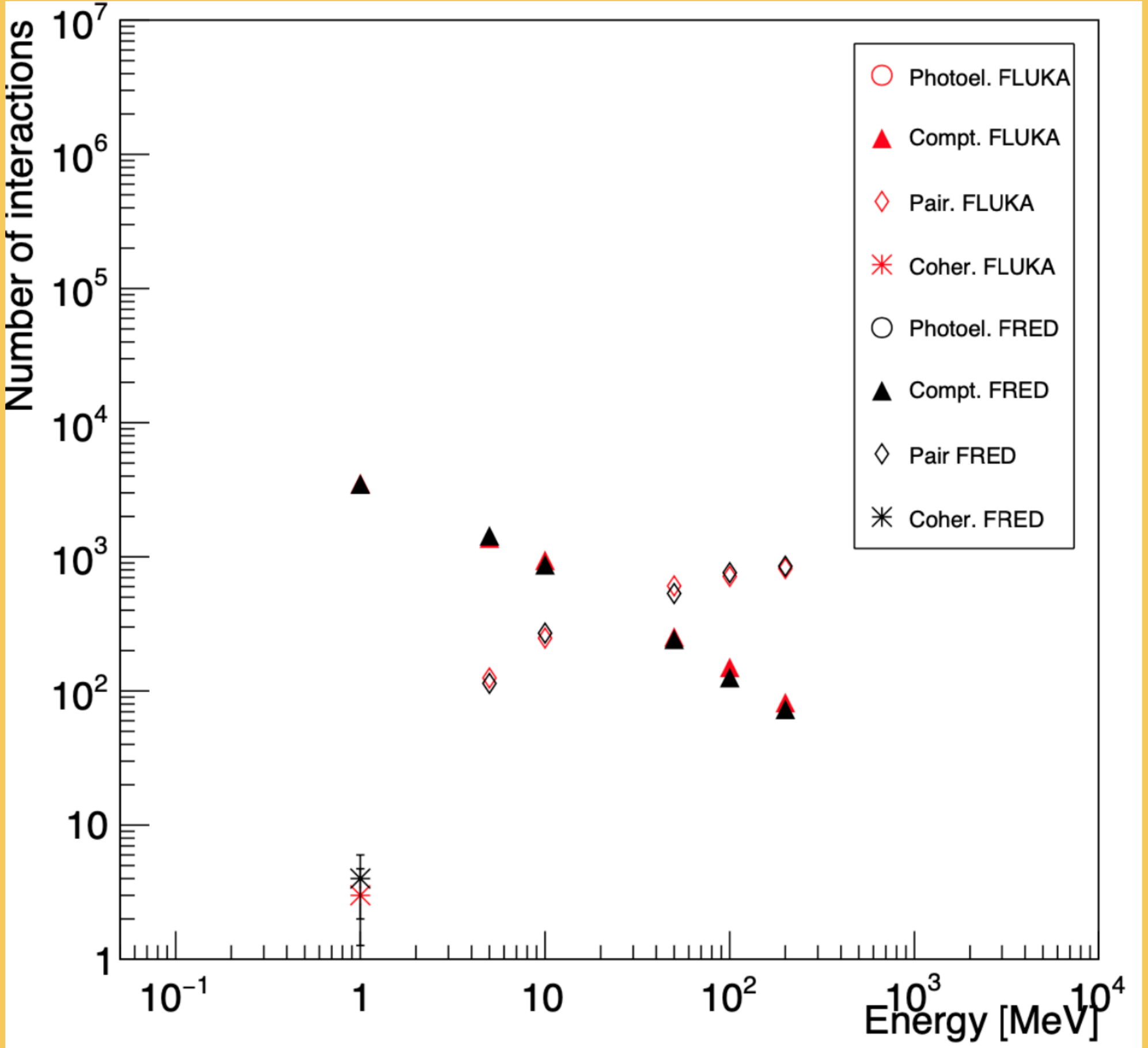
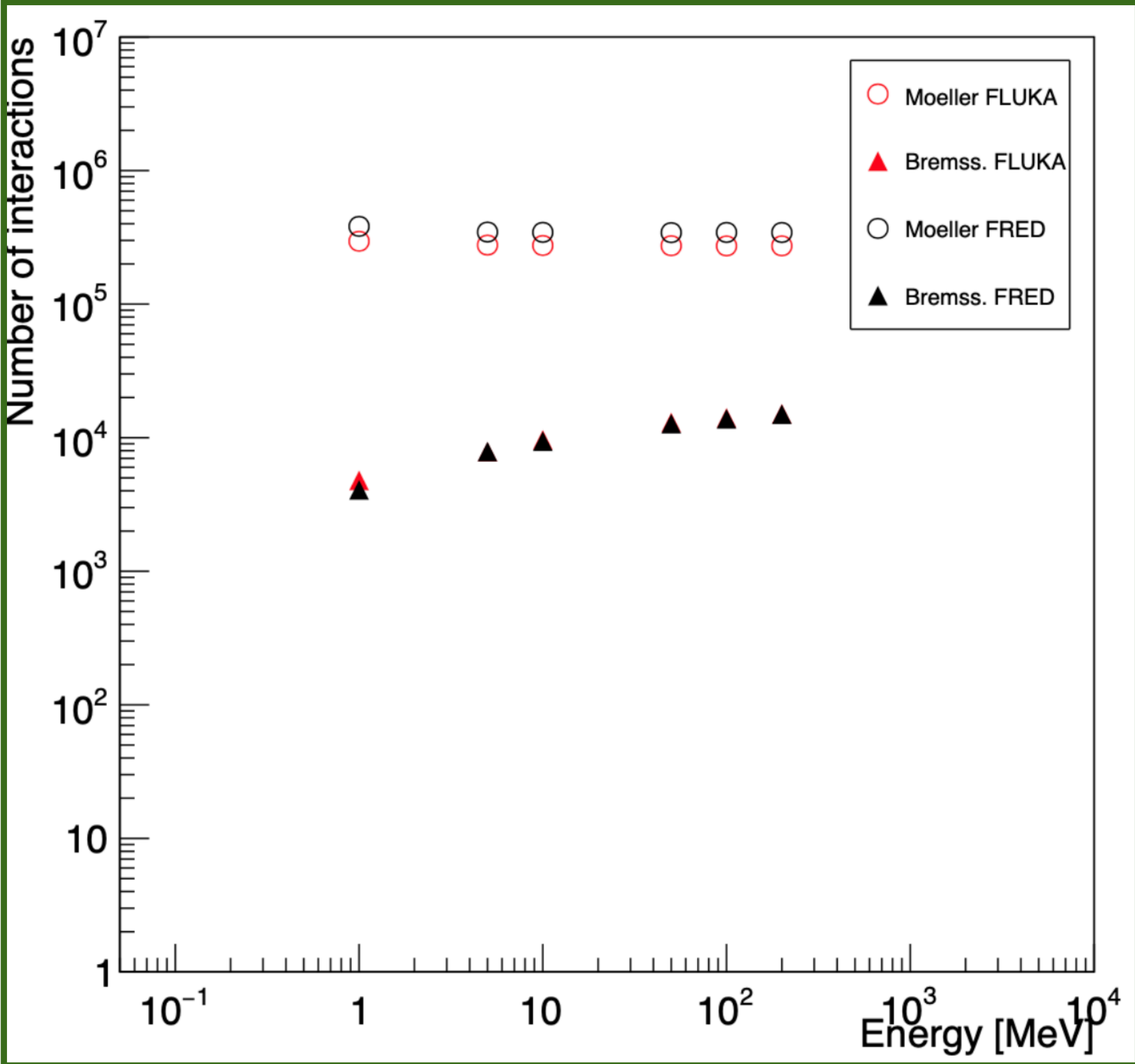


	R100	R80	R50
\varnothing 120 7 MeV	99.00 %	100 %	96.29 %
\varnothing 120 5 MeV	95.00 %	95.57 %	95.00 %
\varnothing 30 7 MeV	98.40 %	99.60 %	99.60 %
\varnothing 30 5 MeV	96.01 %	100 %	96.41 %

Thin target benchmark

FRED-em cross-sections

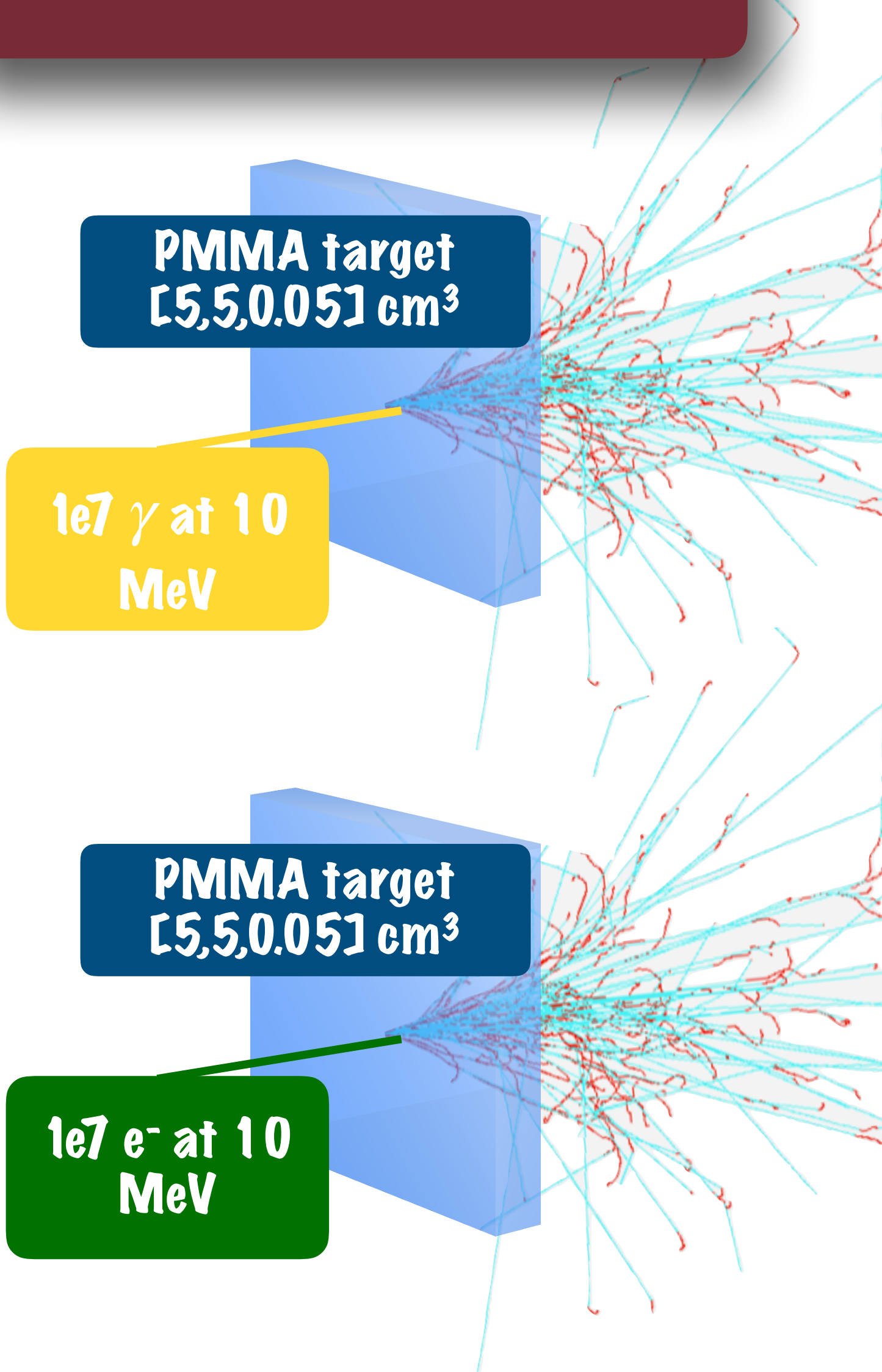
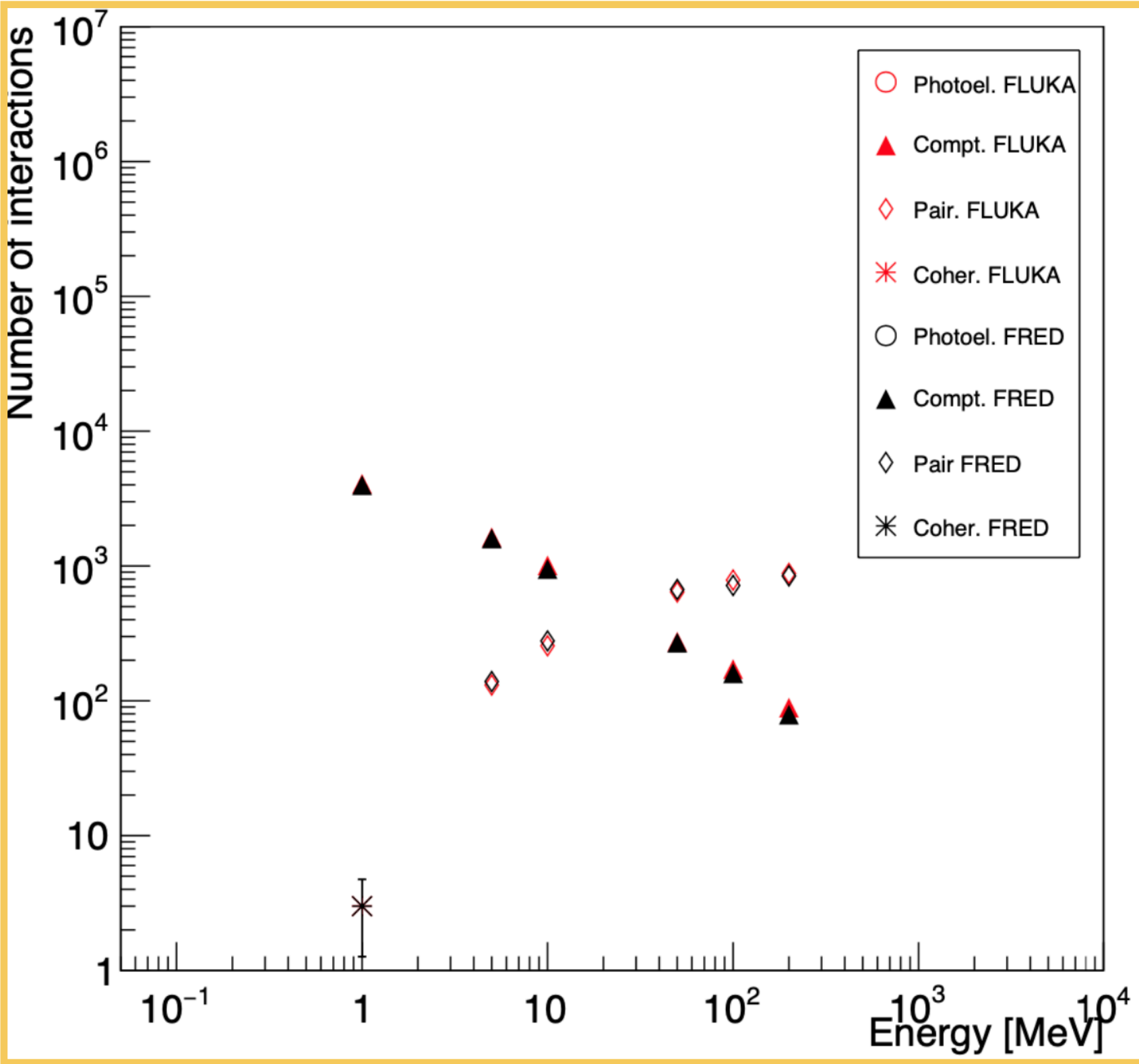
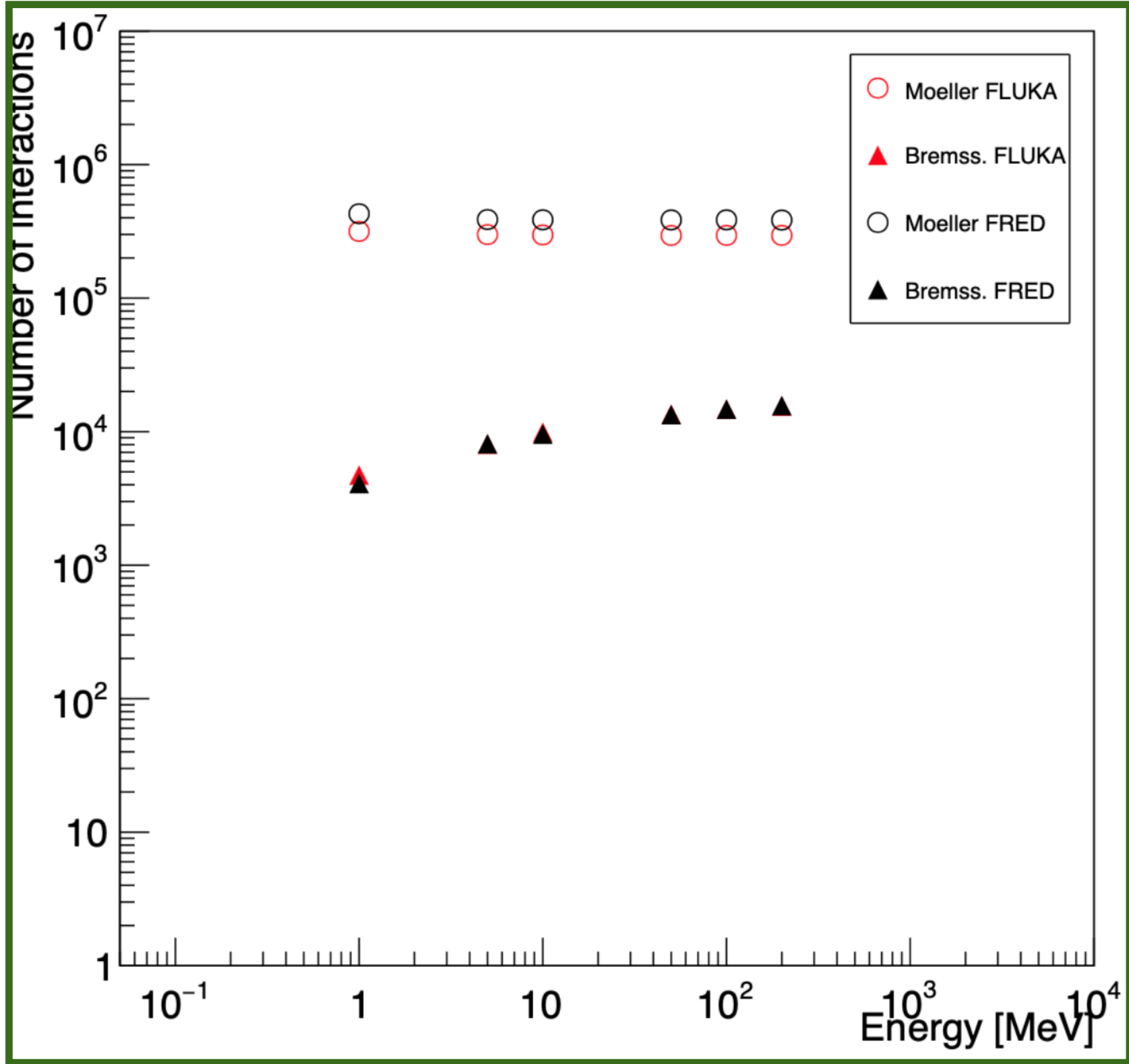
I have checked against **FLUKA** the **cross-section models** by counting the number of times a given process took place during the all simulation run.



Thin target benchmark

FRED-em cross-sections

I have checked against **FLUKA** the **cross-section models** by counting the number of times a given process took place during the all simulation run.



Thick target benchmark

FRED-em dose

Once I have obtained a successful agreement between the **FLUKA** and **FRED** electromagnetic models, I have checked the **dose distribution** released in different materials in the energy range of **[1-200] MeV**.

e^-

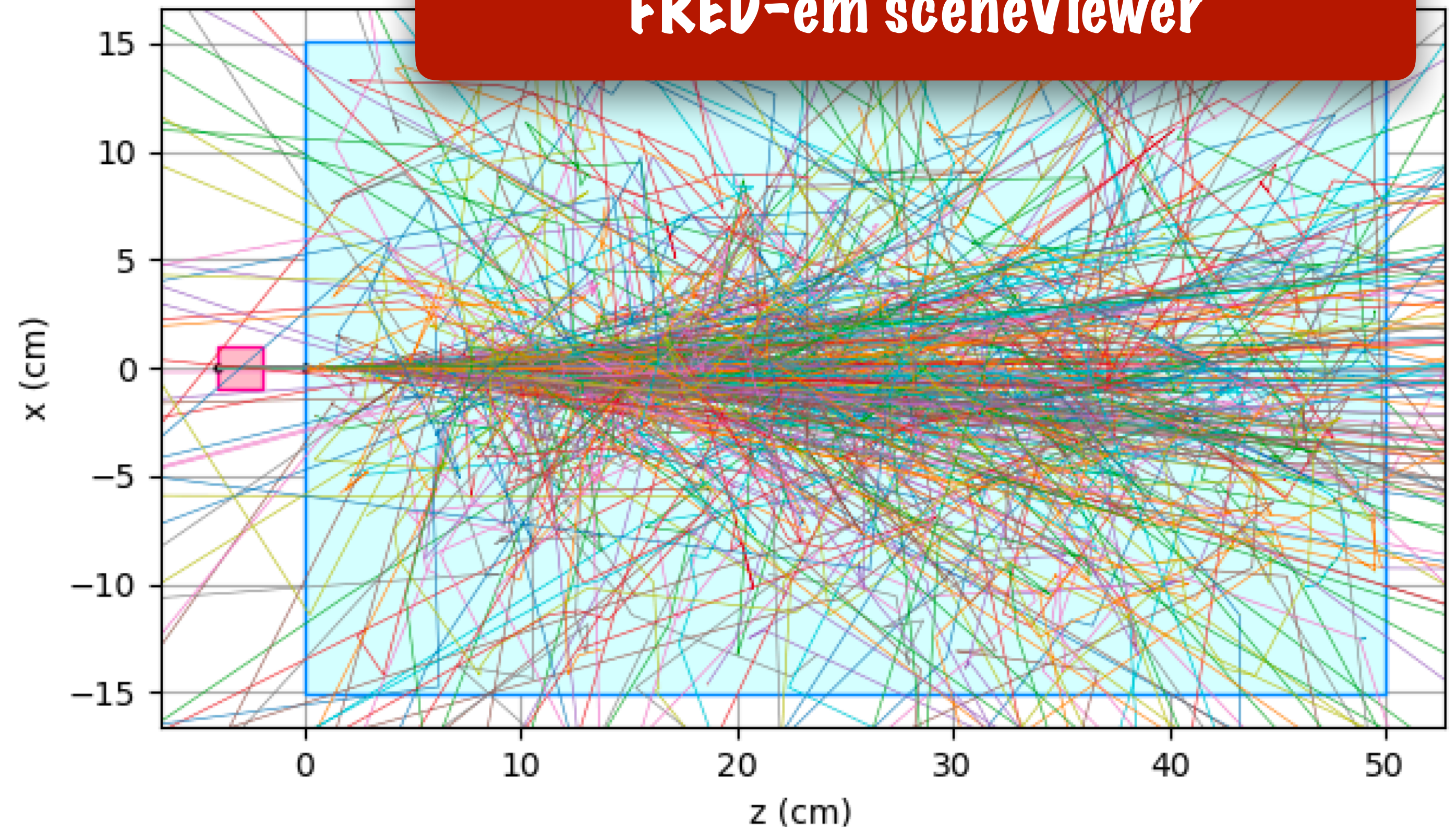
Pencil beam @ **10 MeV** with FWHM = 0 cm impinging on a water target of [40x40x50] cm³

γ

Pencil beam @ **10 MeV** with FWHM = 0 cm impinging on a water target of [40x40x100/200] cm³



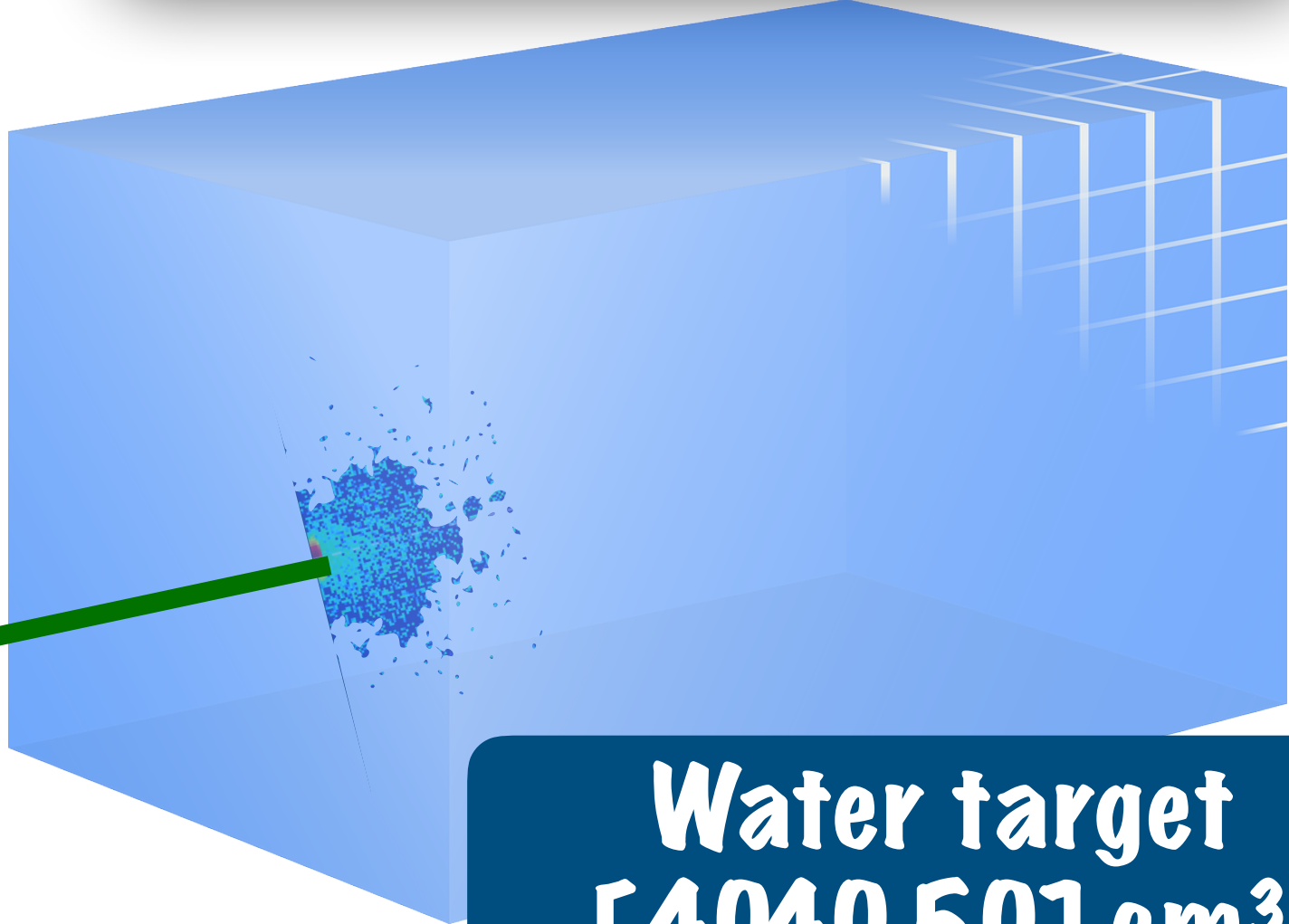
FRED-em sceneViewer



Thick target benchmark

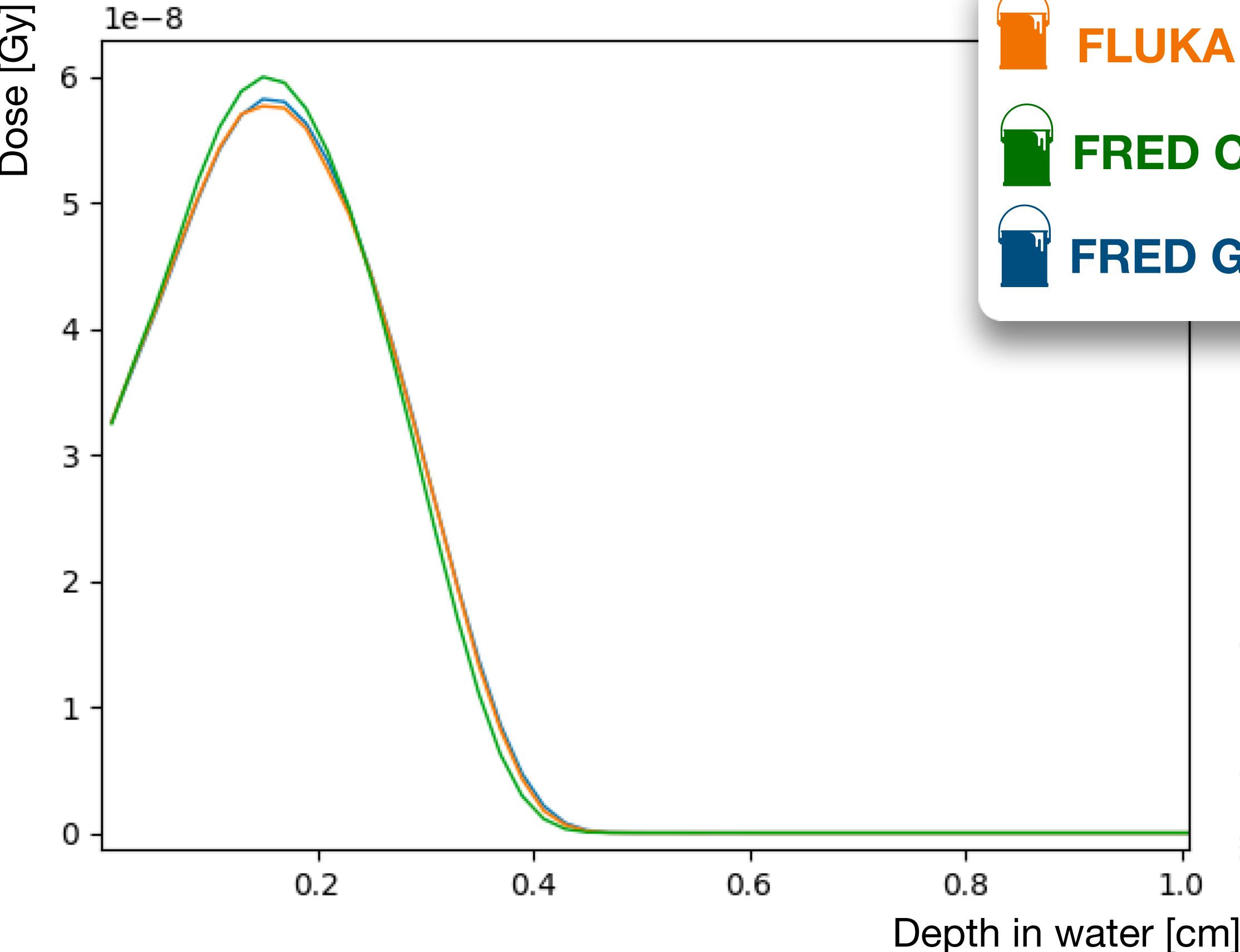
FRED-em dose

Ones I have obtained a successful agreement between the **FLUKA** and **FRED** electromagnetic models, I have checked the **dose distribution** released in different materials.



1e6 e⁻ at 1 MeV

Water target [40,40,50] cm³



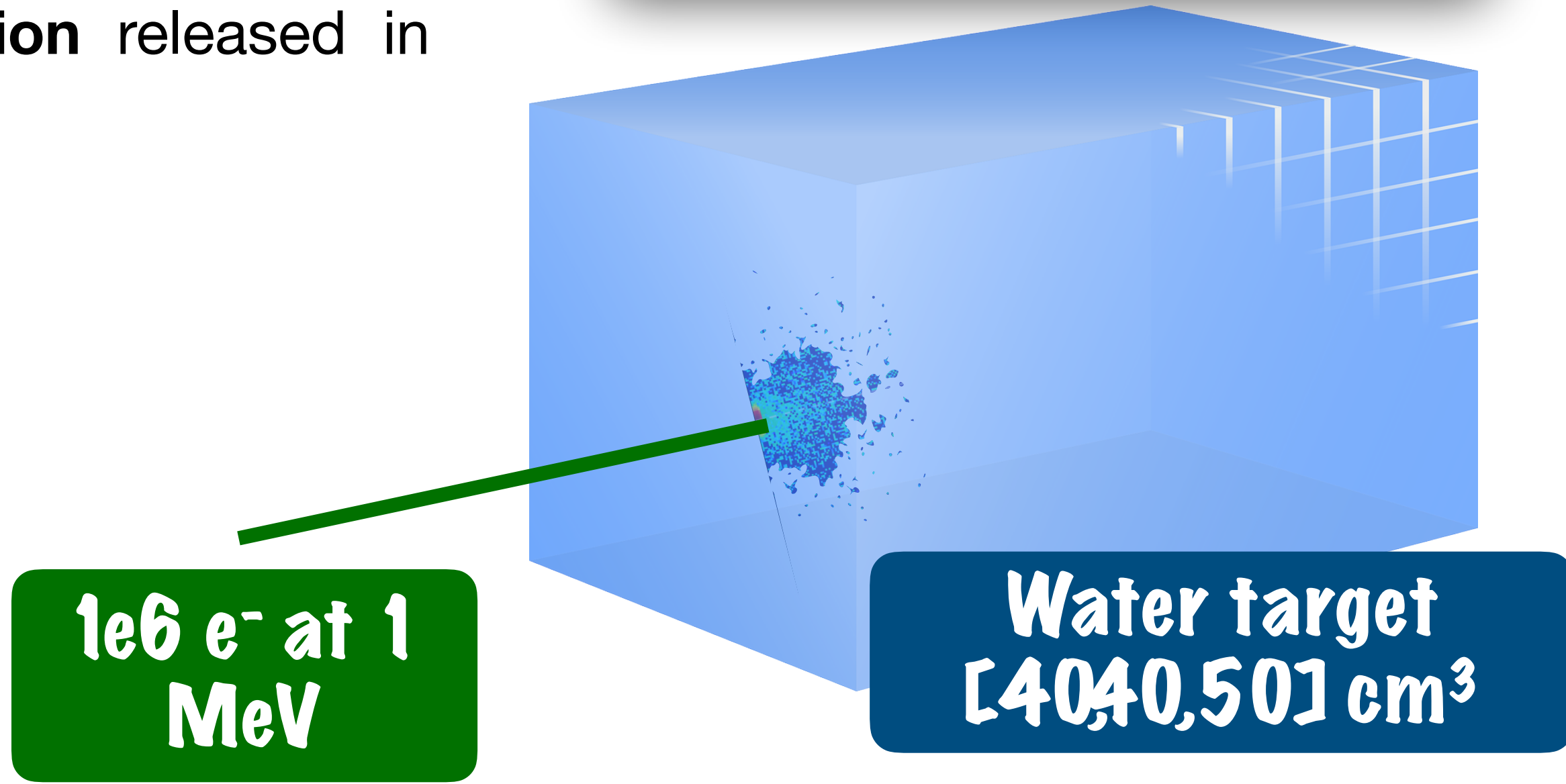
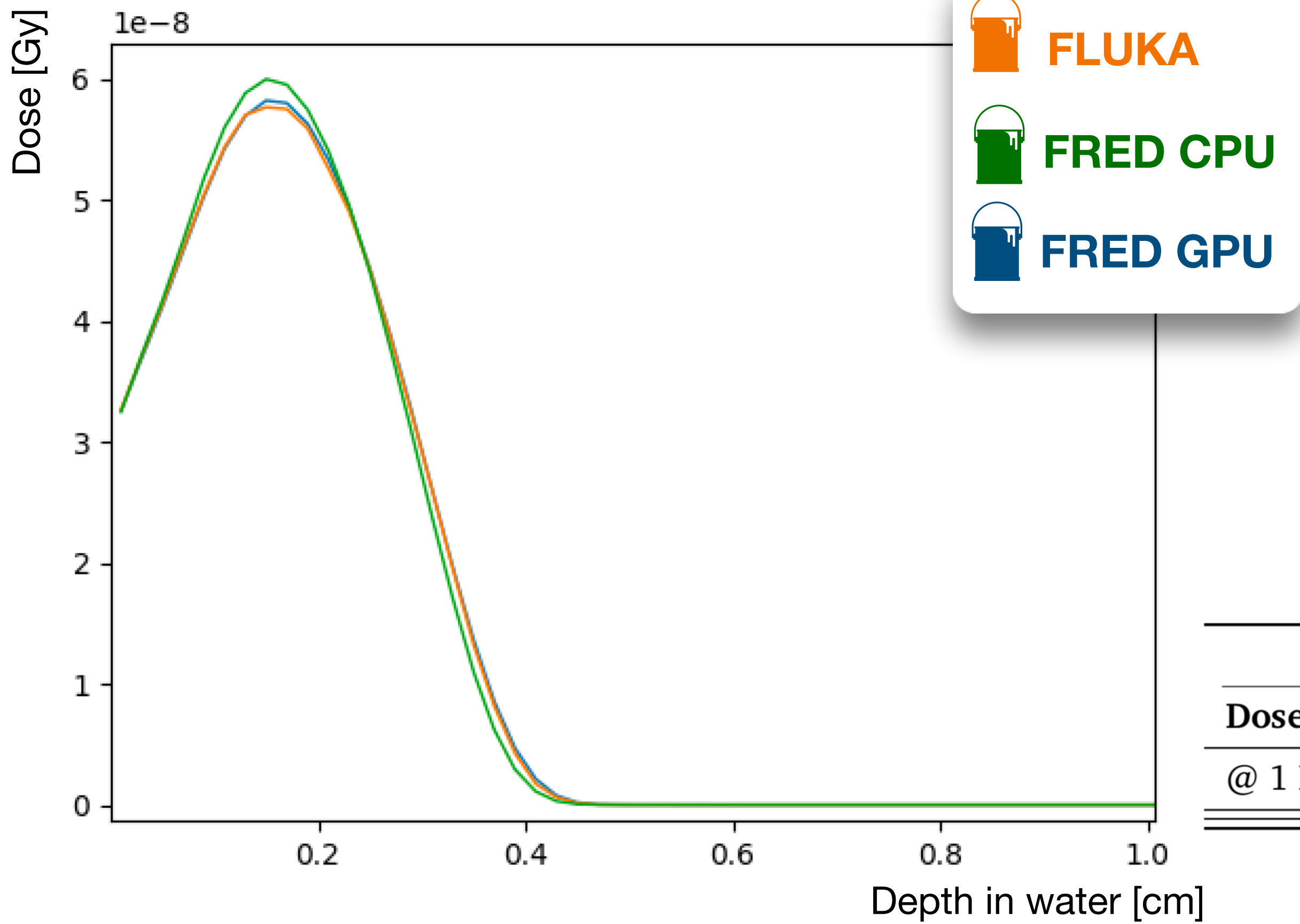
- FLUKA
- FRED CPU
- FRED GPU

Dose integral	FRED-em performance		
	FLUKA	FRED-CPU	FRED-GPU
@ 1 MeV	$7.889 \cdot 10^{-8}$ Gy/primary	$7.809 \cdot 10^{-8}$ Gy/primary	$7.902 \cdot 10^{-8}$ Gy/primary

Thick target benchmark

Once I have obtained a successful agreement between the **FLUKA** and **FRED** electromagnetic models, I have checked the **dose distribution** released in different materials.

FRED-em dose



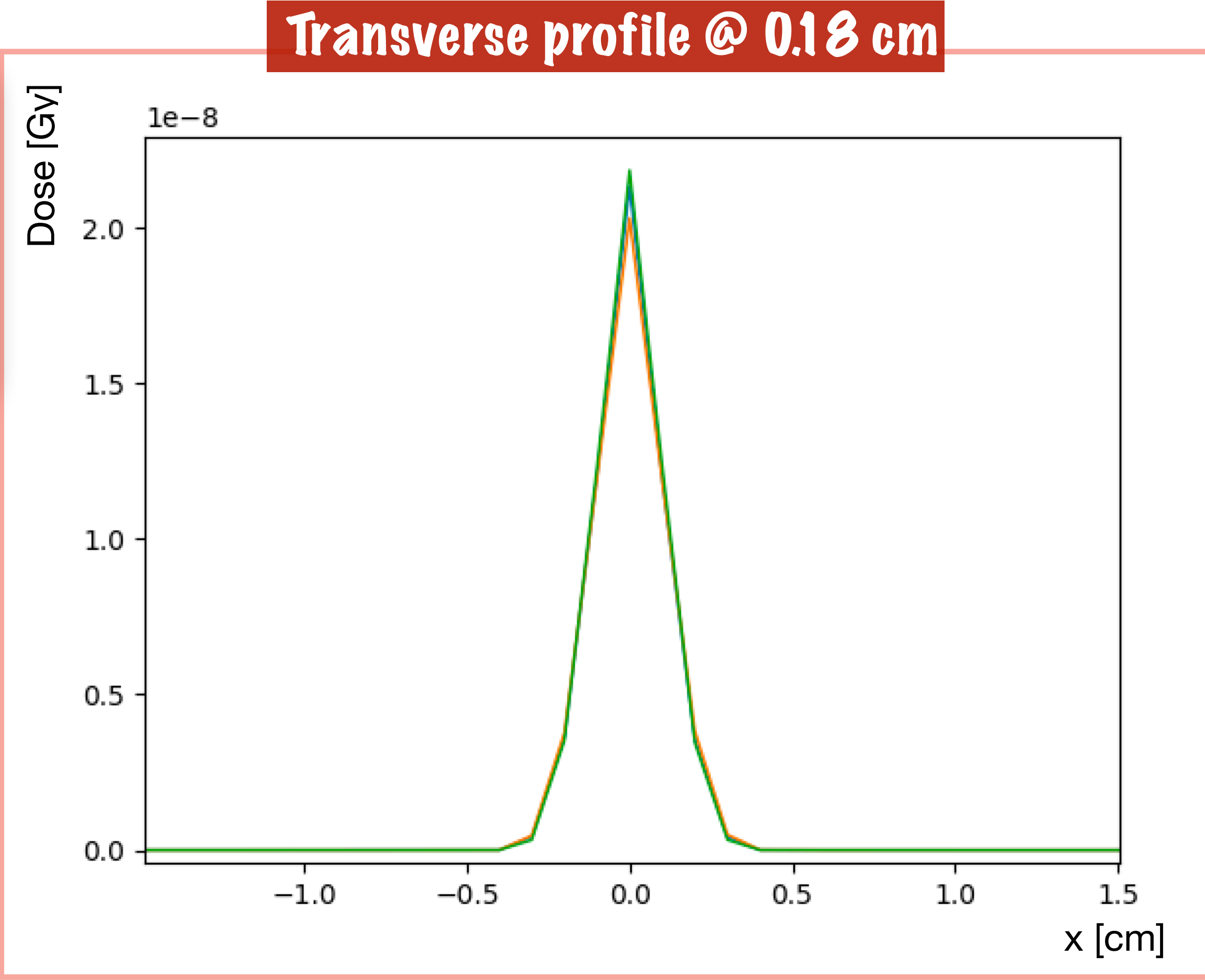
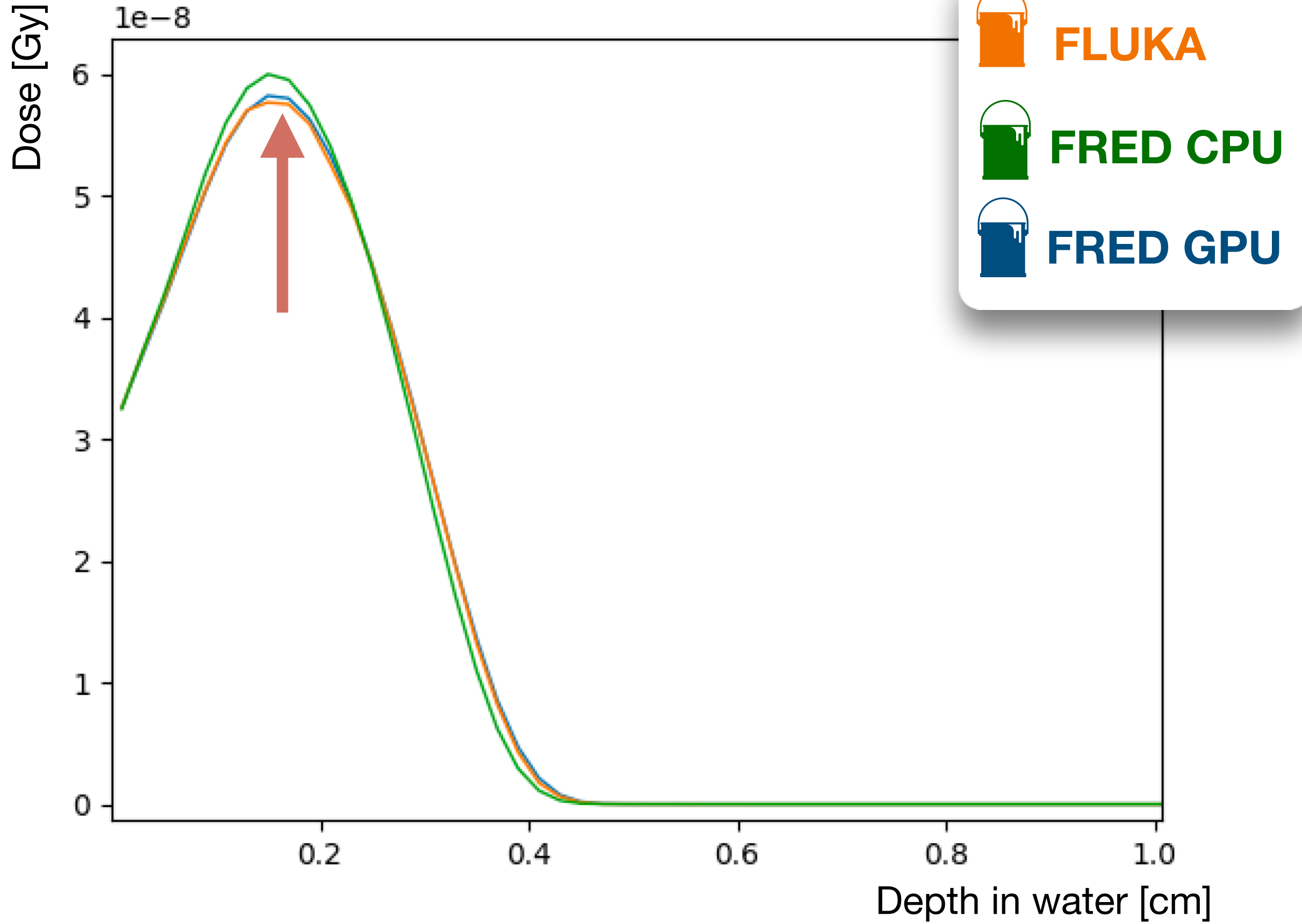
FRED-em performance			
Dose integral	FLUKA	FRED-CPU	FRED-GPU
@ 1 MeV	$7.889 \cdot 10^{-8}$ Gy/primary	$7.809 \cdot 10^{-8}$ Gy/primary	$7.902 \cdot 10^{-8}$ Gy/primary

diff ~ 0.16 %

Thick target benchmark

FRED-em dose

Once I have obtained a successful agreement between the **FLUKA** and **FRED** electromagnetic models, I have checked the **dose distribution** released in different materials.

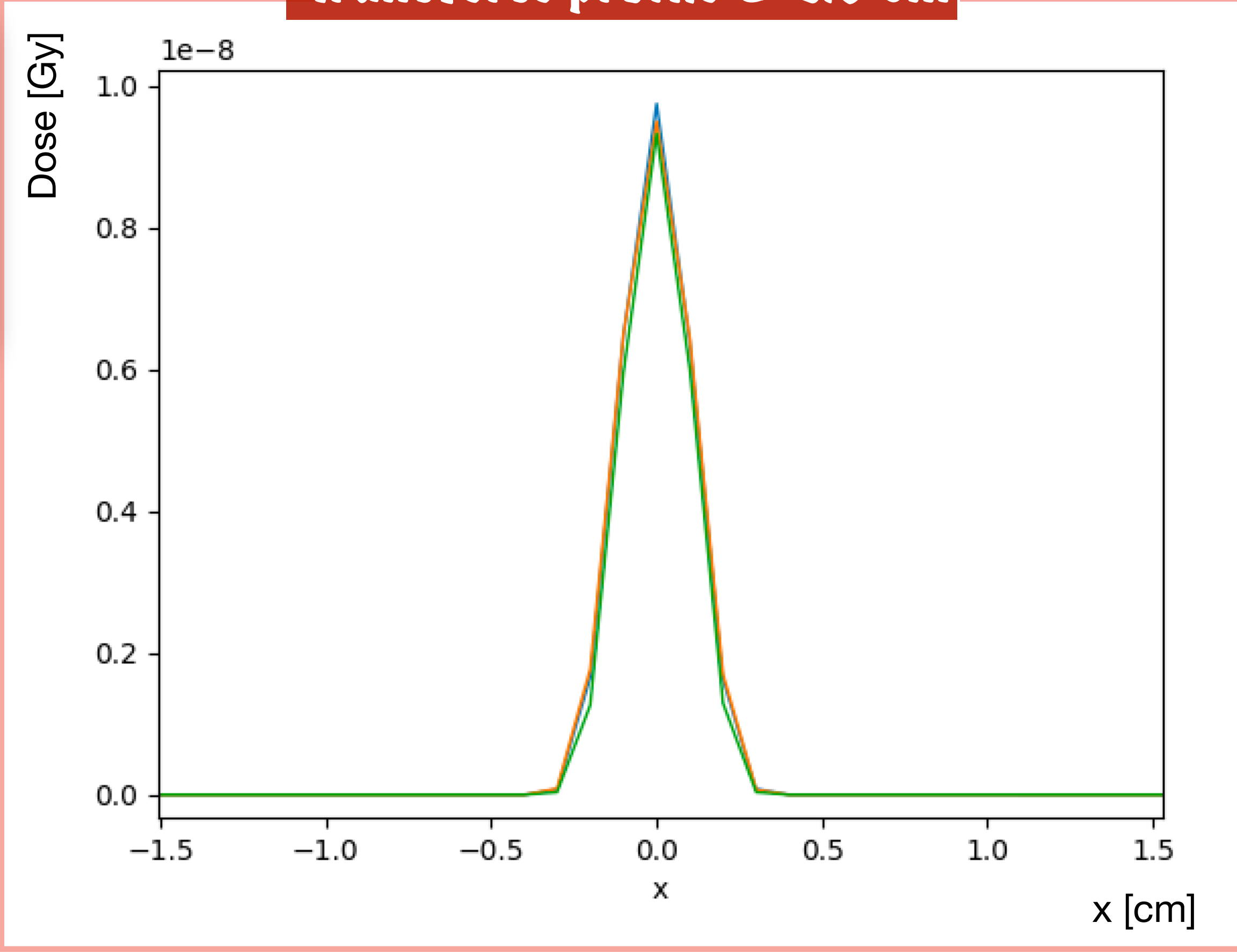
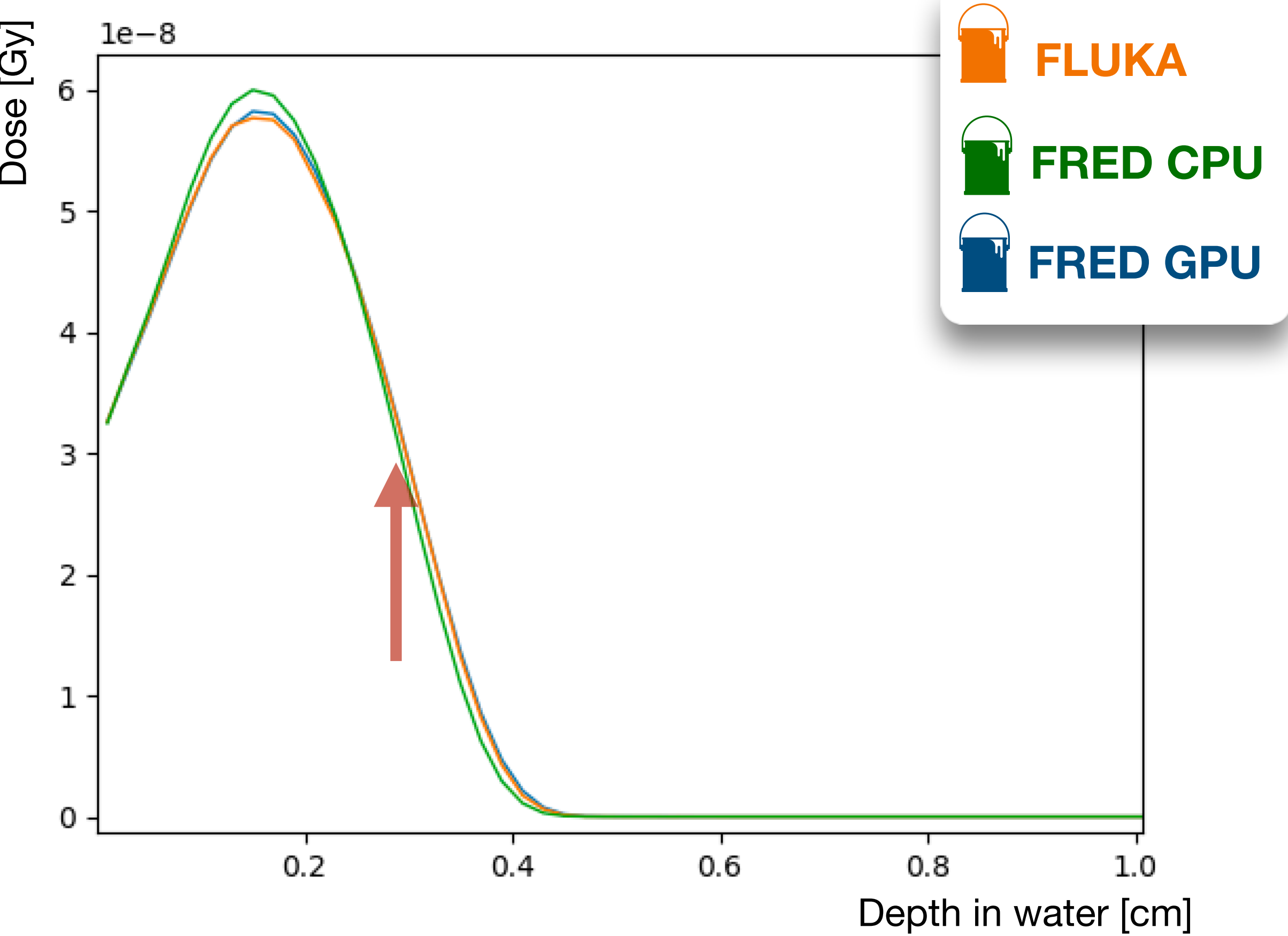


Thick target benchmark

FRED-em dose

Once I have obtained a successful agreement between the **FLUKA** and **FRED** electromagnetic models, I have checked the **dose distribution** released in different materials.

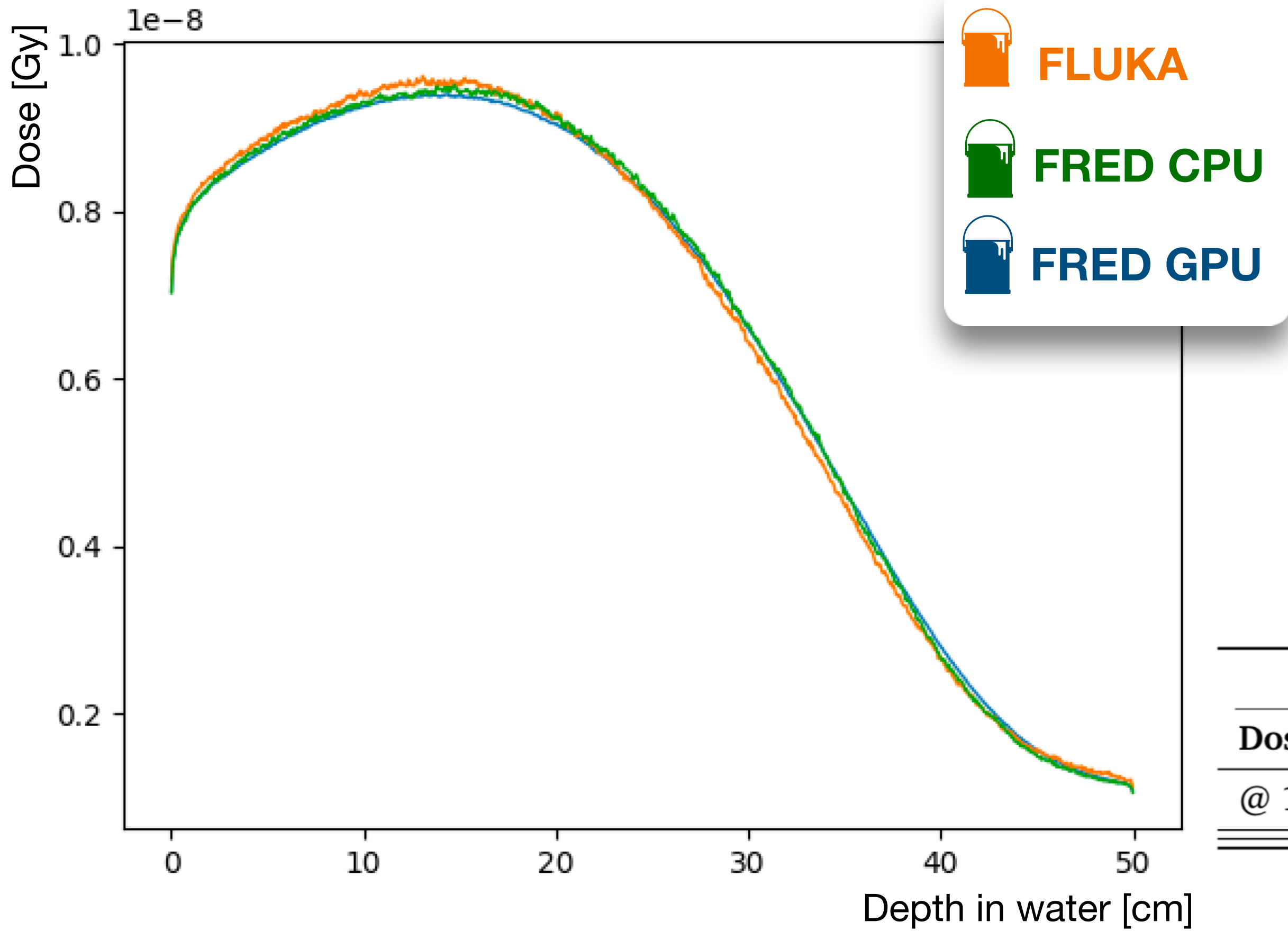
Transverse profile @ 0.3 cm



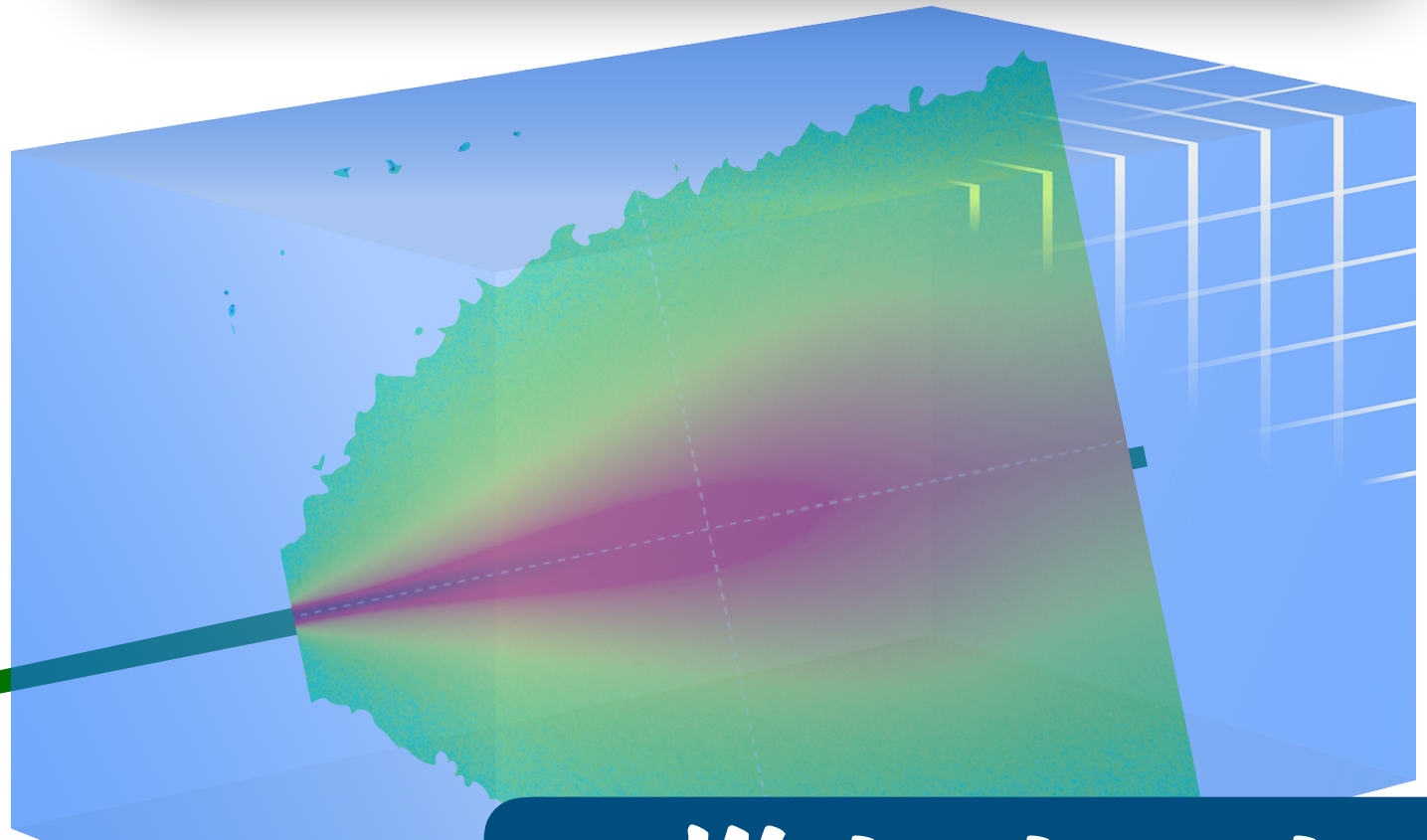
Thick target benchmark

Once I have obtained a successful agreement between the **FLUKA** and **FRED** electromagnetic models, I have checked the **dose distribution** released in different materials.

FRED-em dose



1e6 e⁻ at 100 MeV



Water target [40,40,50] cm³

FRED-em performance			
Dose integral	FLUKA	FRED-CPU	FRED-GPU
@ 100 MeV	$6.497 \cdot 10^{-6}$ Gy/primary	$6.486 \cdot 10^{-6}$ Gy/primary	$6.481 \cdot 10^{-6}$ Gy/primary

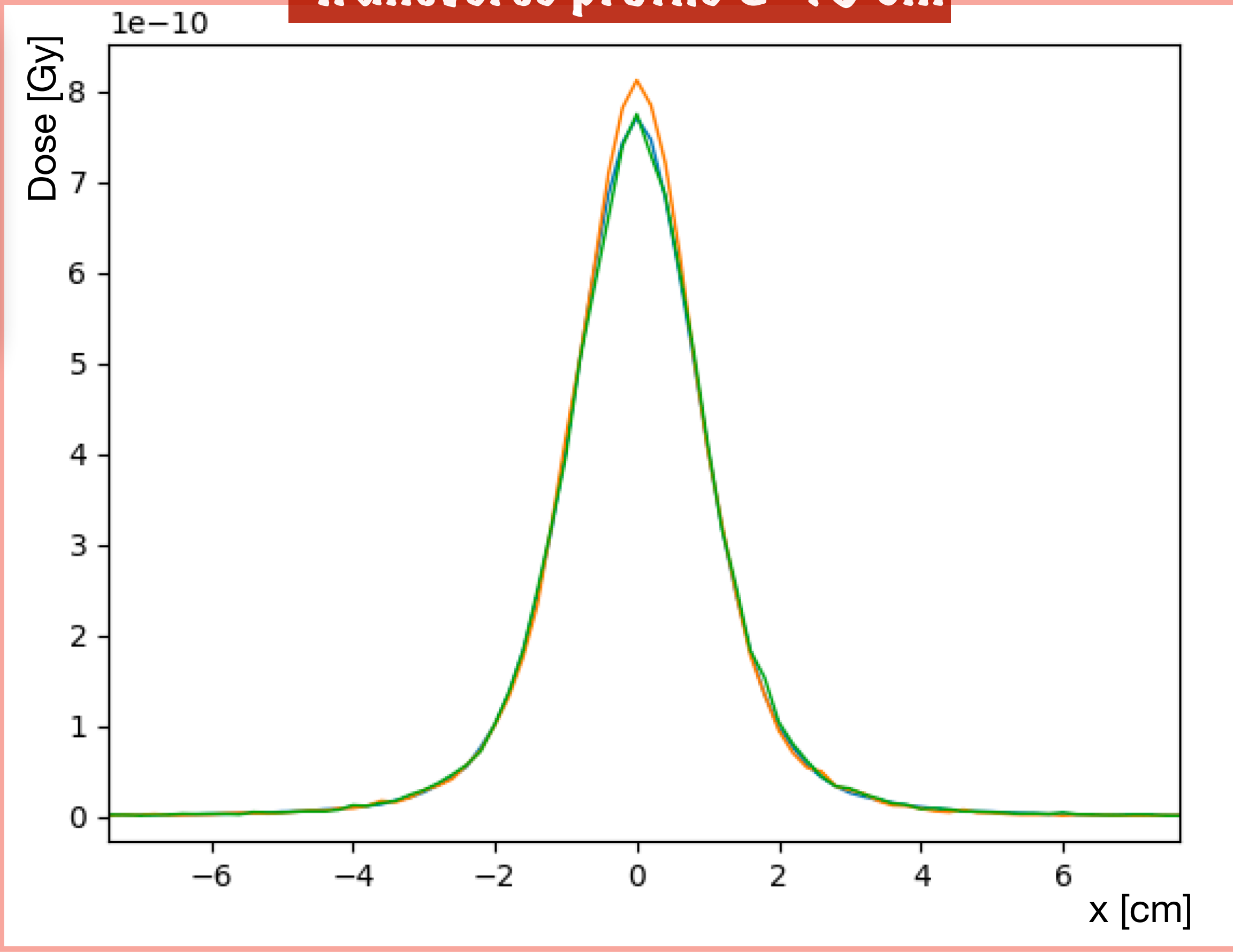
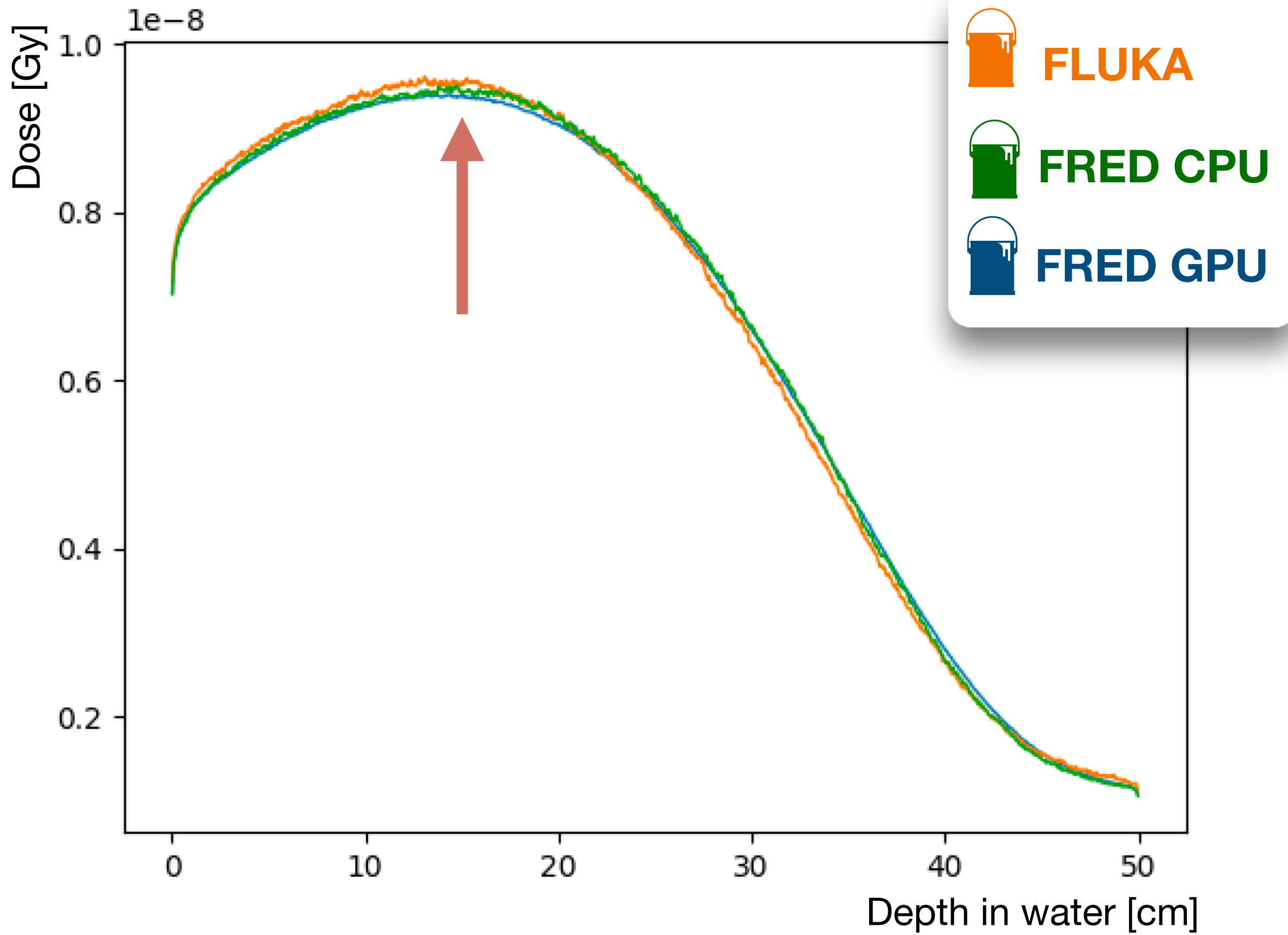
diff ~ 0.24%

Thick target benchmark

FRED-em dose

Once I have obtained a successful agreement between the **FLUKA** and **FRED** electromagnetic models, I have checked the **dose distribution** released in different materials.

Transverse profile @ 15 cm

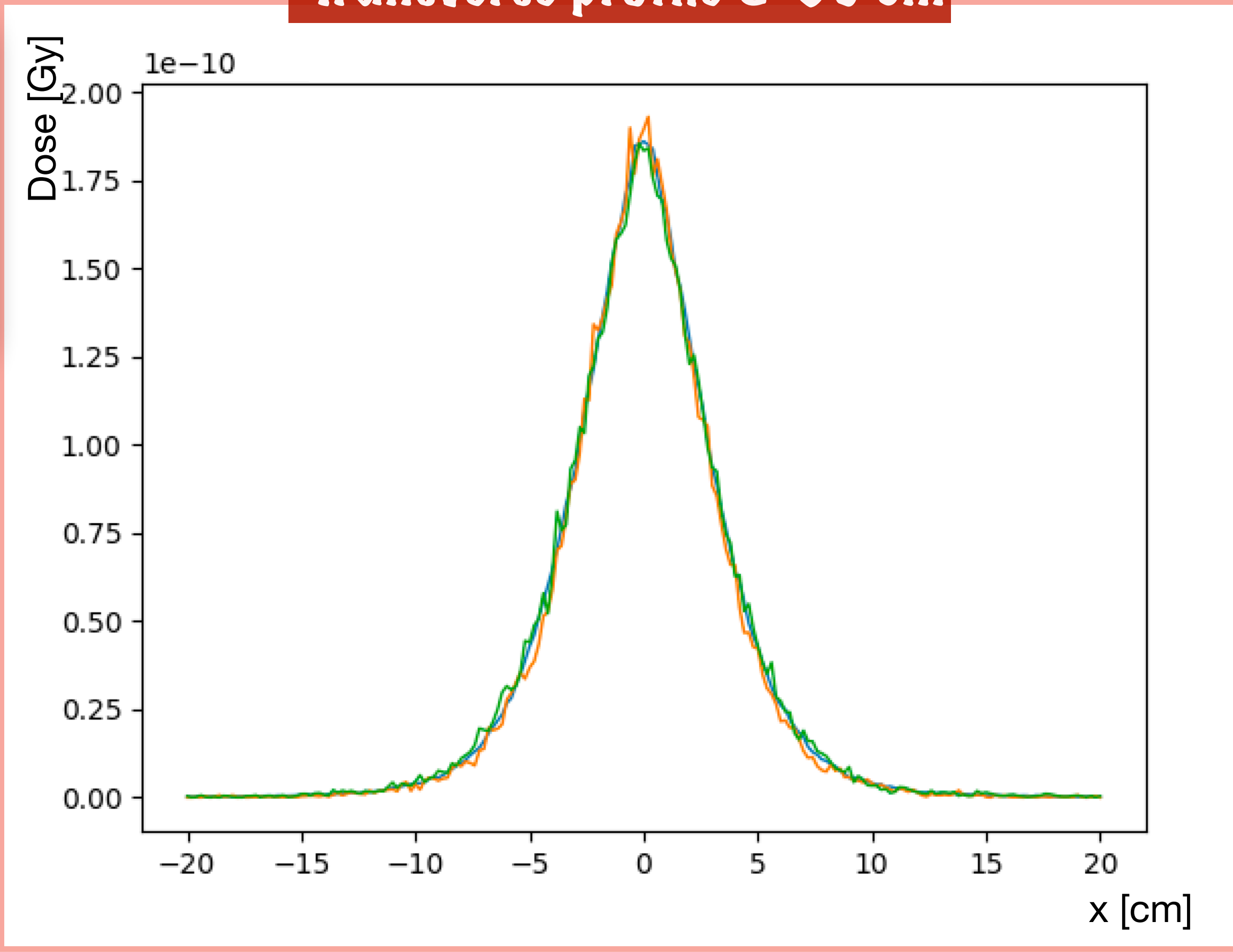
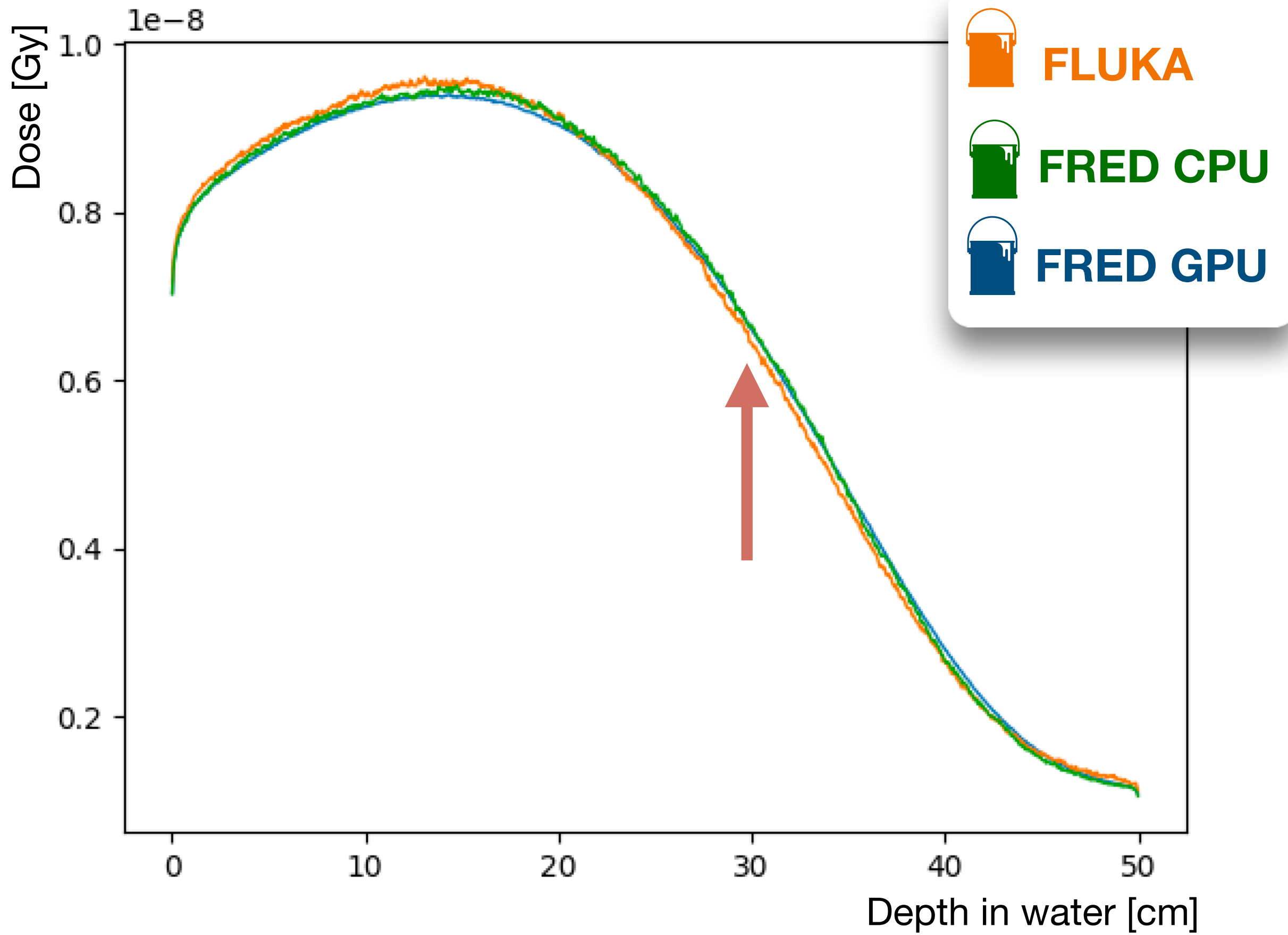


Thick target benchmark

FRED-em dose

Once I have obtained a successful agreement between the **FLUKA** and **FRED** electromagnetic models, I have checked the **dose distribution** released in different materials.

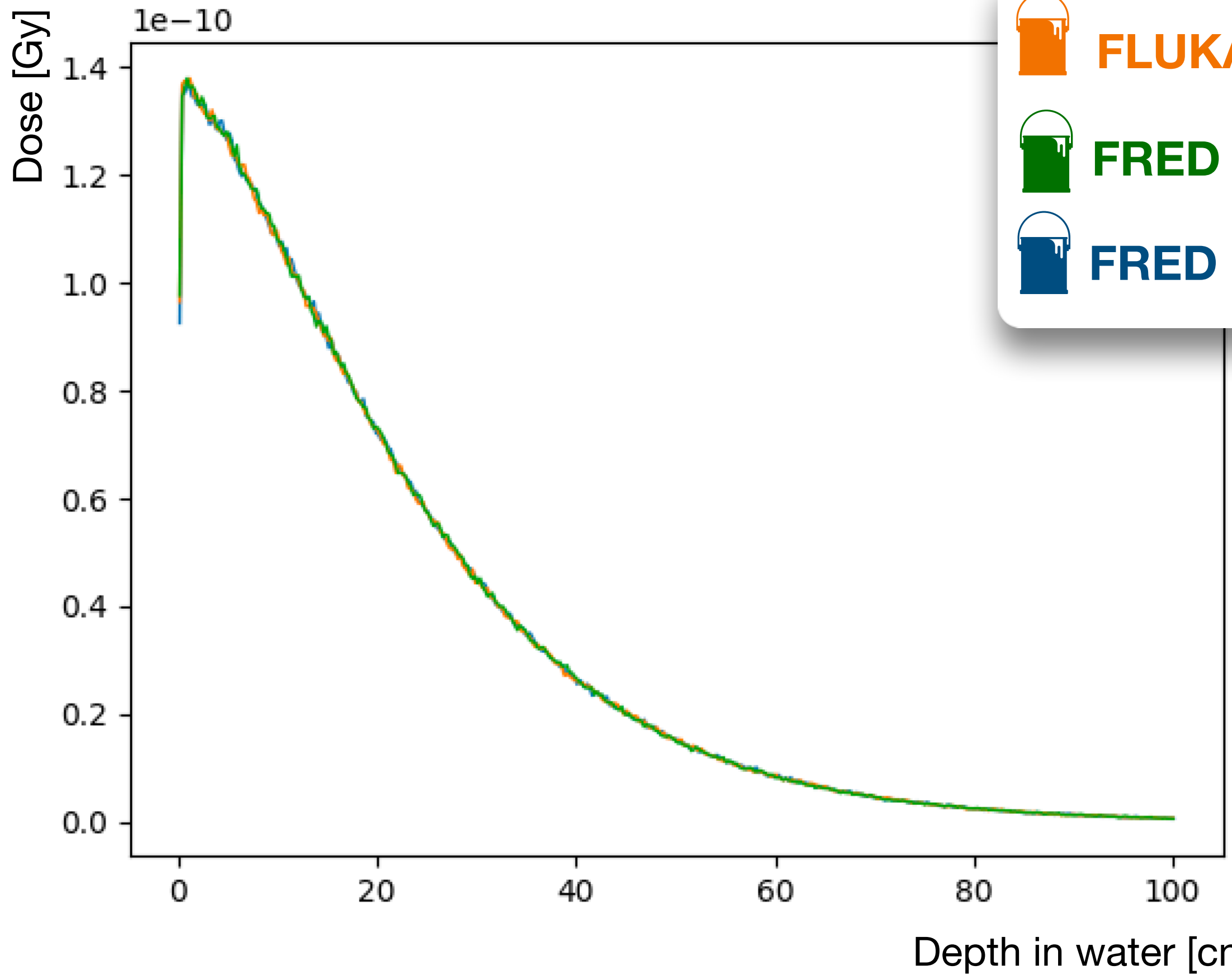
Transverse profile @ 30 cm



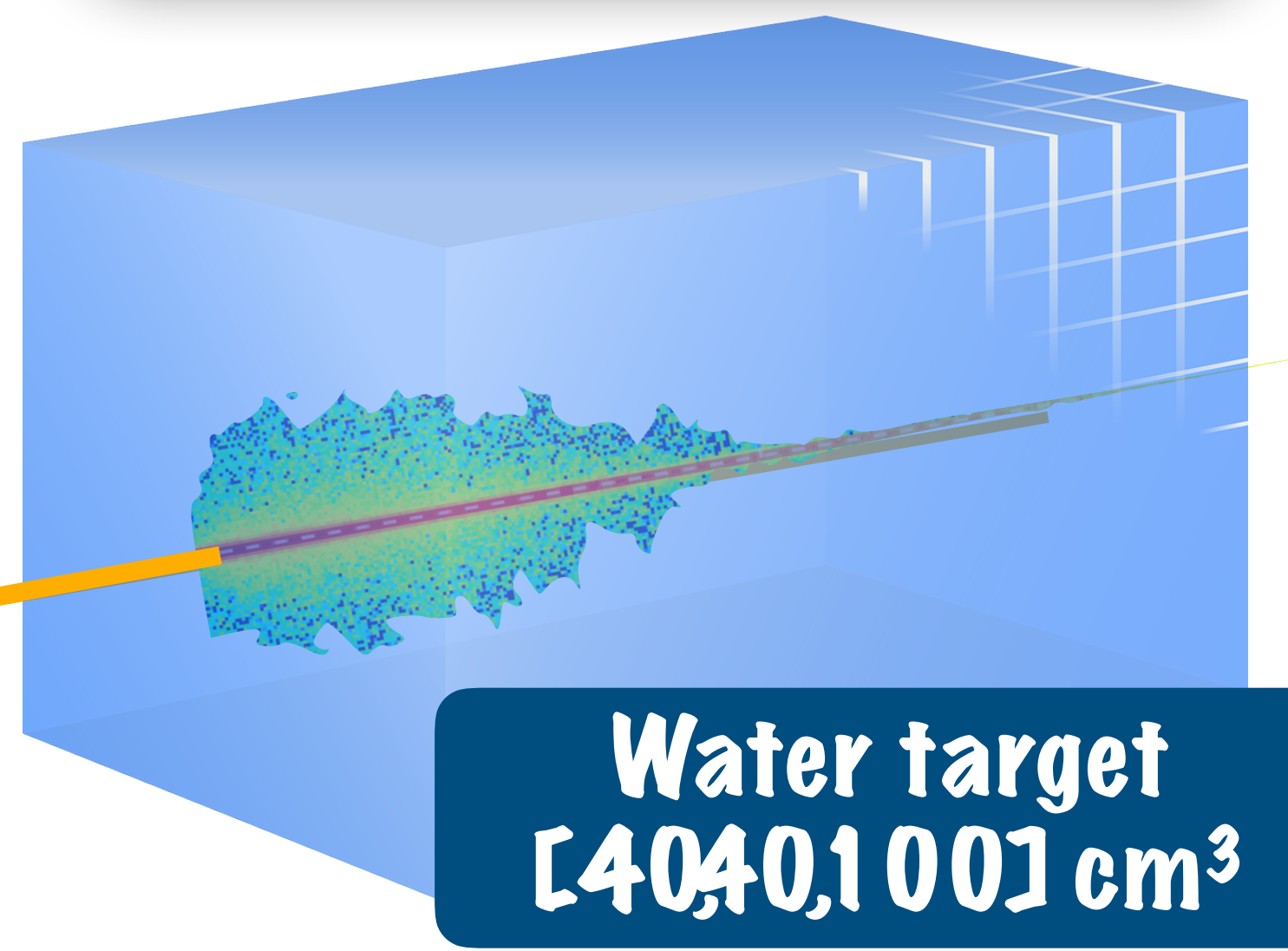
Thick target benchmark

FRED-em dose

Once I have obtained a successful agreement between the **FLUKA** and **FRED** electromagnetic models, I have checked the **dose distribution** released in different materials.



1e6 γ at 1 MeV



FRED-em performance			
Dose integral	FLUKA	FRED-CPU	FRED-GPU
@ 1 MeV	1.404 · 10 ⁻⁸ Gy/primary	1.408 · 10 ⁻⁸ Gy/primary	1.406 · 10 ⁻⁸ Gy/primary

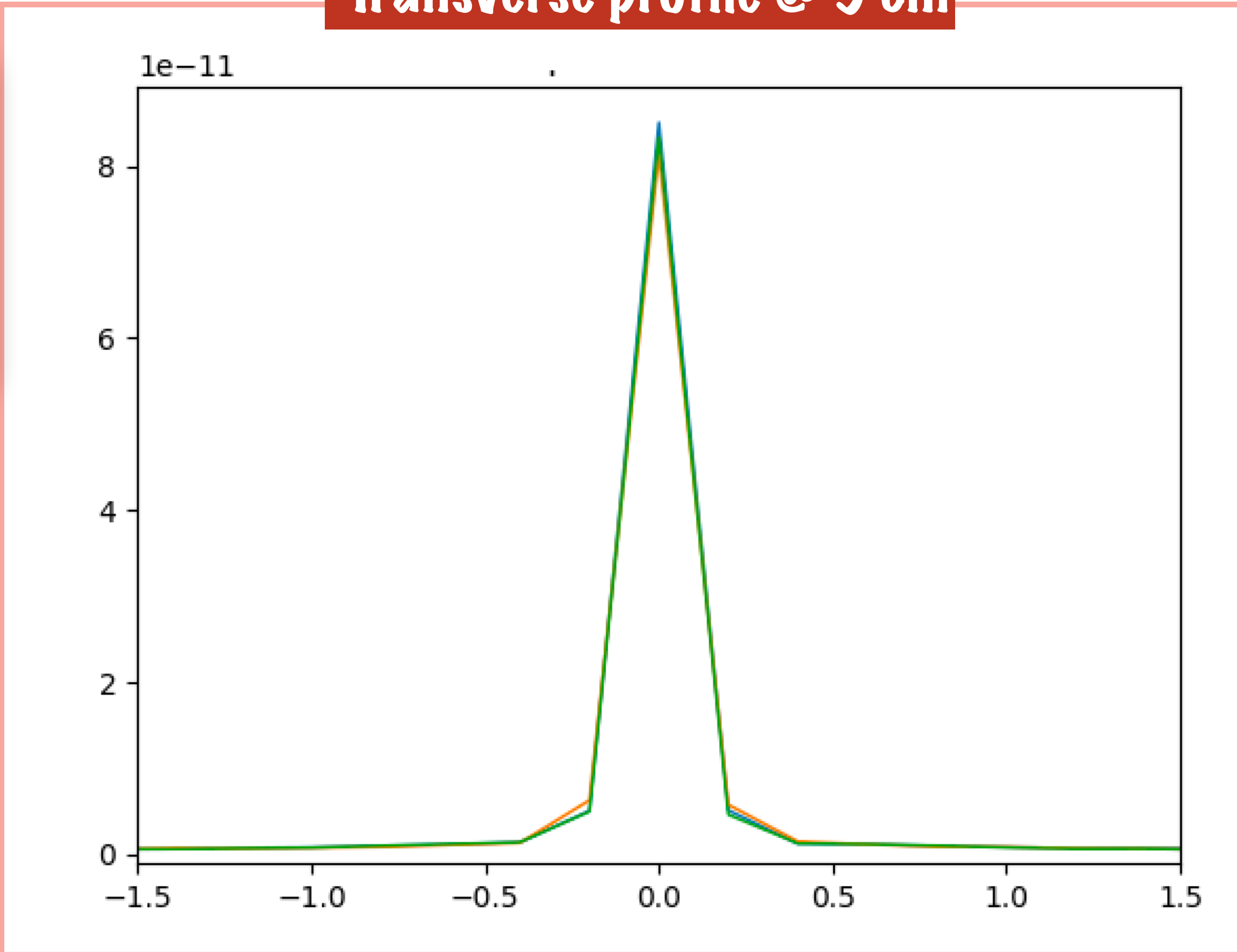
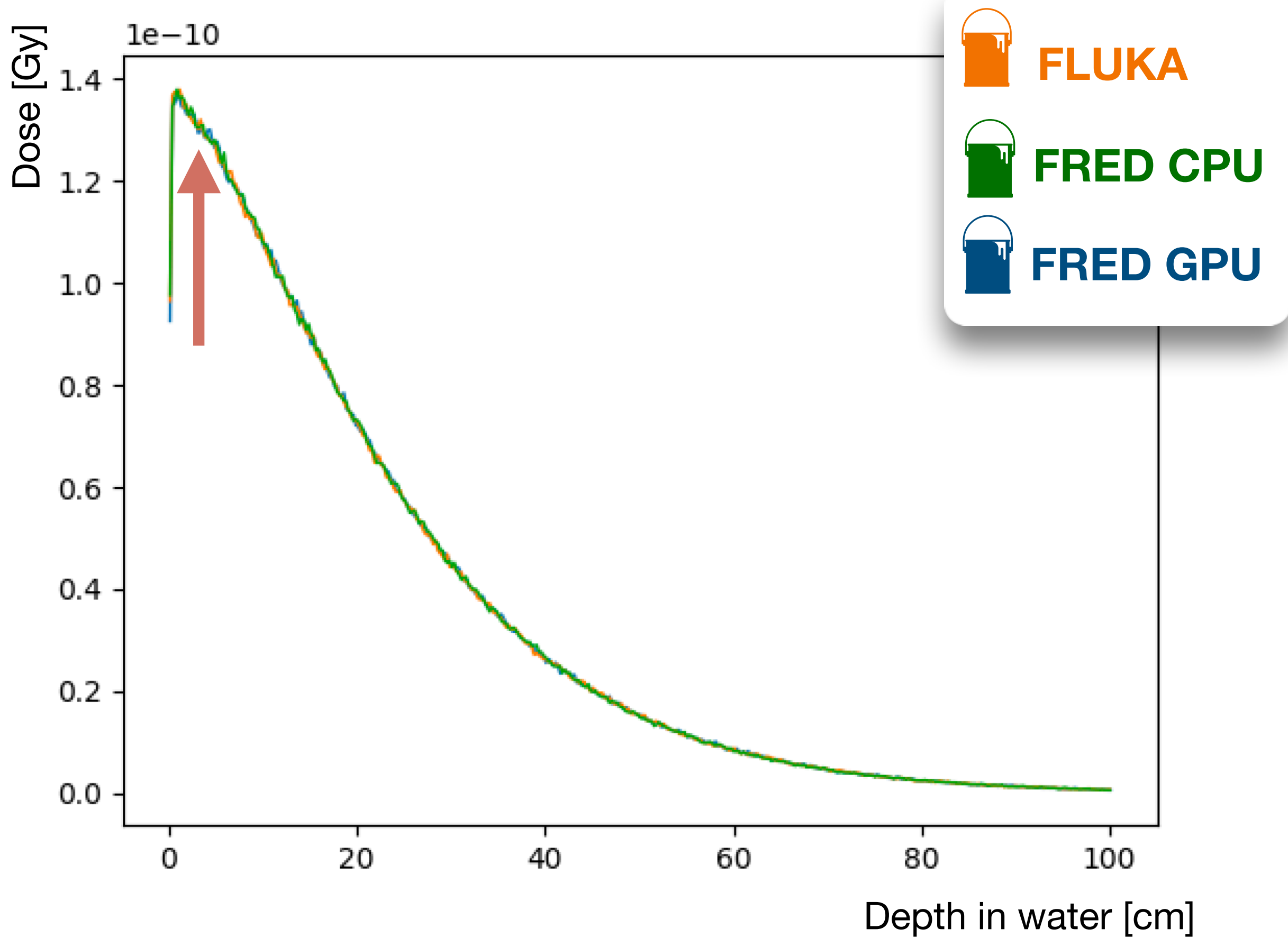
diff ~ 0.14%

Thick target benchmark

FRED-em dose

Once I have obtained a successful agreement between the **FLUKA** and **FRED** electromagnetic models, I have checked the **dose distribution** released in different materials.

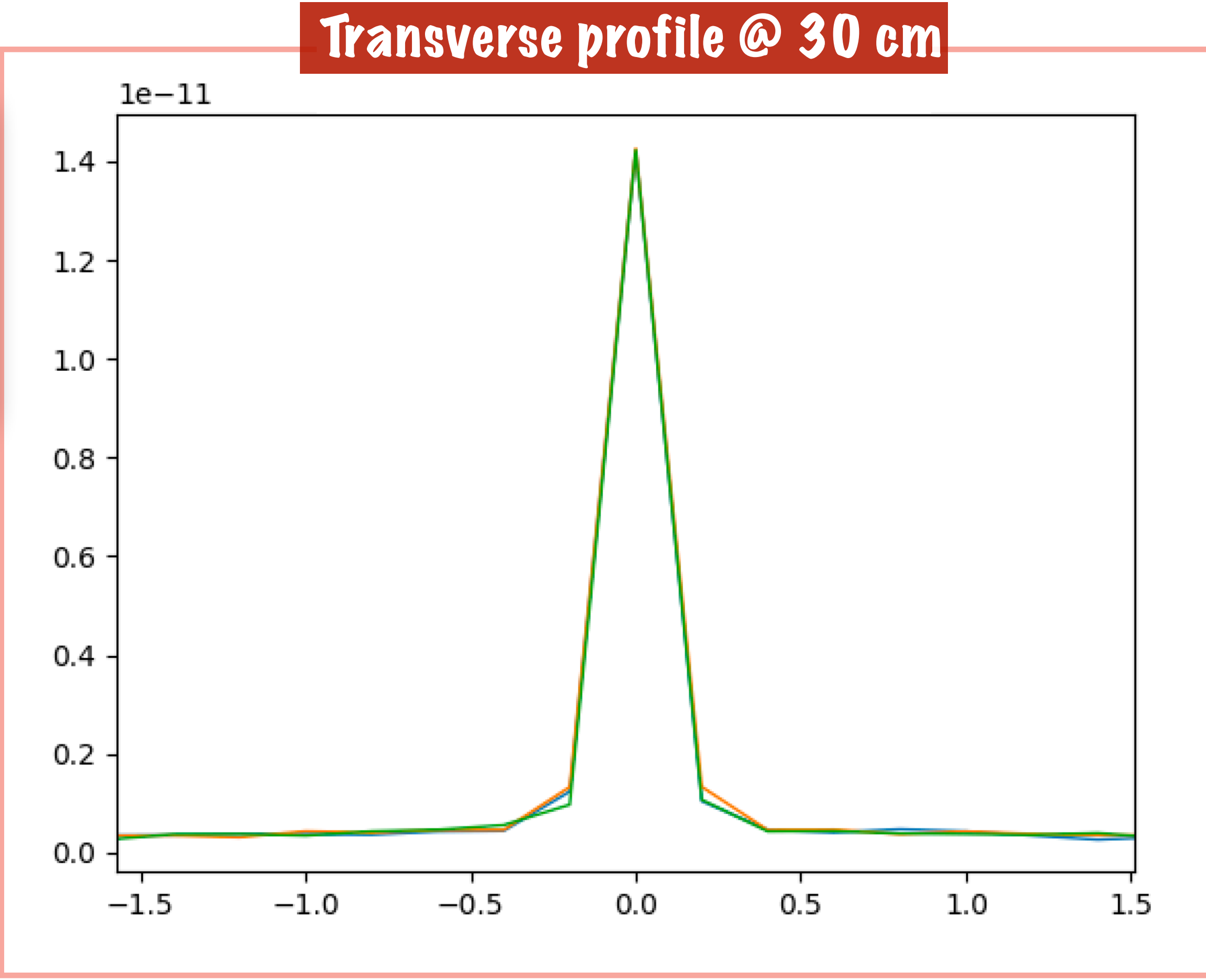
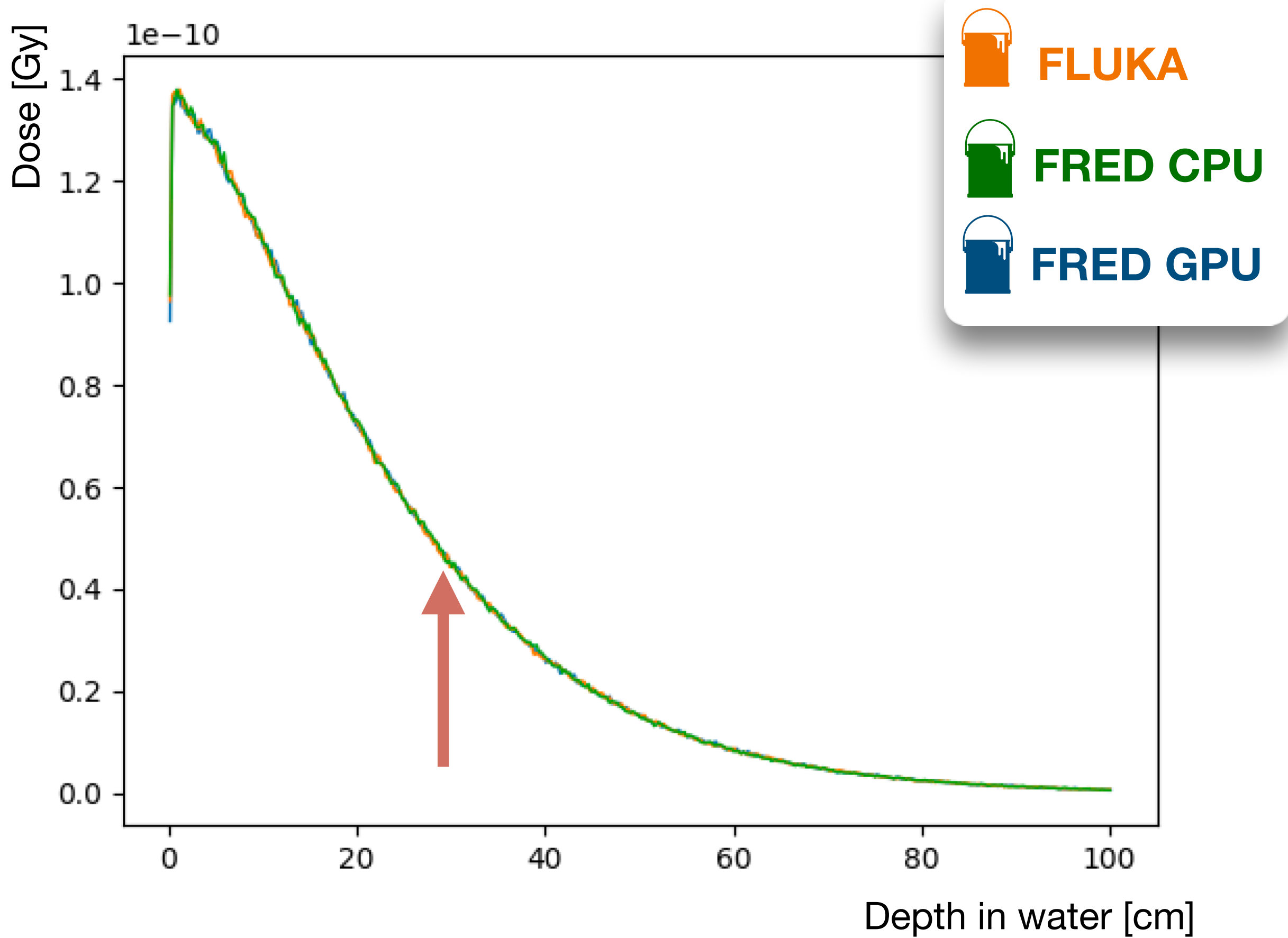
Transverse profile @ 5 cm



Thick target benchmark

FRED-em dose

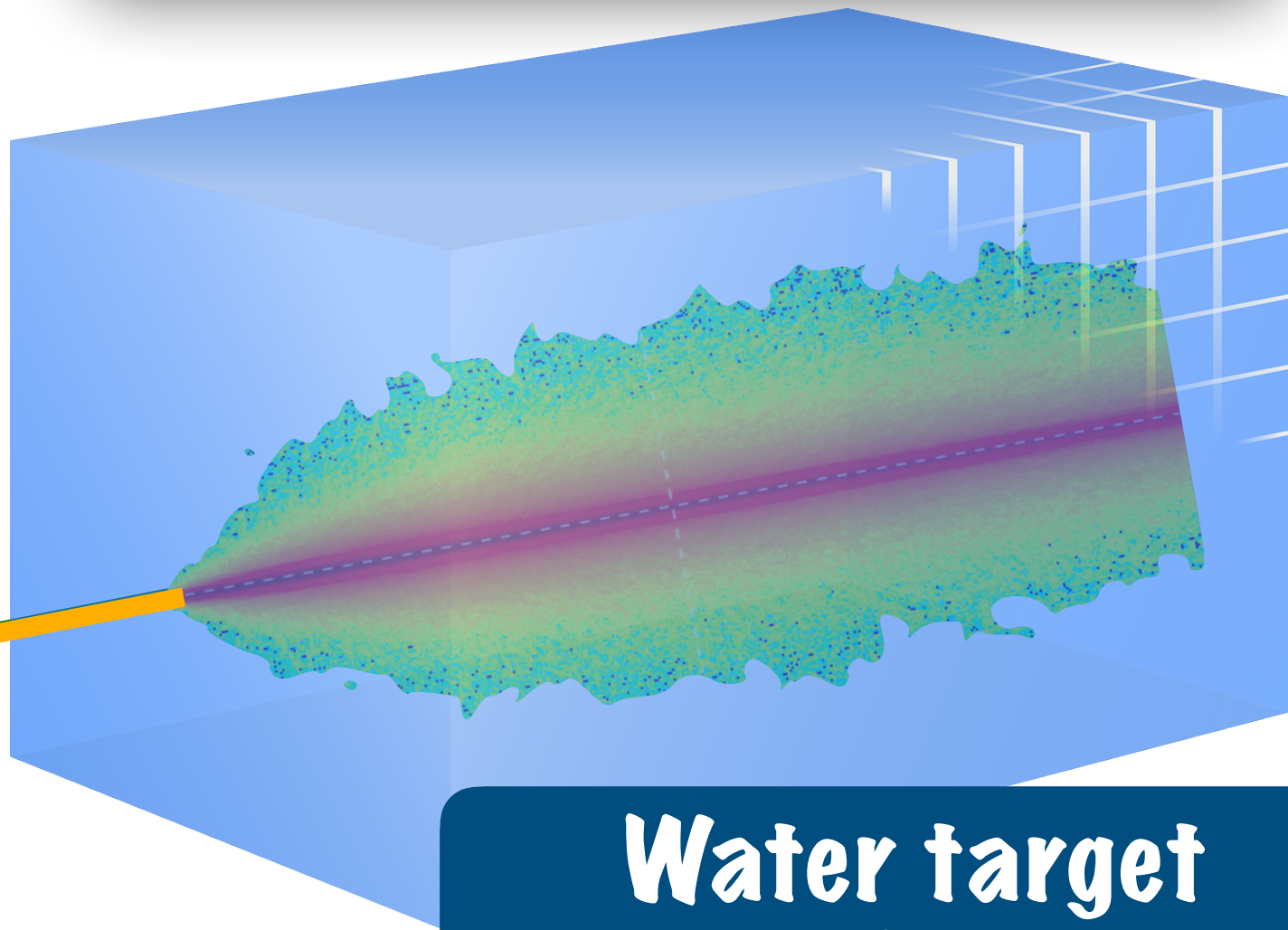
Once I have obtained a successful agreement between the **FLUKA** and **FRED** electromagnetic models, I have checked the **dose distribution** released in different materials.



Thick target benchmark

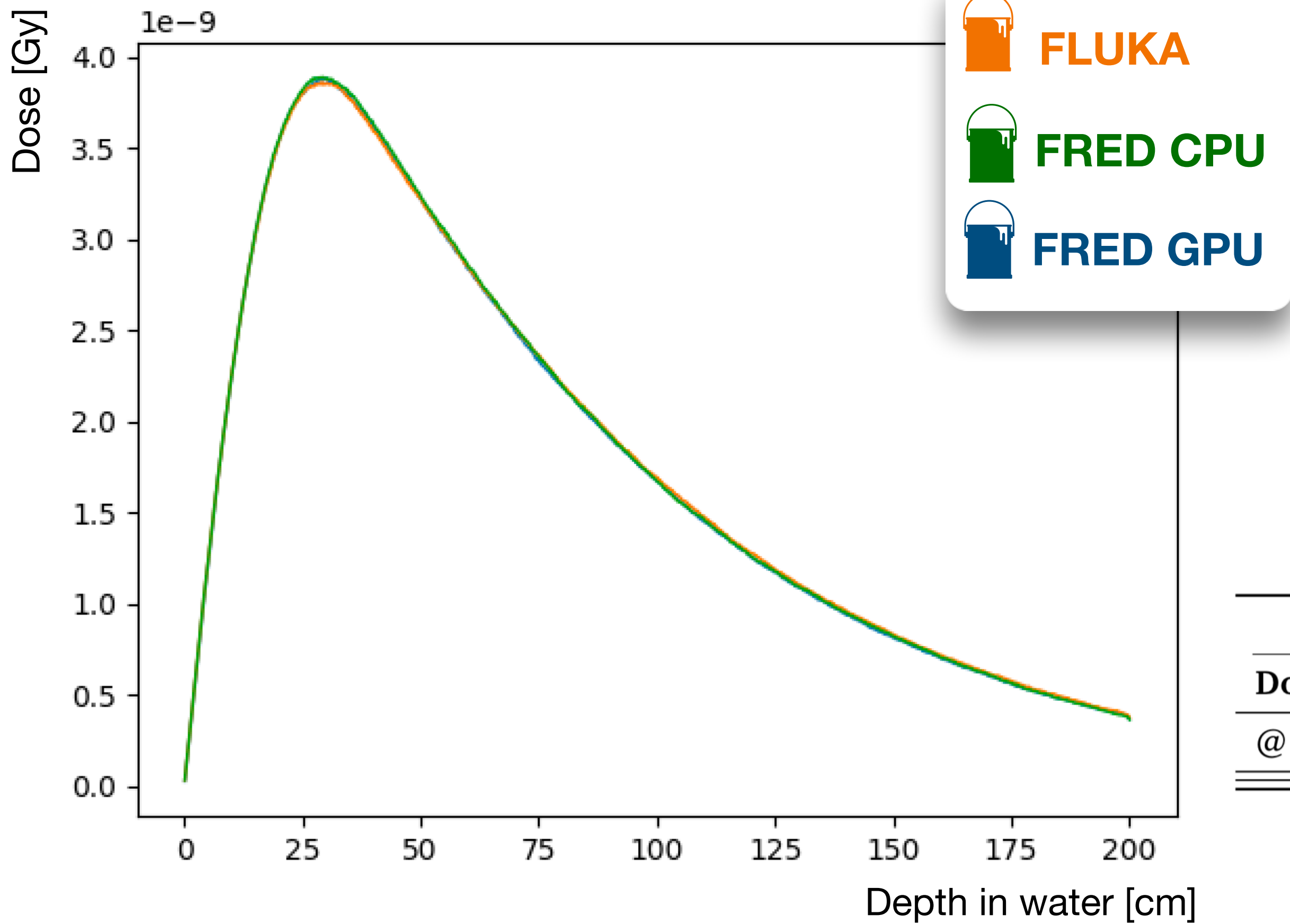
Ones I have obtained a successful agreement between the **FLUKA** and **FRED** electromagnetic models, I have checked the **dose distribution** released in different materials.

FRED-em dose



1e6 γ at 100 MeV

Water target [40, 40, 200] cm³



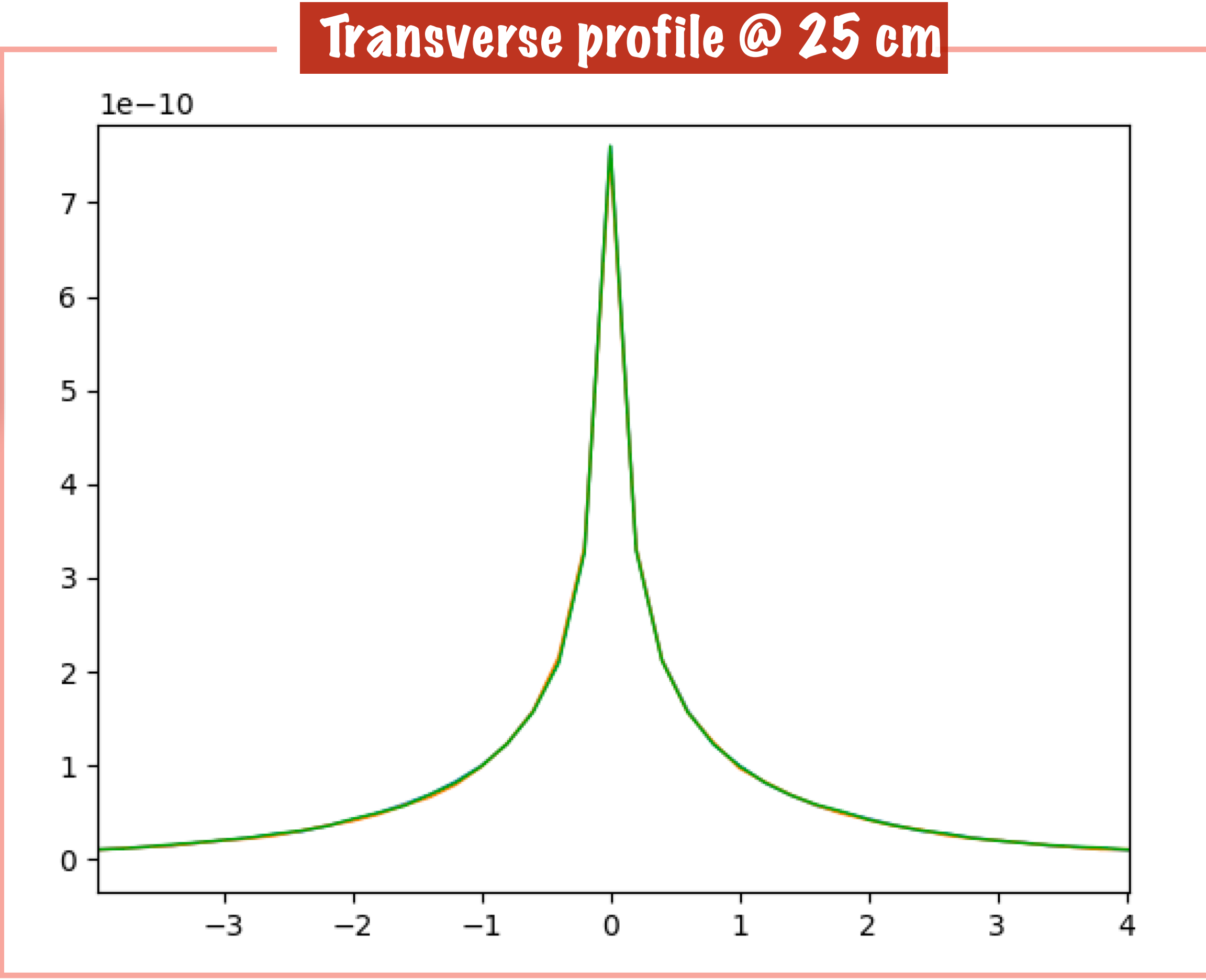
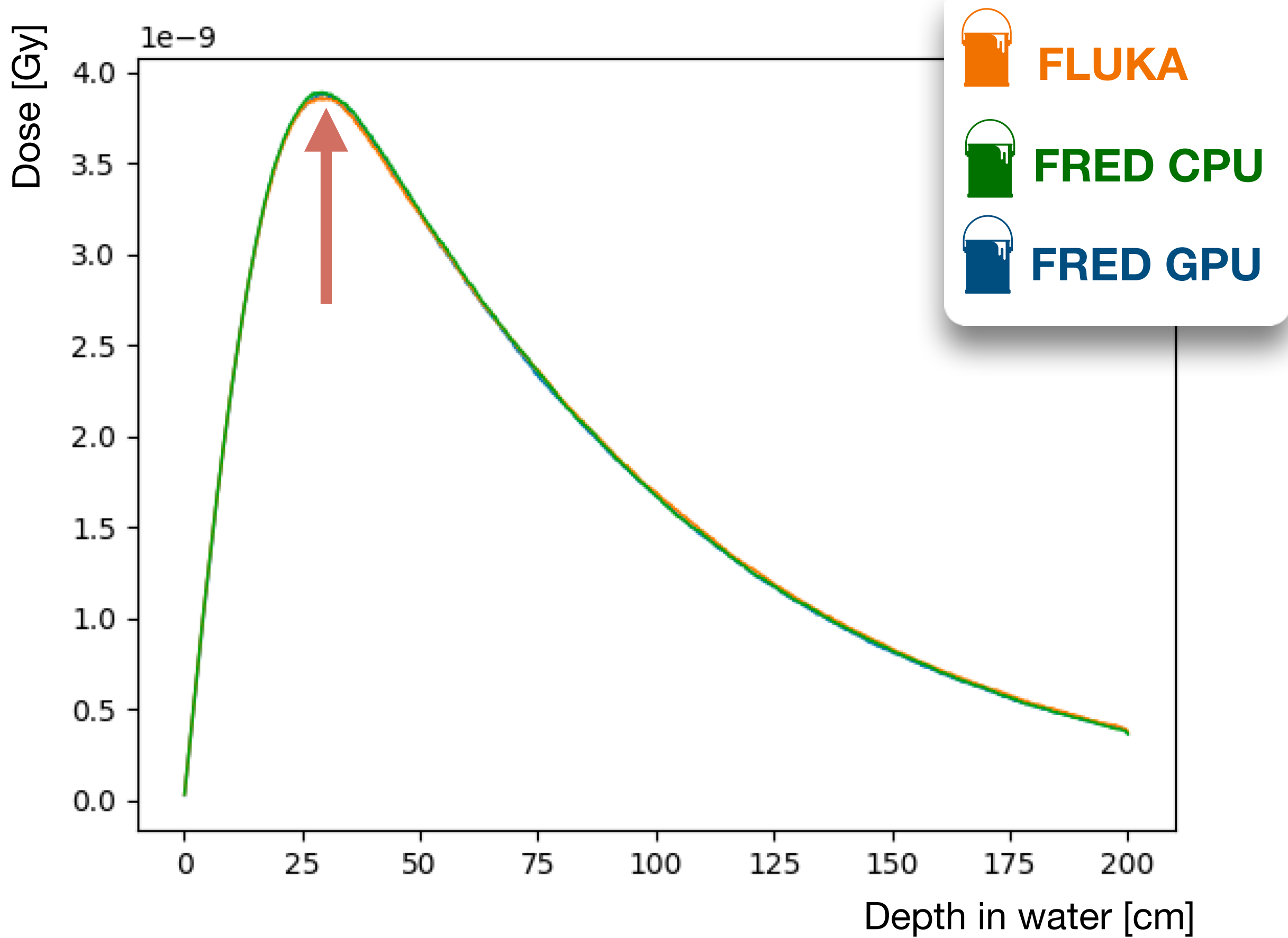
FRED-em performance			
Dose integral	FLUKA	FRED-CPU	FRED-GPU
@ 100 MeV	$1.801 \cdot 10^{-6}$ Gy/primary	$1.799 \cdot 10^{-6}$ Gy/primary	$1.793 \cdot 10^{-6}$ Gy/primary

diff ~ 0.44%

Thick target benchmark

FRED-em dose

Ones I have obtained a successful agreement between the **FLUKA** and **FRED** electromagnetic models, I have checked the **dose distribution** released in different materials.

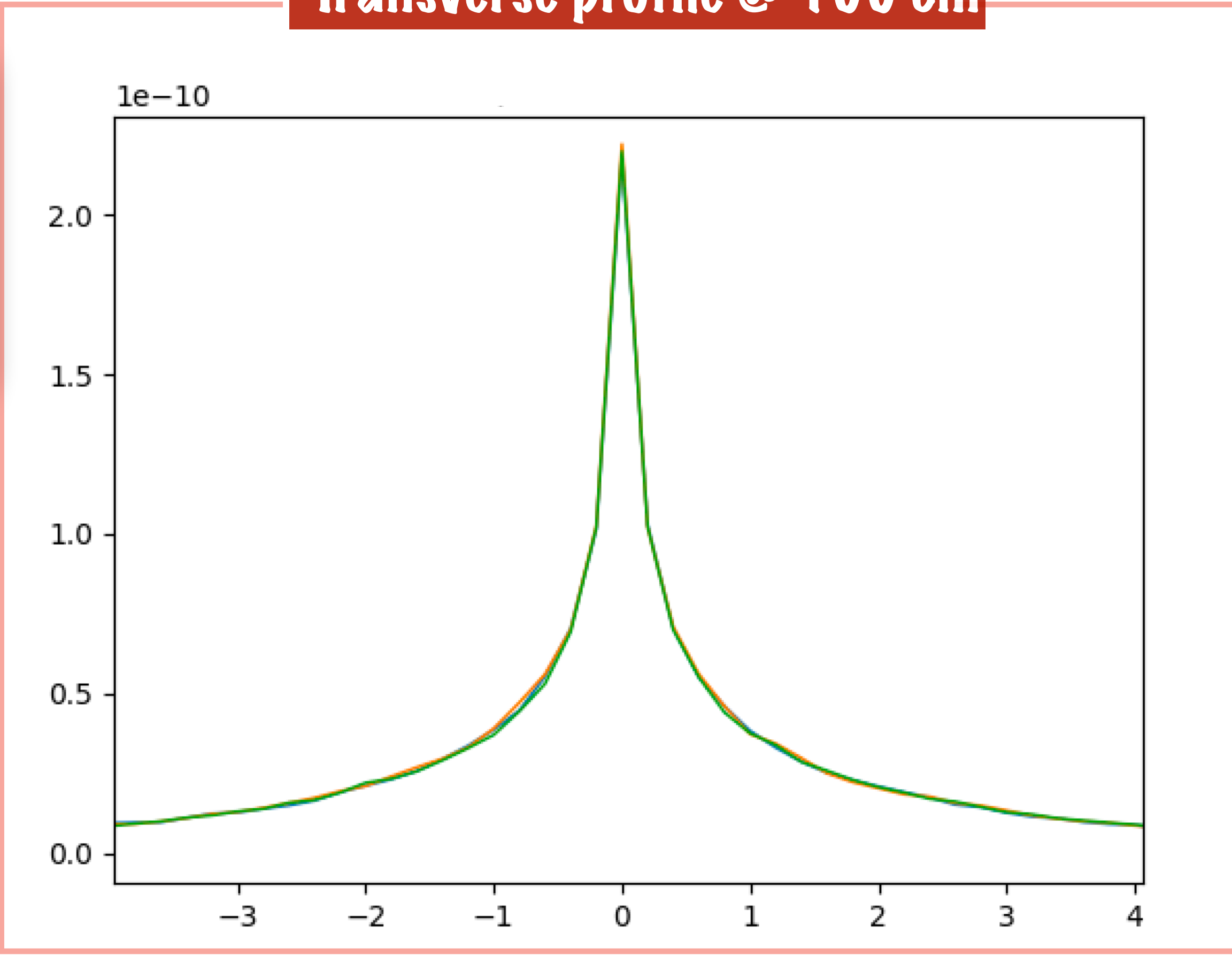
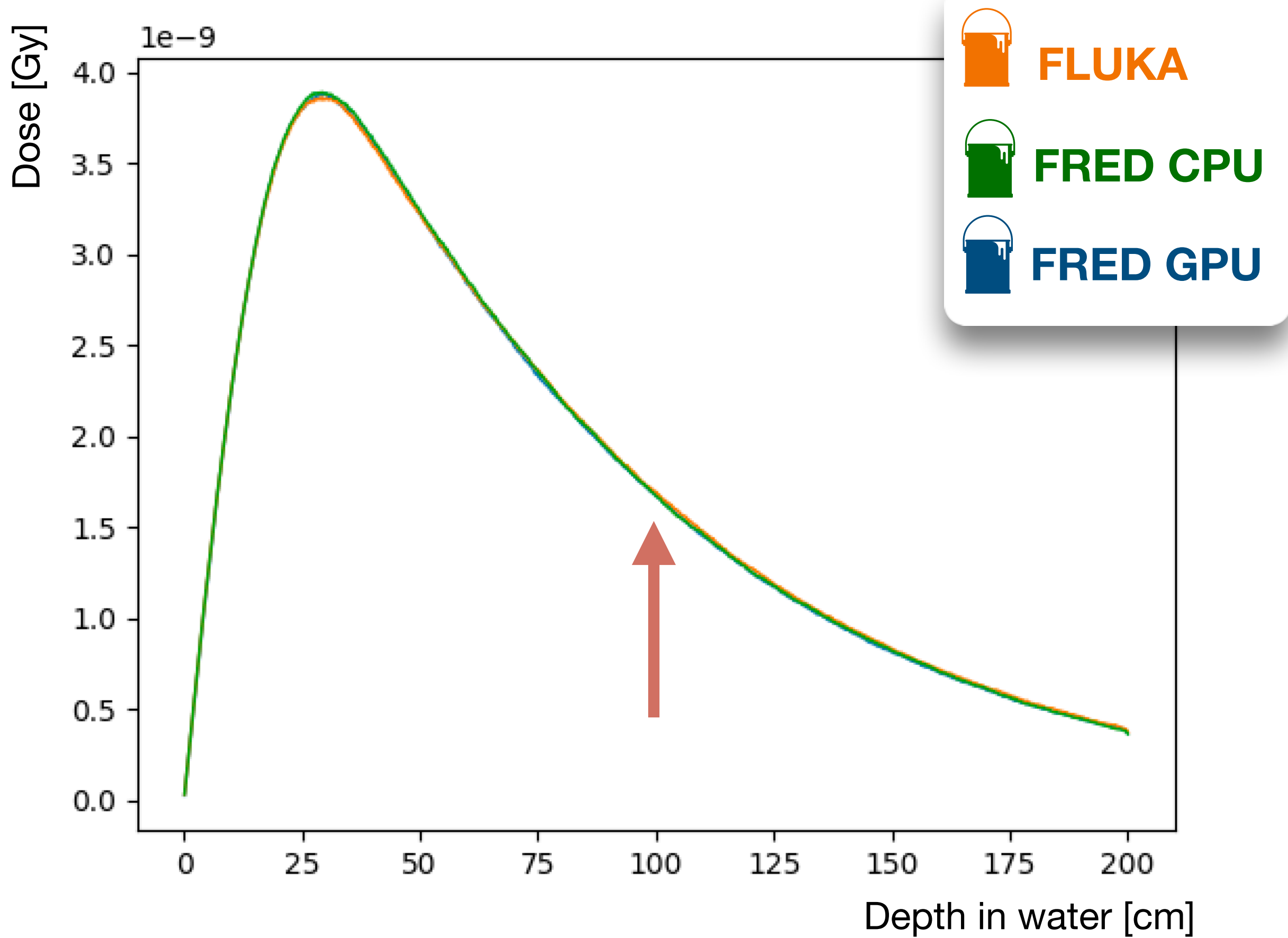


Thick target benchmark

FRED-em dose

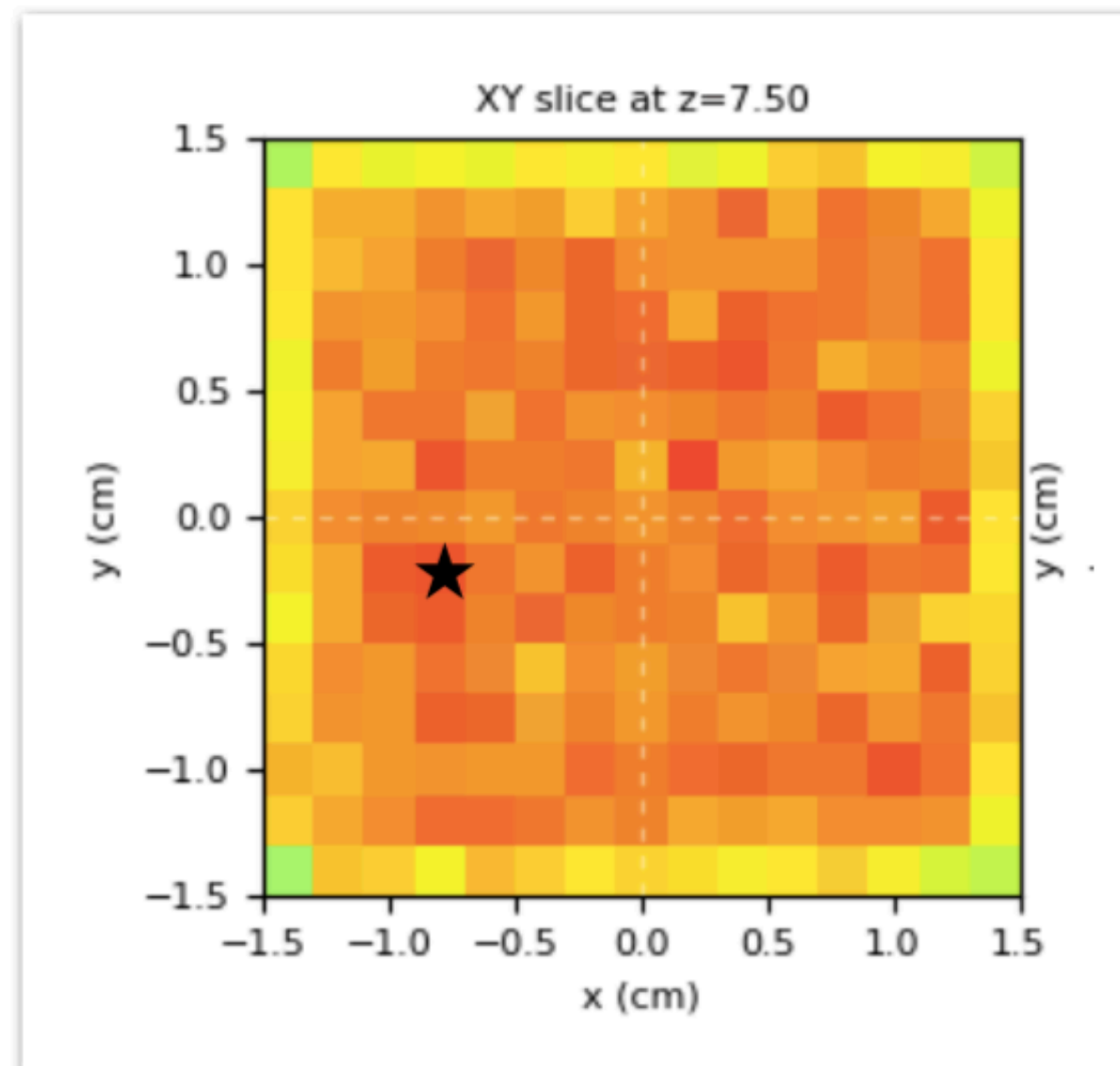
Once I have obtained a successful agreement between the **FLUKA** and **FRED** electromagnetic models, I have checked the **dose distribution** released in different materials.

Transverse profile @ 100 cm

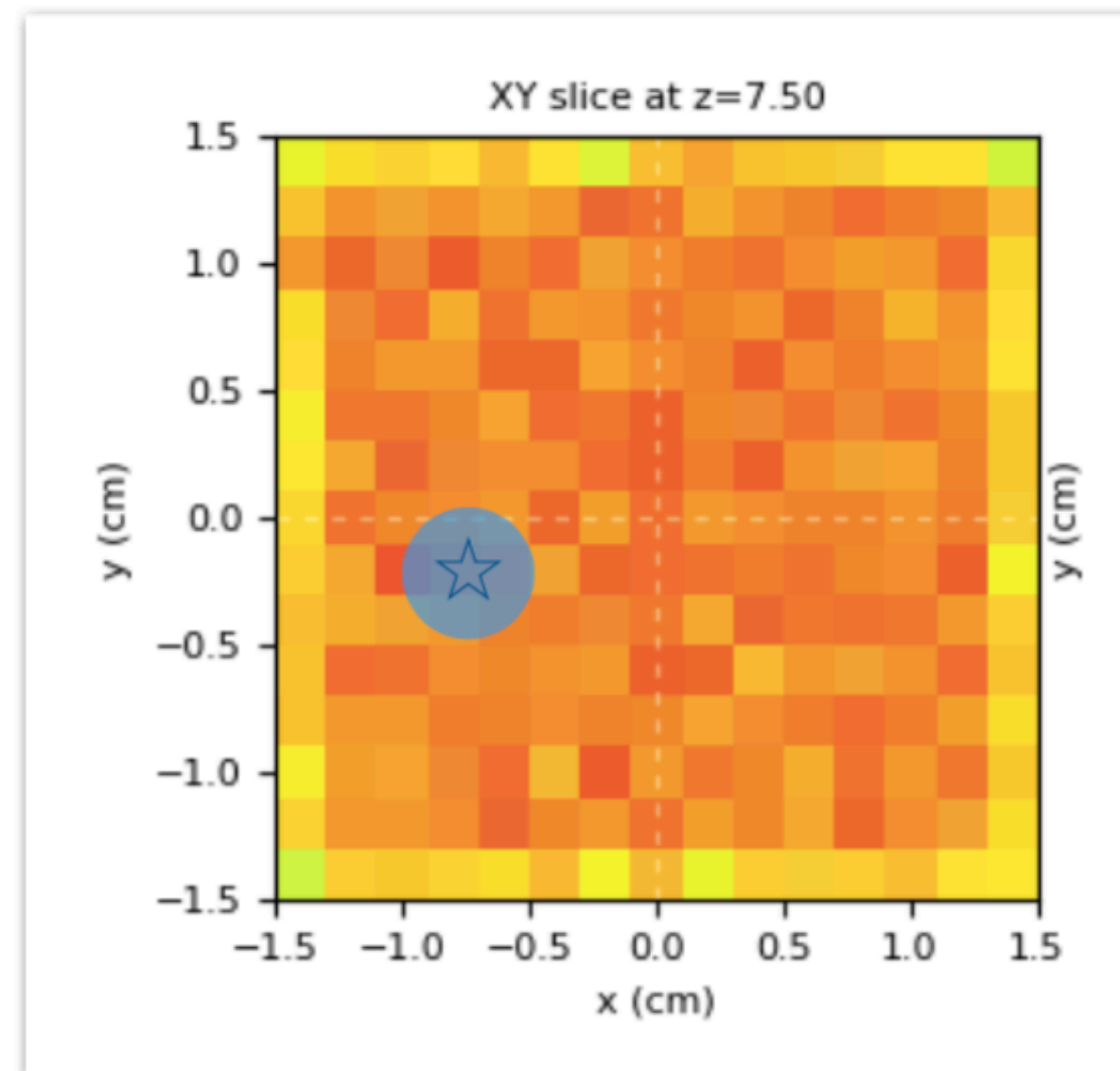


Gamma index analysis

Reference Map



Evaluation Map



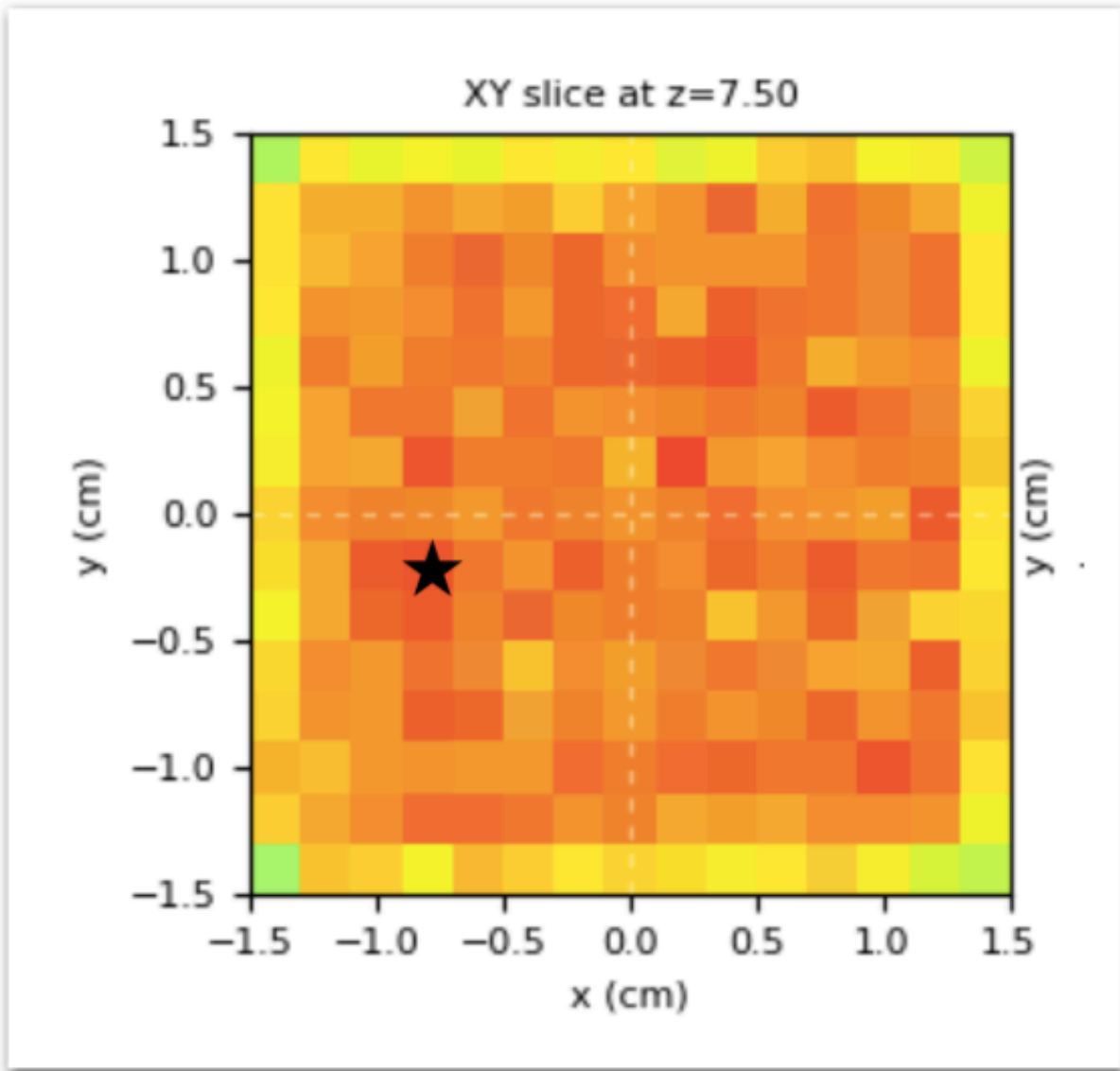
γ -index 2mm/3%

$$\Gamma(\vec{r}_e, \vec{r}_r) = \sqrt{\frac{|\vec{r}_e - \vec{r}_r|^2}{\Delta r^2} + \frac{[D_e(\vec{r}_e) - D_r(\vec{r}_r)]^2}{\Delta D^2}}$$

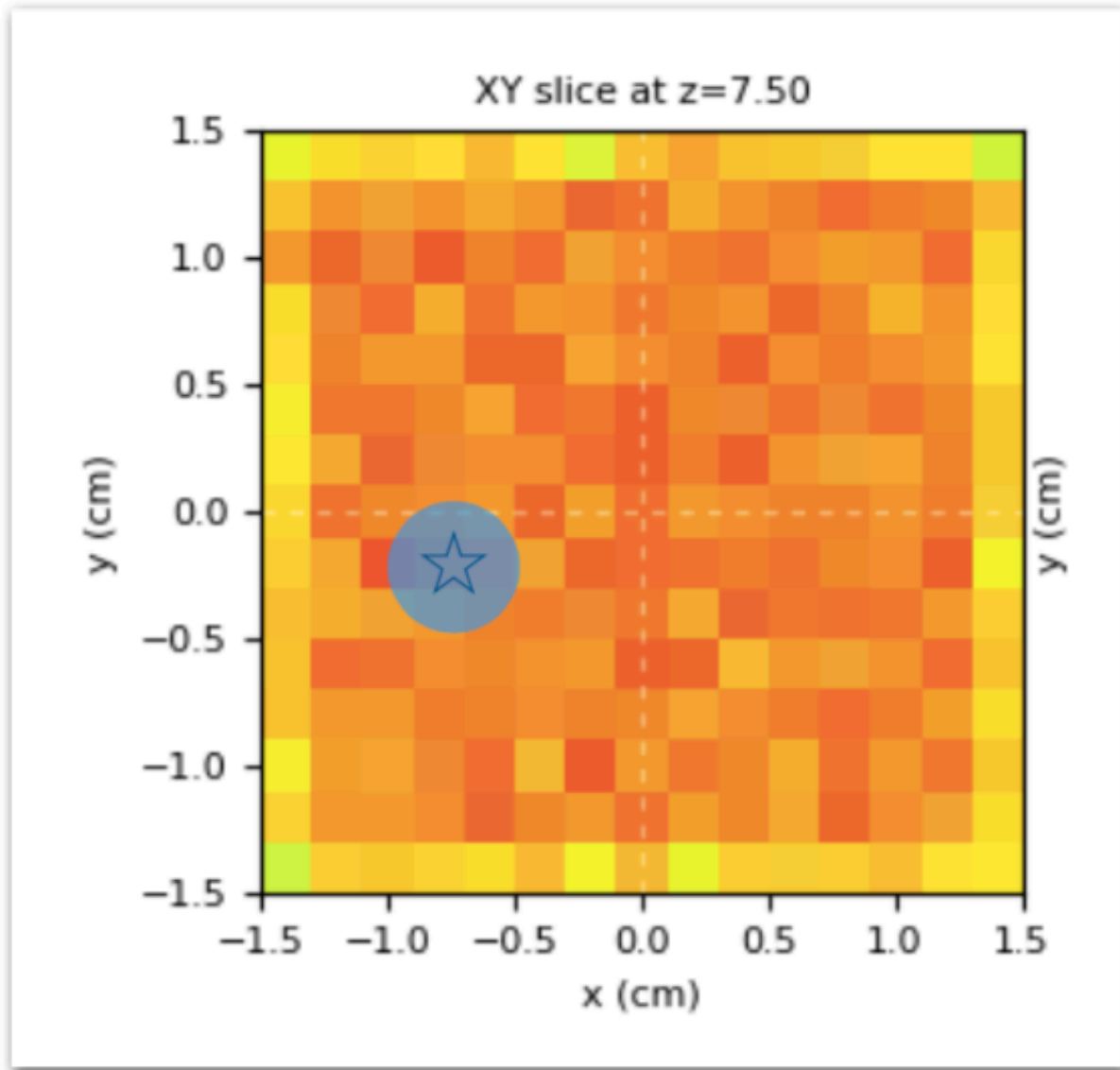
D= dose (D_r of the reference map, D_e of the evaluation map)
r = position of the evaluated point (r_r of the reference map, r_e of the evaluation map)

Gamma index analysis

Reference Map



Evaluation Map



$$\gamma(\vec{r}_r) = \min\{\Gamma(\vec{r}_e, \vec{r}_r)\} \forall \{\vec{r}_e\}$$

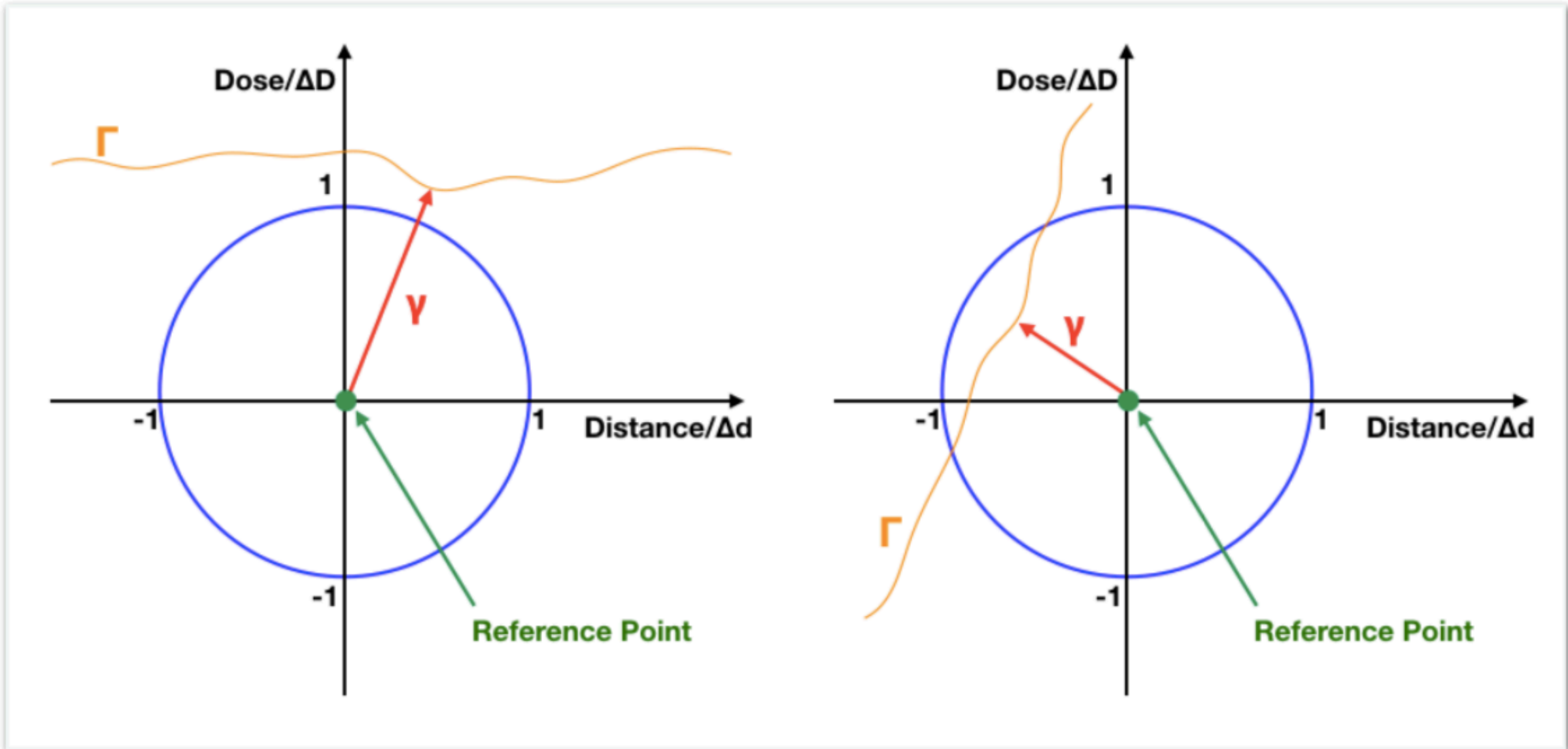
$\gamma \leq 1$ = test passed
 $\gamma > 1$ = test NOT passed

pass rate $\geq 92\%$
 clinical acceptance

γ -index 2mm/3%

$$\Gamma(\vec{r}_e, \vec{r}_r) = \sqrt{\frac{|\vec{r}_e - \vec{r}_r|^2}{\Delta r^2} + \frac{[D_e(\vec{r}_e) - D_r(\vec{r}_r)]^2}{\Delta D^2}}$$

D= dose (D_r of the reference map, D_e of the evaluation map)
 r = position of the evaluated point (r_r of the reference map, r_e of the evaluation map)



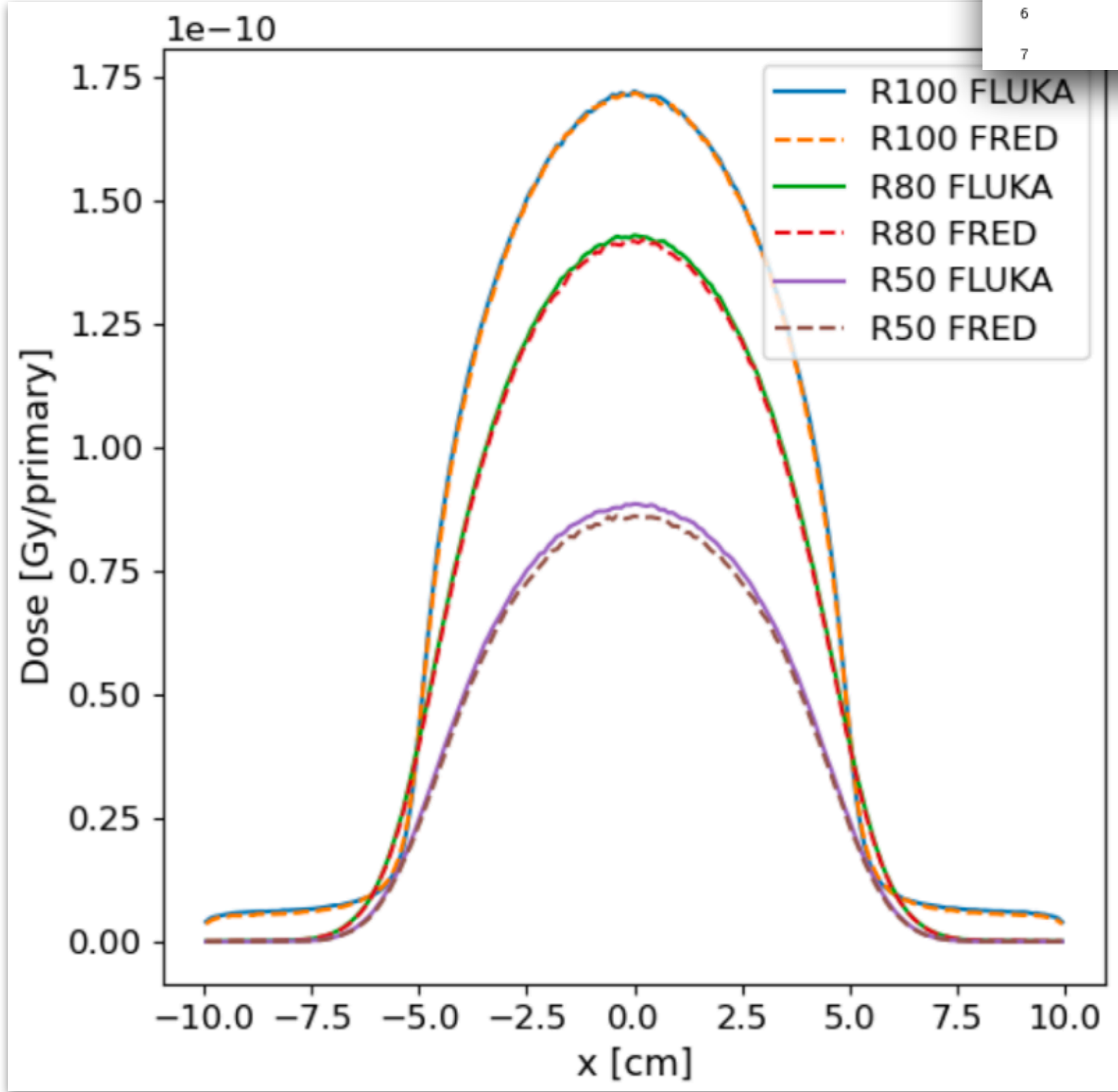
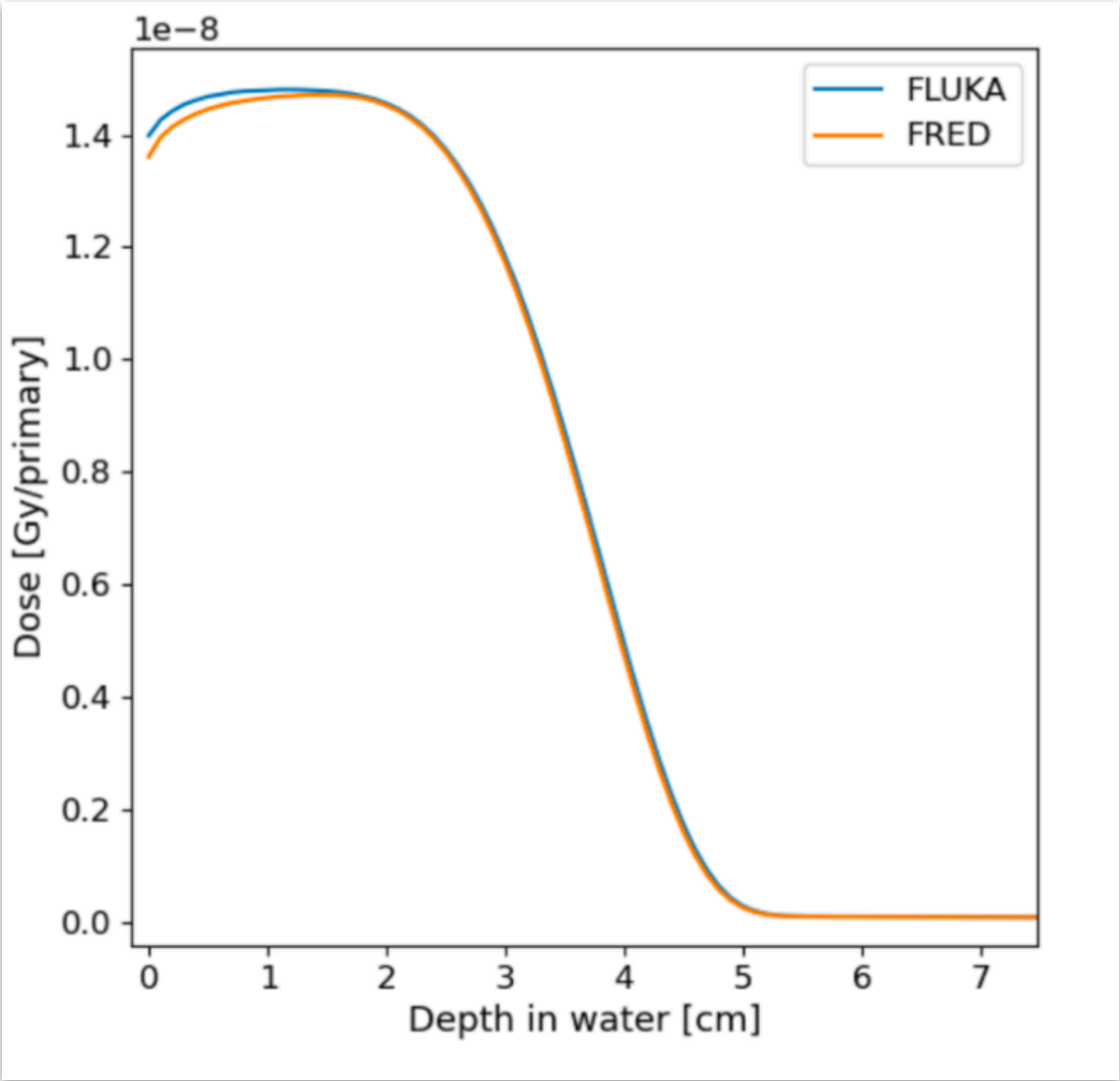
FRED-em applicator: FLUKA benchmark



To test step-by-step the performance of the FRED simulation I have compared the FRED outputs with the ones obtained using an equal **FLUKA** simulation that was previously validated by comparing it with the experimental data.

1 Preliminary study on the correlation between accelerated
 2 current and dose in water for an electron based linac
 3 **G. Franciosini^a**, S. Muraro^c, S. Barone^d, P. De Maria^e, M. De
 4 Simon^f, M. Di Francesco^d, F. Di Martino^f, G. Felici^d, M.
 5 Fischetti^{a,b}, F. Galante^d, L. Grasso^d, M. Marafini^{g,b}, M. Pacitti^d, V.
 6 Patera^{a,b}, A. Sarti^{a,b}, A. Schiavi^a, M. Toppi^{h,*}, G. Traini^{a,b}, G.
 7 Battistonⁱ

to be soon published



$D_{MEAN} = 5.72e-7$ Gy/primary

$D_{MEAN} = 5.43e-7$ Gy/primary

diff ~ 5%

- R100: 100% of the peak value ~ 1.3 cm**
- R80: 80% of the peak value ~ 3.0 cm**
- R50: 50% of the peak value ~ 3.7 cm**

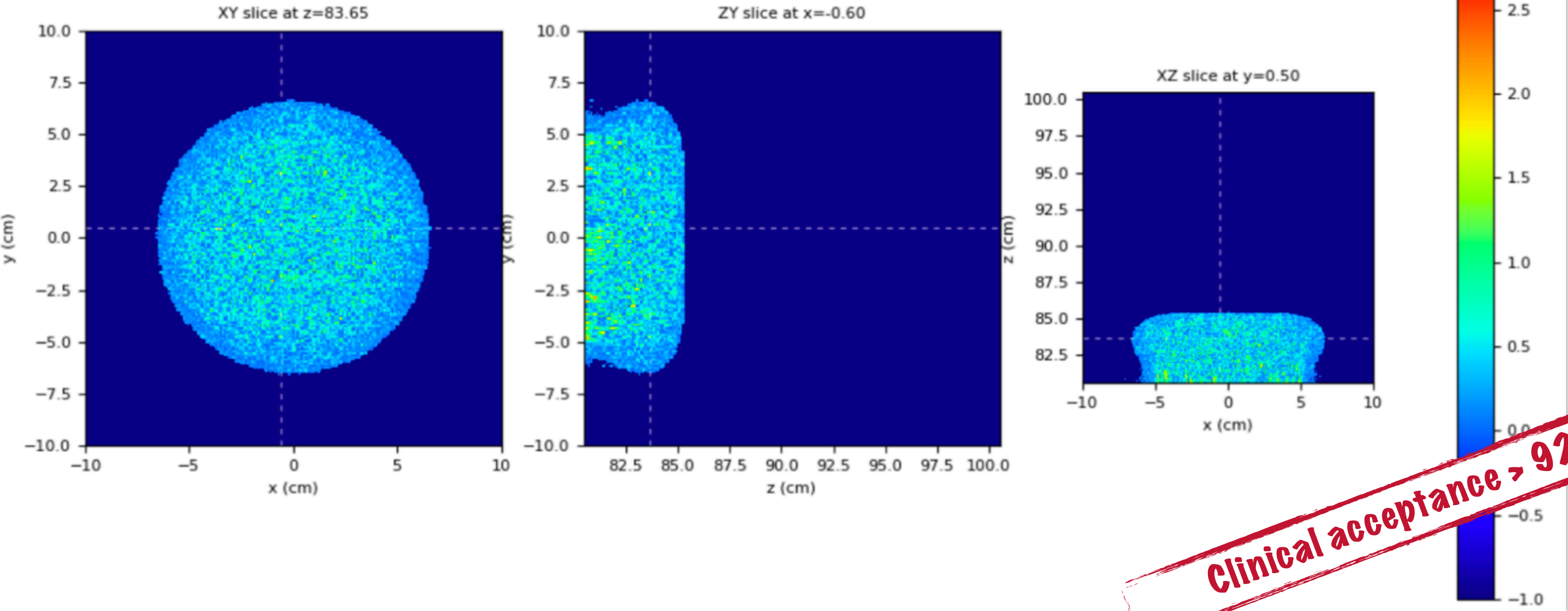
FRED-em applicator: FLUKA benchmark



To test step-by-step the performance of the FRED simulation I have compared the FRED outputs with the ones obtained using an equal **FLUKA** simulation that was previously validated by comparing it with the experimental data.

1 Preliminary study on the correlation between accelerated
 2 current and dose in water for an electron based linac
 3 **G. Franciosini^a**, S. Muraro^c, S. Barone^d, P. De Maria^e, M. De
 4 Simon^f, M. Di Francesco^d, F. Di Martino^f, G. Felici^d, M.
 5 Fischetti^{a,b}, F. Galante^d, L. Grasso^d, M. Marafini^{g,b}, M. Pacitti^d, V.
 6 Patera^{a,b}, A. Sarti^{a,b}, A. Schiavi^a, M. Toppi^{h,*}, G. Traini^{a,b}, G.
 7 Battistoni^c

to be soon published



Gamma-index 3mm/3%
 pass rate: 93.18%

Clinical acceptance > 92%

FLASH effect

Several pre-clinical studies recently claimed that the toxicity in healthy tissues related to tumour treatments can be significantly reduced (from 80% down to 60%), while keeping the same efficacy in cancer killing, if the dose rate is radically increased (~**10 Gy/s**, or even more) with respect to conventional treatments (~**0.01 Gy/s**).

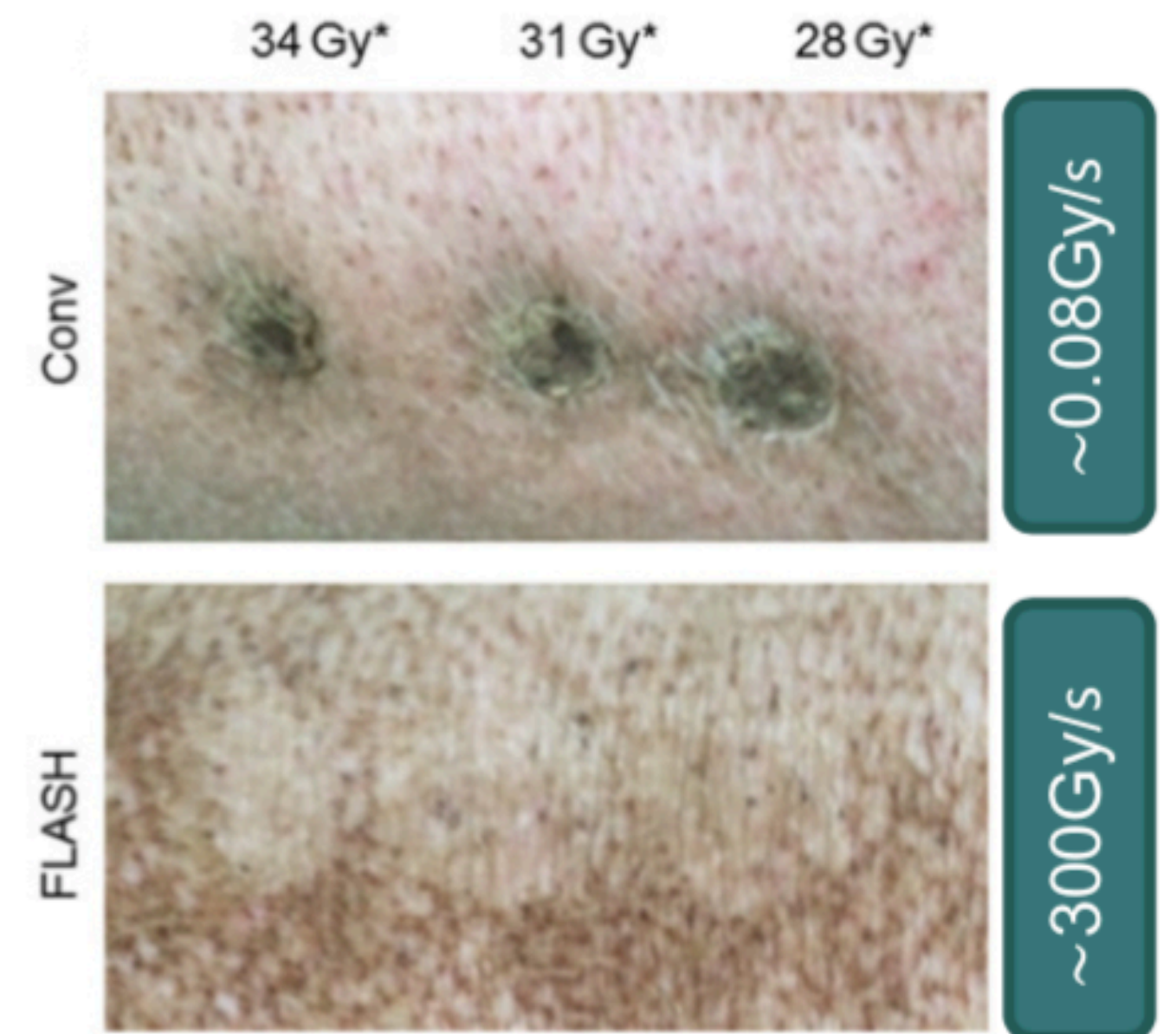
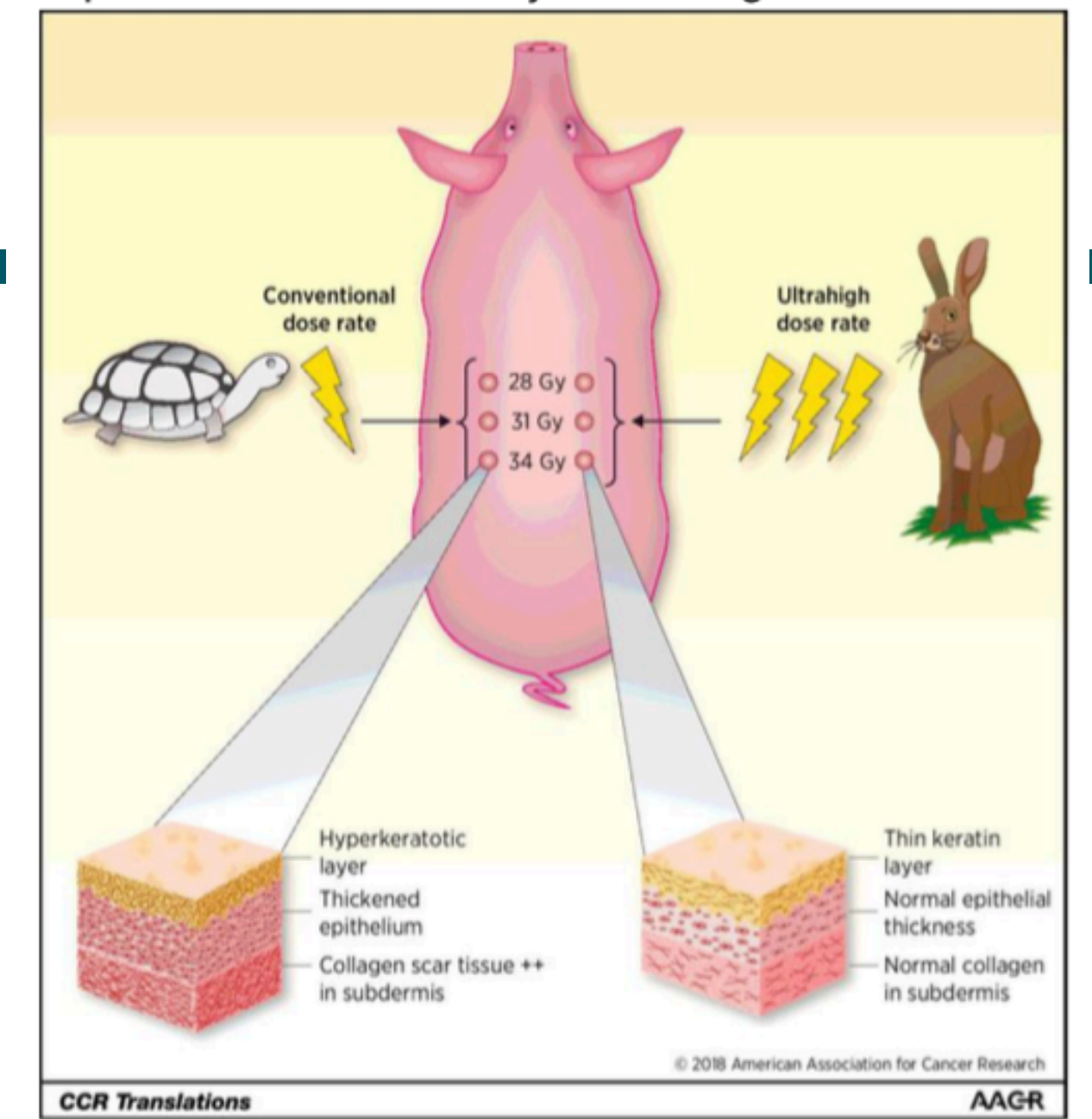


1. Tumor response, analogous to the one obtained with conventional RT
2. Reduced radiation-induced toxicities in the healthy tissues

The mechanism responsible for reduced tissue toxicity following FLASH radiotherapy is yet to be clarified



?Modification of the immune response?



DOI: 10.1158/1078-0432.CCR-17-3375

Moeller/Bhabha scattering

Total cross-section for Moeller scattering (e^-e^-)

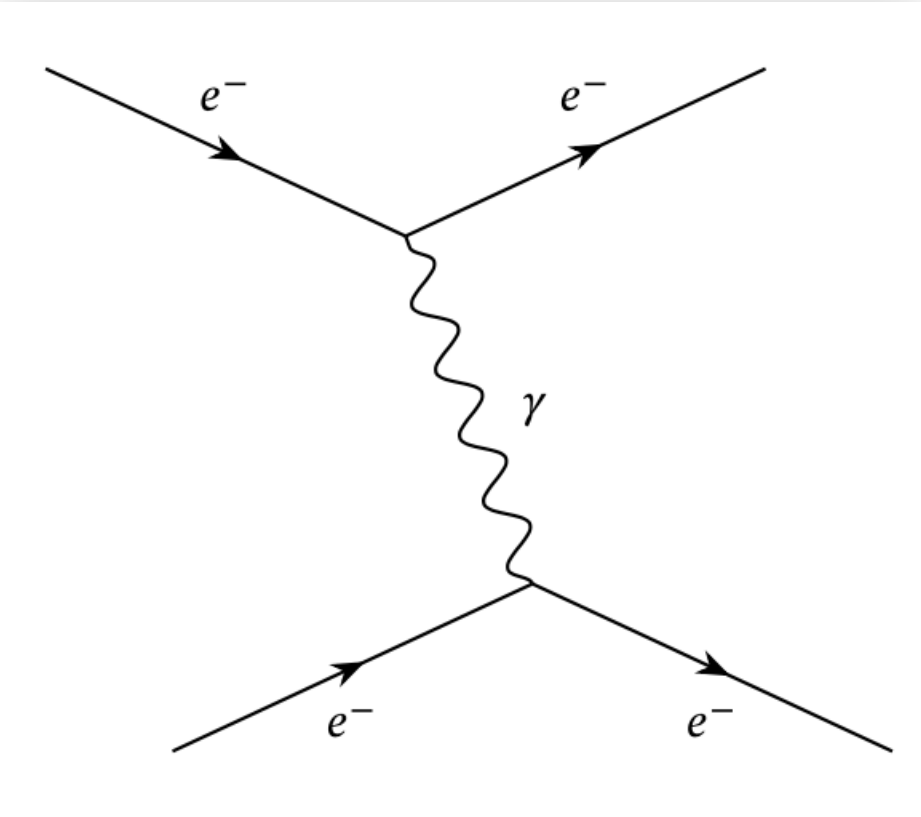
$$\sigma(Z, E, T_{cut}) = \frac{2\pi r_e^2 Z}{\beta^2(\gamma - 1)} \left[\frac{(\gamma - 1)^2}{\gamma^2} \left(\frac{1}{2} - x \right) + \frac{1}{x} - \frac{1}{1 - x} - \frac{2\gamma - 1}{\gamma^2} \ln \frac{1 - x}{x} \right]$$

Total cross-section for Bhabha scattering e^+e^-

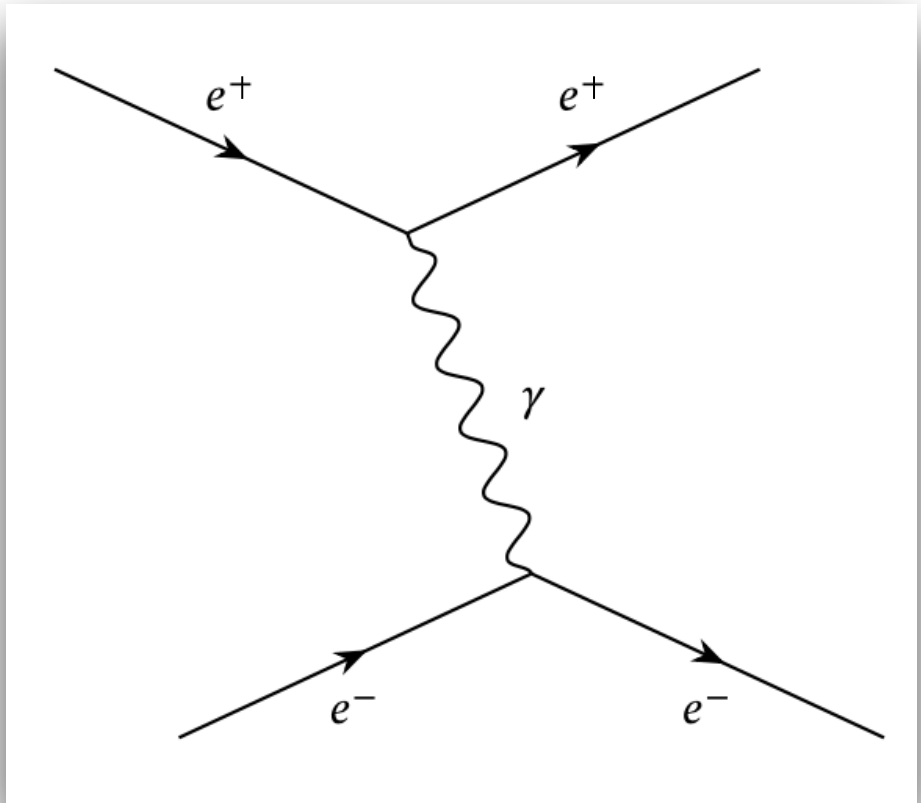
$$\sigma(Z, E, T_{cut}) = \frac{2\pi r_e^2 Z}{(\gamma - 1)} \left[\frac{1}{\beta^2} \left(\frac{1}{x} - 1 \right) + B_1 \ln x + B_2(1 - x) - \frac{B_3}{2}(1 - x^2) + \frac{B_4}{3}(1 - x^3) \right]$$

with

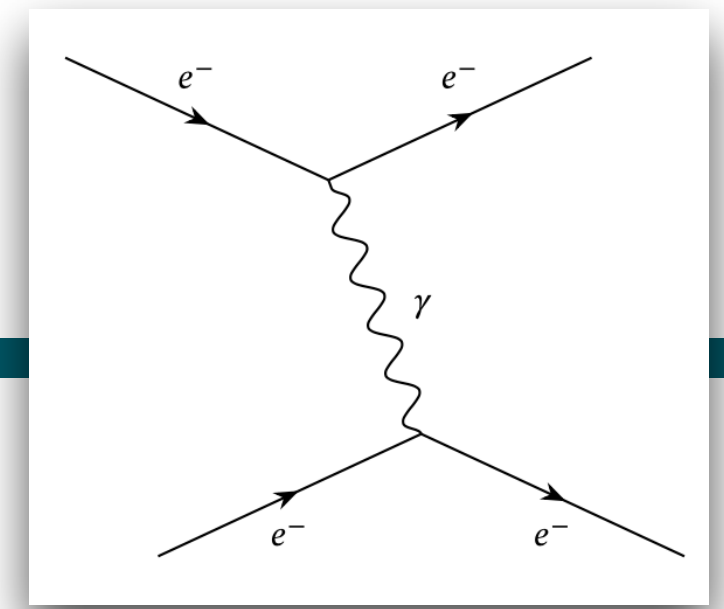
γ	$= E/mc^2$	B_1	$= 2 - y^2$
β^2	$= 1 - (1/\gamma^2)$	B_2	$= (1 - 2y)(3 + y^2)$
x	$= T_{cut}/(E - mc^2)$	B_3	$= (1 - 2y)^2 + (1 - 2y)^3$
y	$= 1/(\gamma + 1)$	B_4	$= (1 - 2y)^3.$



$T_{cut} = 1 \text{ keV}$



Moeller scattering: energy and angle sampling



Differential cross-section

$$\frac{d\sigma}{d\epsilon} = \frac{2\pi r_e^2 Z}{\beta^2(\gamma - 1)} \left[\frac{(\gamma - 1)^2}{\gamma^2} + \frac{1}{\epsilon} \left(\frac{1}{\epsilon} - \frac{2\gamma - 1}{\gamma^2} \right) + \frac{1}{1 - \epsilon} \left(\frac{1}{1 - \epsilon} - \frac{2\gamma - 1}{\gamma^2} \right) \right]$$

$$\epsilon = T / (E - mc^2)$$

Kinetic energy of the impinging electron

1 keV

The kinematic limit for ϵ is: $\epsilon_0 = \frac{T_{cut}}{E - mc^2} \leq \epsilon \leq \frac{1}{2}$

Sampling

We can write the cross-section as:

$$\frac{d\sigma}{d\epsilon} = f(\epsilon)g(\epsilon)$$

$$f(\epsilon) = \frac{1}{\epsilon^2} \frac{\epsilon_0}{1 - 2\epsilon_0}$$

$$g(\epsilon) = \frac{4}{9\gamma^2 - 10\gamma + 5} \left[(\gamma - 1)^2 \epsilon^2 - (2\gamma^2 + 2\gamma - 1) \frac{\epsilon}{1 - \epsilon} + \frac{\gamma^2}{(1 - \epsilon)^2} \right]$$

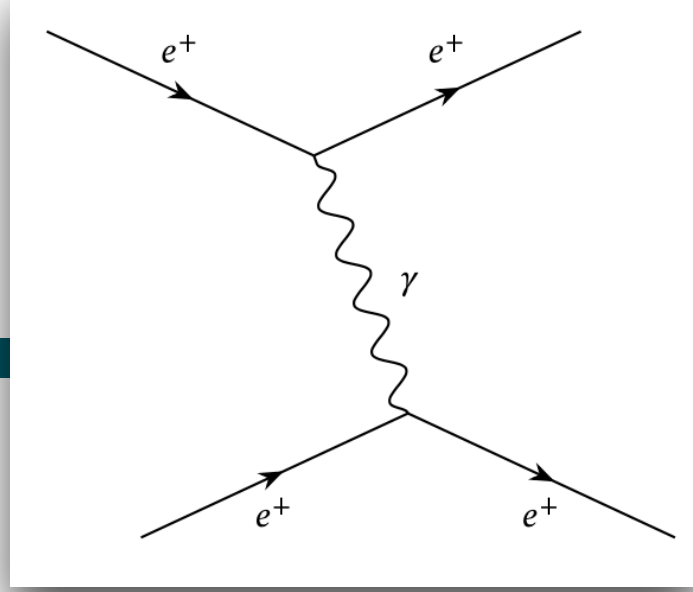
To choose ϵ , and hence the **delta ray energy**

1. ϵ is sampled from $f(\epsilon)$
2. the rejection function $g(\epsilon)$ is calculated using the sampled value of ϵ
3. ϵ is accepted with probability $g(\epsilon)$

The **azimuthal angle** φ is generated isotropically and the **polar angle** θ is calculated from energy-momentum conservation



Bhabha scattering : energy and angle sampling



Differential cross-section

$$\frac{d\sigma}{d\epsilon} = \frac{2\pi r_e^2 Z}{(\gamma - 1)} \left[\frac{1}{\beta^2 \epsilon^2} - \frac{B_1}{\epsilon} + B_2 - B_3 \epsilon + B_4 \epsilon^2 \right]$$

$\epsilon = T / (E - mc^2)$
 Kinetic energy of the impinging electron

The kinematic limit for ϵ is:
 1 keV $\epsilon_0 = \frac{T_{cut}}{E - mc^2} \leq \epsilon \leq 1$

$\gamma = E/mc^2$	$B_1 = 2 - y^2$
$\beta^2 = 1 - (1/\gamma^2)$	$B_2 = (1 - 2y)(3 + y^2)$
$x = T_{cut}/(E - mc^2)$	$B_3 = (1 - 2y)^2 + (1 - 2y)^3$
$y = 1/(\gamma + 1)$	$B_4 = (1 - 2y)^3$

Sampling

We can write the cross-section as:

$$\frac{d\sigma}{d\epsilon} = f(\epsilon)g(\epsilon)$$

$$f(\epsilon) = \frac{1}{\epsilon^2} \frac{\epsilon_0}{1 - \epsilon_0}$$

$$g(\epsilon) = \frac{B_0 - B_1\epsilon + B_2\epsilon^2 - B_3\epsilon^3 + B_4\epsilon^4}{B_0 - B_1\epsilon_0 + B_2\epsilon_0^2 - B_3\epsilon_0^3 + B_4\epsilon_0^4} \quad B_0 = \gamma^2 / (\gamma^2 - 1)$$

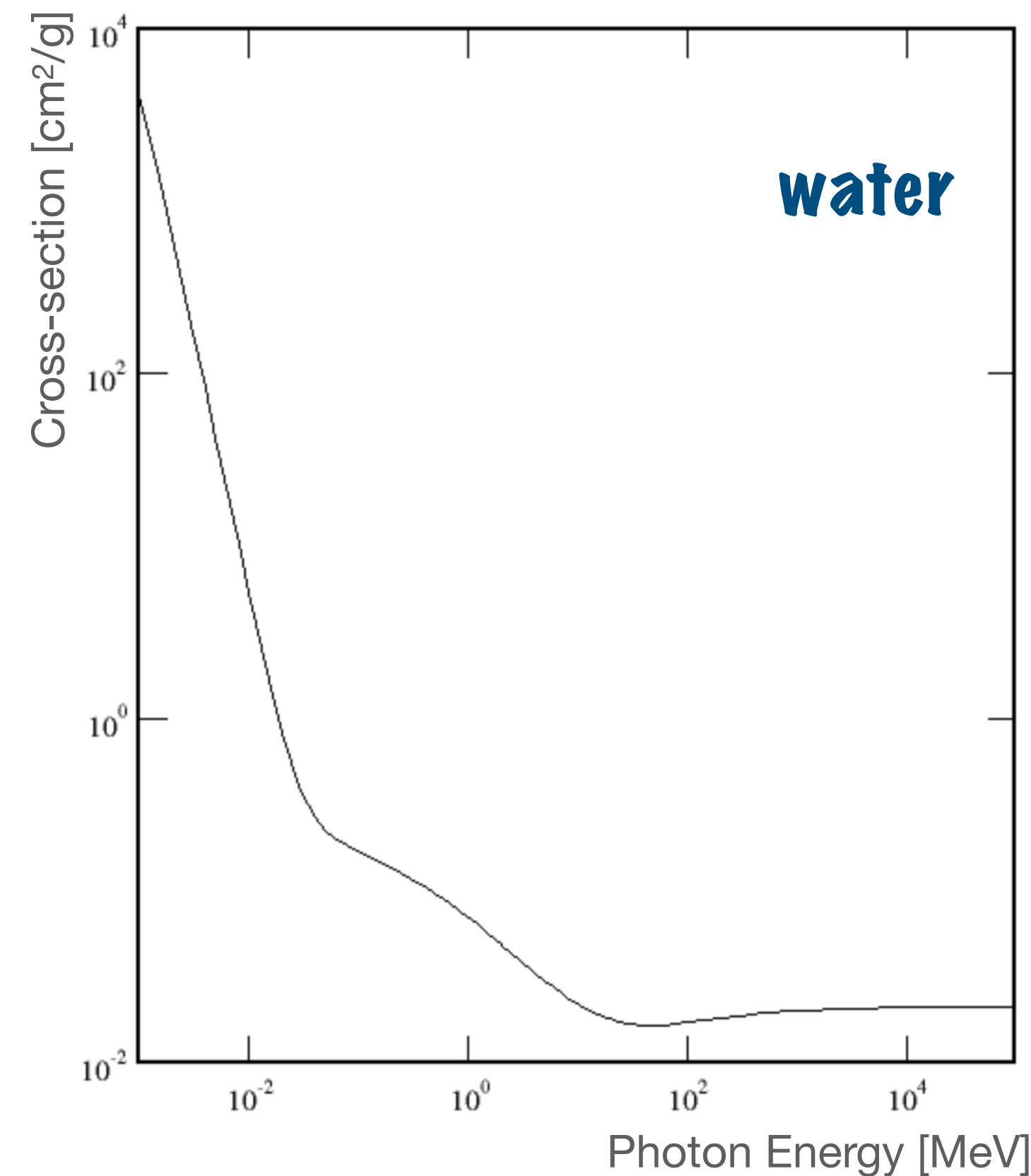
- To choose ϵ , and hence the **delta ray energy**
- ϵ is sampled from $f(\epsilon)$
 - the rejection function $g(\epsilon)$ is calculated using the sampled value of ϵ
 - ϵ is accepted with probability $g(\epsilon)$

The **azimuthal angle** ϕ is generated isotropically and the **polar angle** θ is calculated from energy-momentum conservation

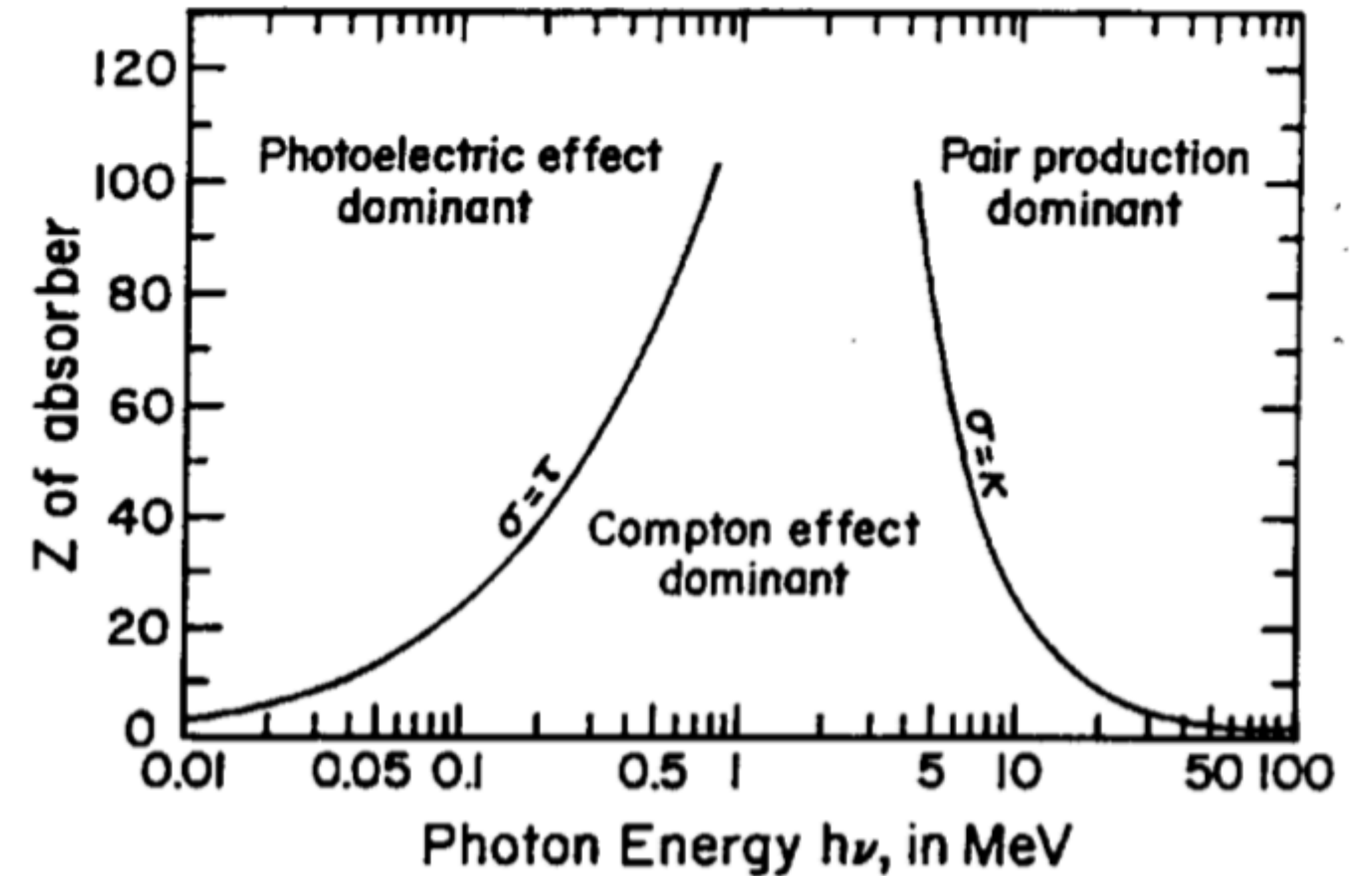


Photons interaction

From NIST XCOM database we have download the cross-sections of **photons** with **energy** ranging from **1 keV** to **1 GeV** and for material with **Z** value from **1** (Hydrogen) to **99** (Einsteinium) for:

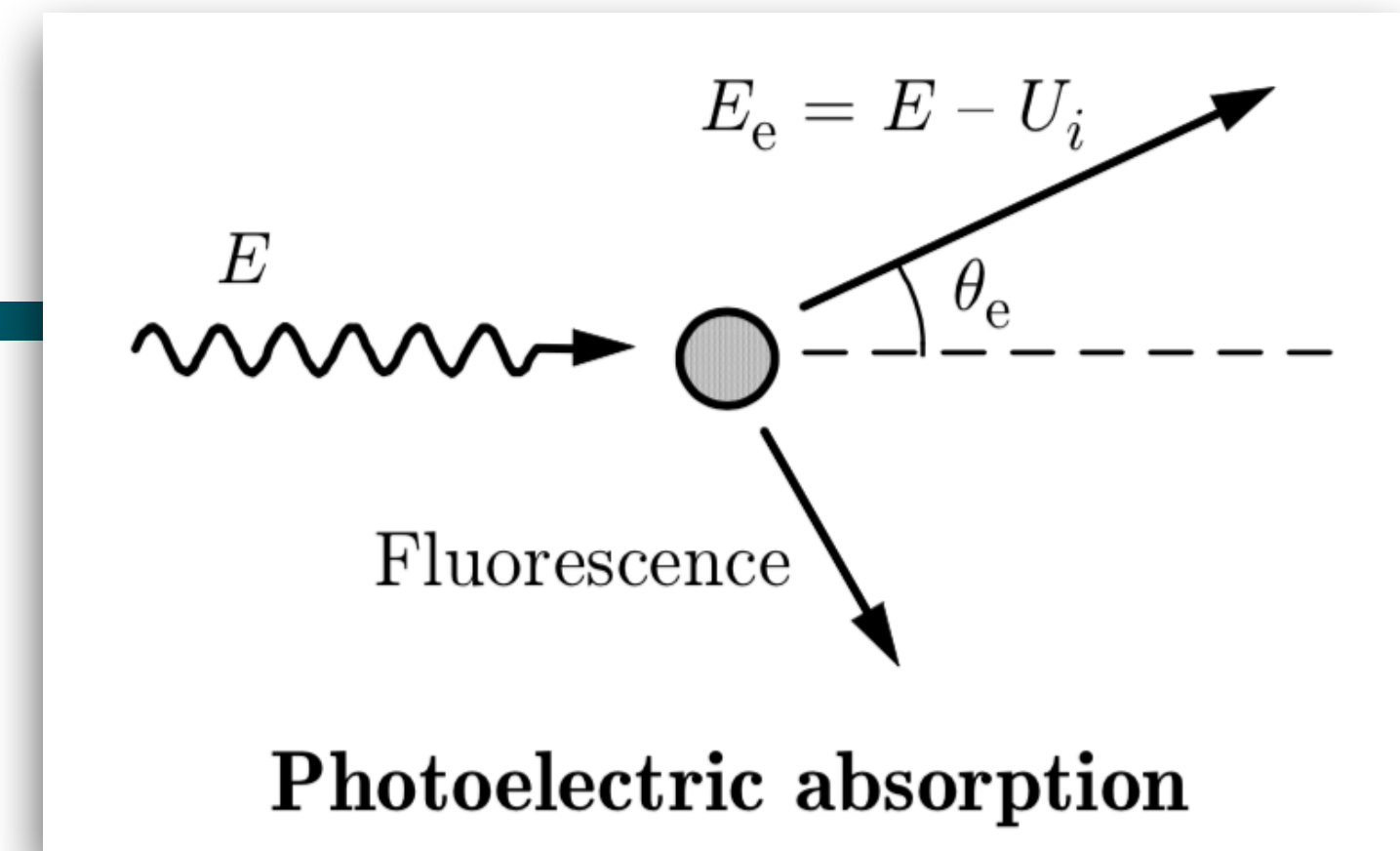


- Coherent scattering
- Photoelectric effect
- Compton scattering
- Pair production



NIST XCOM photons Cross-sections Database: <https://www.nist.gov/pml/xcom-photon-cross-sections-database>

Photoelectric effect



Depending on the interacted atomic shell (B=K,M,L ...) the energy of the emitted electron is set to:

$$E'_e = k - E_B$$

where the kinetic energy of the impinging photon must be greater than the binding energy of the selected shell:

$$k > E_B$$

Then the electron angle is sampled from:

$$\nu = 1 - \cos \theta_e$$

$$p(\nu) = (2 - \nu) \left[\frac{1}{A + \nu} + \frac{1}{2} \beta \gamma (\gamma - 1) (\gamma - 2) \right] \frac{\nu}{(A + \nu)^3}, \quad A = \frac{1}{\beta} - 1$$

This probability can be factorized as:

$$p(\nu) = g(\nu) \pi(\nu)$$

$$g(\nu) = (2 - \nu) \left[\frac{1}{A + \nu} + \frac{1}{2} \beta \gamma (\gamma - 1) (\gamma - 2) \right]$$

$$\pi(\nu) = \frac{A(A + 2)^2}{2} \frac{\nu}{(A + \nu)^3}$$

To choose the **electron angle**:

1. Generate ν from $\pi(\nu)$
2. Generate a random number ξ
3. if $\xi g(0) > g(\nu)$ go to step 1.
4. Deliver $\cos \theta_e = 1 - \nu$.

pyPENELOPE

Compton Scattering

The PDF of the polar deflection $\cos\theta$ of the scattered photon is given by

$$P_{\theta}(\cos\theta) = \left(\frac{E_C}{E}\right)^2 \left(\frac{E_C}{E} + \frac{E}{E_C} - \sin^2\theta\right)$$

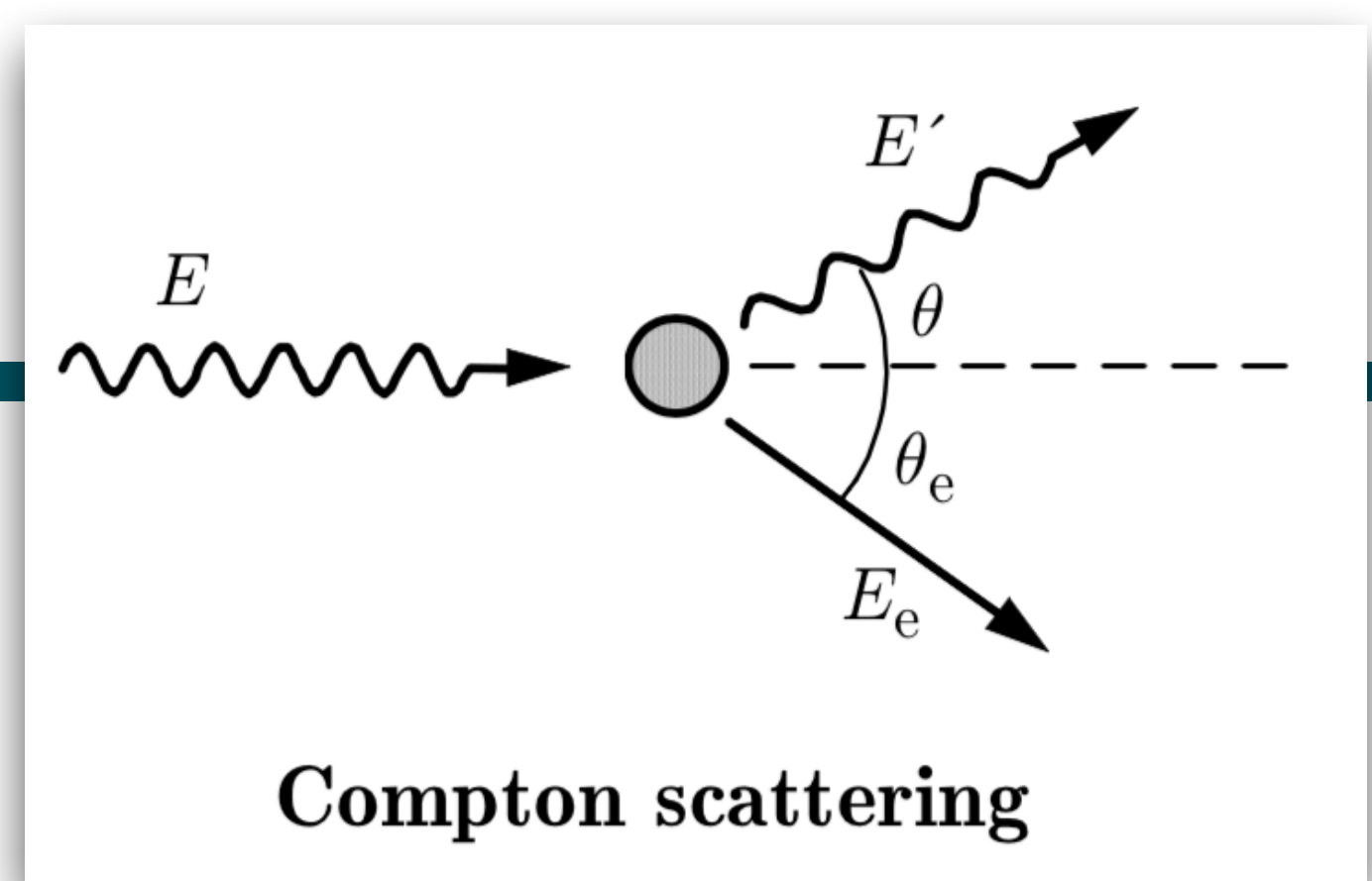
where

$$E' \equiv \frac{E}{1 + \kappa(1 - \cos\theta)} \equiv E_C \quad \text{is the energy of photons scattered in the direction } \theta \text{ by free electrons **at rest**}$$

However we have to consider the **Doppler effect**: the atomic electrons are not at rest, but move with a certain momentum distribution.

We perform a **Lorentz boost**, moving in the reference frame in which the atomic electron is at rest ($p_e = 0$). Then we simulate the all process sampling the energy and angle of the electron and scattered photon and at the end we move again in the initial reference frame ($p_e \neq 0$).

Depending on the impinging photon energy the i -th shell is selected and the atomic electron momentum is chosen from tables (**FLUKA**)



Klein-Nischina

Random values of $\cos \theta$ from the PDF can be generated by using the following algorithm:

Let's define

$$\tau \equiv \frac{E_C}{E} = \frac{1}{1 + \kappa(1 - \cos \theta)} \quad \text{with} \quad \kappa \equiv \frac{E}{m_e c^2}.$$

The PDF of this variable is:

$$P_\tau(\tau) = P_\theta(\cos \theta) \frac{d(\cos \theta)}{d\tau} = \left(\frac{1}{\tau^2} + \frac{\kappa^2 - 2\kappa - 2}{\tau} + (2\kappa + 1) + \kappa^2 \tau \right)$$

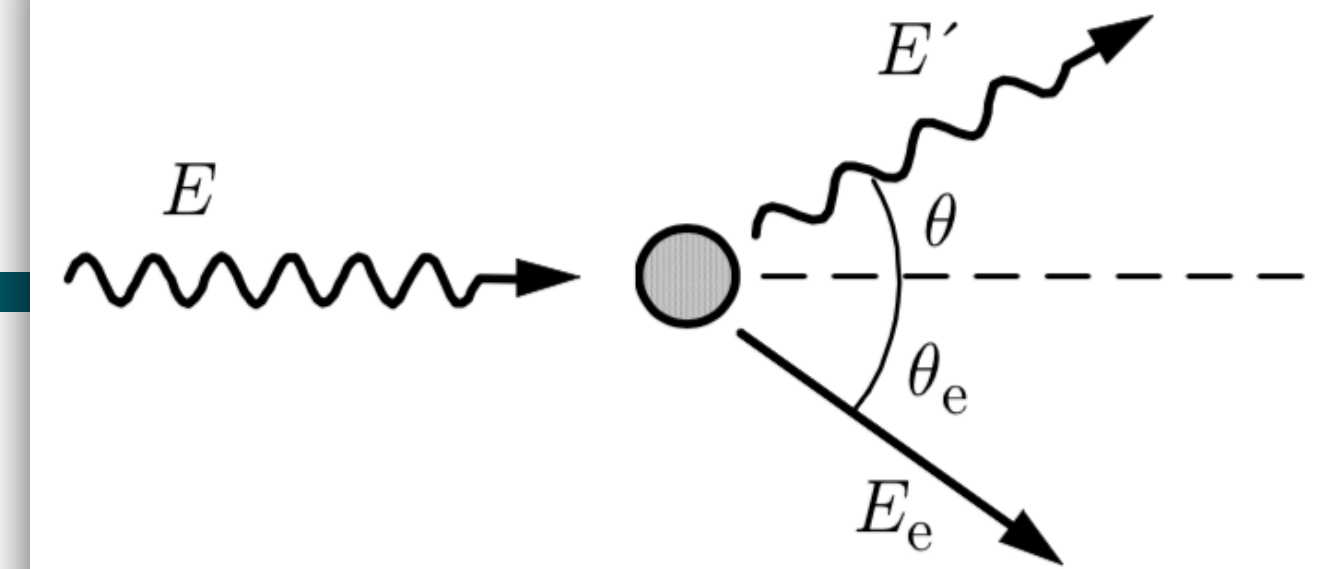
We can write the PDF as:

$$P_\tau(\tau) = [a_1 P_1(\tau) + a_2 P_2(\tau)] T(\cos \theta),$$

$$P_1(\tau) = \frac{1}{\ln(1 + 2\kappa)} \frac{1}{\tau}, \quad P_2(\tau) = \frac{(1 + 2\kappa)^2}{2\kappa(1 + \kappa)} \tau$$

$$T(\cos \theta) = \left\{ 1 - \frac{(1 - \tau) [(2\kappa + 1)\tau - 1]}{\kappa^2 \tau (1 + \tau^2)} \right\}$$

$$a_1 = \ln(1 + 2\kappa), \quad a_2 = \frac{2\kappa(1 + \kappa)}{(1 + 2\kappa)^2},$$



Compton scattering

Klein-Nischina

To choose the **scatter photon angle** ϑ :

1. Sample a value of the integer i ($=1,2$) according to the point probabilities:

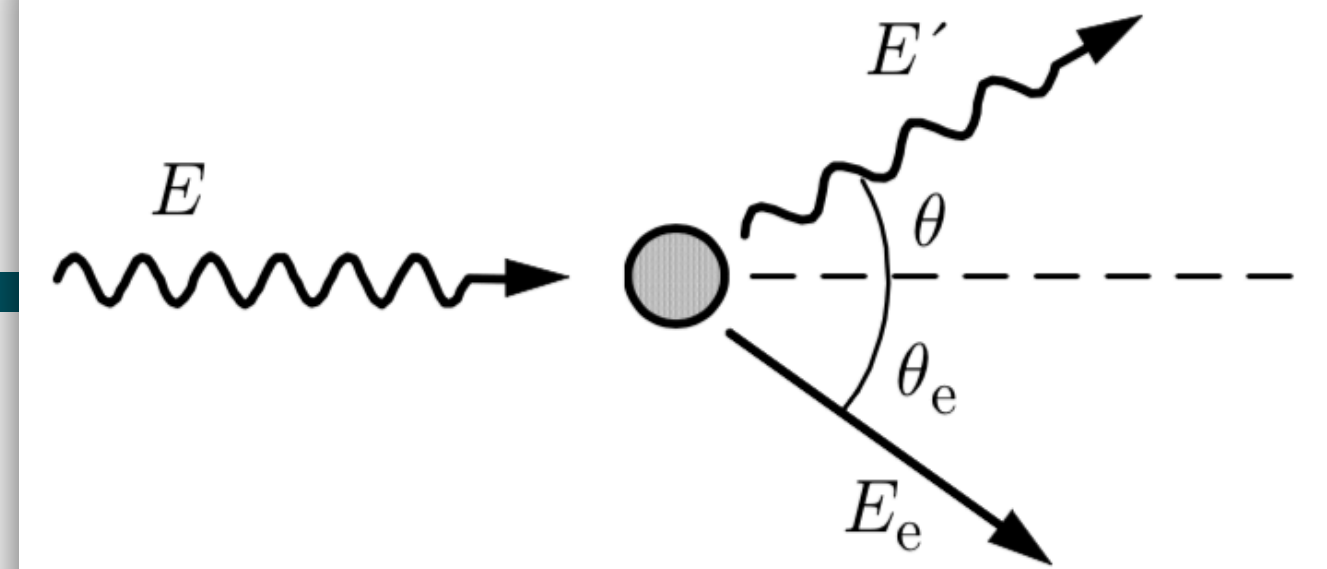
$$\pi(1) = \frac{a_1}{a_1 + a_2} \quad \pi(2) = \frac{a_2}{a_1 + a_2}$$

2. Sample τ from the inverse-transform method:
$$\tau = \begin{cases} \tau_{\min}^{\xi} & \text{if } i = 1, \\ [\tau_{\min}^2 + \xi(1 - \tau_{\min}^2)]^{1/2} & \text{if } i = 2, \end{cases}$$

3. Determine

$$\cos \theta = 1 - \frac{1 - \tau}{\kappa T},$$

4. Generate a random number r
5. If $r > T(\cos \vartheta)$ go to step 1.
6. Deliver $\cos \vartheta$



Compton scattering

From **kinematic the scattered photon energy** is:

$$E' \equiv \frac{E}{1 + \kappa(1 - \cos \theta)}$$

The **electron angle and energy** is then:

$$E_e = E - E' - U_i$$

$$\cos \theta_e = \frac{E - E' \cos \theta}{\sqrt{E^2 + E'^2 - 2EE' \cos \theta}}$$